Suppression of hepatic fibrosis by efficient Col1a1 silencing using shRNA inducible mouse models

Dissertation

Zur Erlangung des Grades

Doktor der Naturwissenschaften

Am Fachbereich Biologie

Der Johannes Gutenberg-Universität Mainz

Olena Molokanova

geb. am 4 October 1965 in Nikolajew, Ukraine

Mainz, 2018

Tag der mündlichen Prüfung: 12.06.2018

Table of Contents

1. Introduction

1.1. Liver fibrosis and cirrhosis

Hepatic fibrosis is the result of a wound-healing response of the liver to repeated injury. This is associated with an altered, usually low grade chronic inflammation that causes excess deposition of scar tissue (extracellular matrix, ECM), composed of collagens, structural proteins, glycoproteins, proteoglycans and hyaluronan. Liver fibrosis often progresses to cirrhosis, which is characterized by a distortion of the liver vasculature and architecture, and which is the major determinant of morbidity and mortality in patients with liver disease, predisposing to liver failure and primary liver cancer (1-3).

The spectrum of chronic liver injuries includes viral hepatitis, autoimmune and cholestatic liver diseases, genetic disorders resulting in storage diseases, and alcoholic and non-alcoholic fatty liver disease. These conditions usually lead to chronic hepatic inflammation, fibrosis and cirrhosis (4).

One central mechanism underlying progression towards cirrhosis is damage to hepatocytes, the predominant functional liver cells. This damage induces e.g. the release of cellular contents, such as DNA and proteins, i.e., “damage-associated molecular patterns”, DAMPs, or reactive oxygen species that activate resident macrophages (Kupffer cells) or freshly recruited monocytes to release pro-inflammatory factors like tumor necrosis factor alpha (TNFα), interleukin-1β (IL-1β), interleukin 6 (IL-6), interleukin 8 (IL-8), or chemokine ligand 2 (CCL2), monocyte chemoattractant protein 1 (MCP-1) and pro-fibrogenic factors, especially transforming growth factor beta 1 (TGFβ1), that can induce fibrogenic activation of myofibroblasts (MF) and hepatic stellate cells (HSC), or further recruit inflammatory cells (5).

Fibrogenesis is also characterized by downregulation of ECM degrading enzymes, especially the matrix metalloproteinases (MMPs), such as MMP-1, -3, -8, -9, -12, and -13, and by upregulation the tissue inhibitors of MMPs (TIMPs), especially TIMP-1, the major physiological inhibitor of most MMPs (1).

Activated HSC and (portal) MF are the major effector cells of hepatic fibrosis via production of most of the excess ECM in fibrosis. A subgroup of these cells, approx.

30%, is characterized by expression of a-smooth muscle actin (α-SMA), and they all can produce excessive amounts of the major scar tissue proteins, collagens type I and type III. Thus, inhibition of translation of type I (and type III) collagen should in principle lead to a prominent attenuation of fibrosis.

The aim of this work was to engineer mice with endogenous, HSC and MF specific and inducible downregulation of type I procollagen *in vivo* during liver fibrosis progression, to assess the relevance of collagen type I in liver fibrosis and the relative role of procollagen type I as a prime target for antifibrotic therapies. Moreover, these mice should permit the HSC and MF specific deletion of other relevant fibrosis related proteins. Notably, similar mice had not been generated before and would represent an invaluable tool to explore HSC and MF specific fibrogenic (or fibrolytic) as well as immune modulatory mechanisms in different models of (liver) injury and fibrosis.

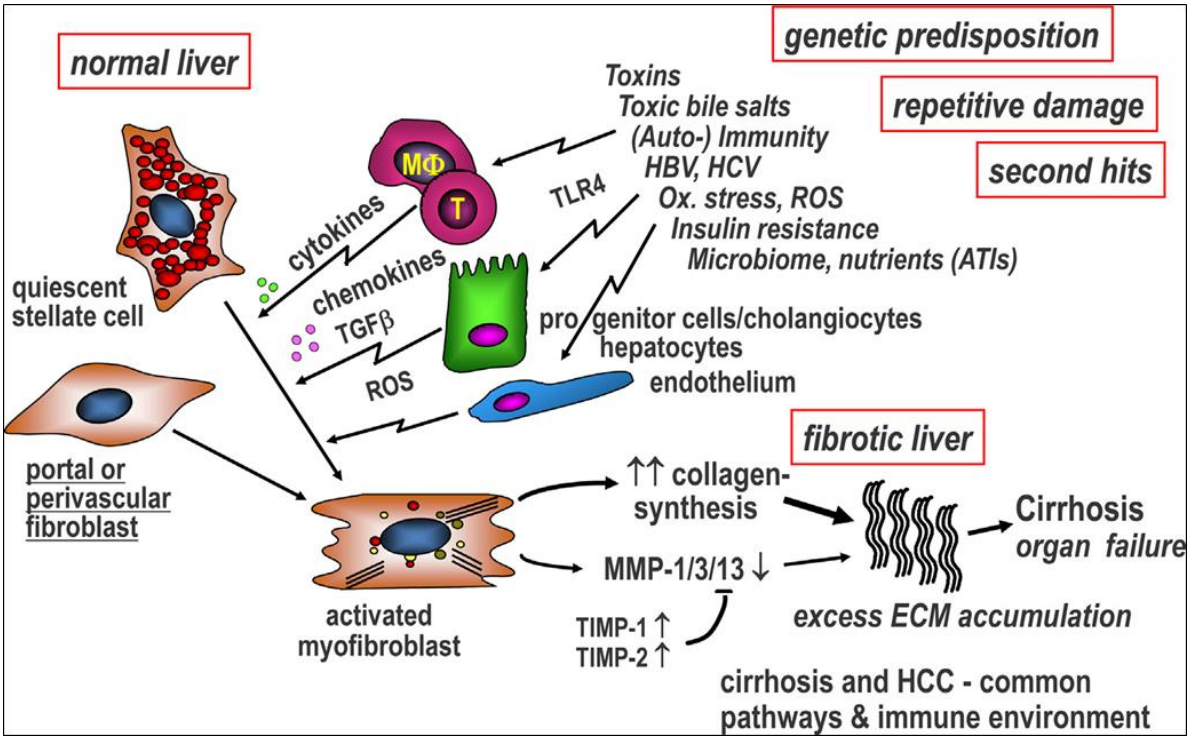

Figure 1. Common cellular mechanisms of liver fibrogenesis (1).

1.2. Extracellular matrix (ECM)

The extracellular matrix (ECM) is a combination of biological molecules secreted by cells. It supports establishment, separation and maintenance of differentiated tissues and organs. ECM is a complex network within which defined molecules are precisely organized. Importantly, the ECM directs cellular differentiation, migration, proliferation, and fibrogenic activation or deactivation. Most of the structural ECM molecules are collagens, noncollagenous glycoproteins, and proteoglycans. Some of them share different functional domains creating multidomain proteins tailored to the needs of the organism (6). Via defined oligopeptide sequences or structural domains, the ECM transfers specific signals to cells that act in concert with growth factors/cytokines. These signals either confer stress activation, with a resultant fibrogenic response, or stress relaxation, with a fibrolytic response (6).

Thus ECM is a complex of all secreted molecules that are immobilized outside a cell, including growth factors, cytokines and cell adhesion molecules and macromolecules that are mainly responsible for tissue-type specific extracellular architecture.
The mature ECM undergoes dynamic remodeling in response to environmental stimuli, such as applied force or injury, which enables the tissue to maintain homeostasis and to respond to physiological challenges and stresses, including disease (7).

As the liver becomes fibrotic, significant qualitative changes of the ECM occur, while the total content of collagens and noncollagenous components increases up to tenfold accompanied by pathological changes of tissue and function of the liver (6).

1.3. Collagens

Collagens are the major proteins in the extracellular matrix and in connective tissues. 80 – 90 percent of the collagens consists of types I, II, and III. The collagens types I, III, IV, V, and VI are characterized as constituents of the hepatic ECM, of both the normal and fibrotic liver. Each collagen is composed of three polypeptide chains, which may be all identical or may be of two or three different chains (Table 1) (1,6,8).

Collagen type	Chain composition	Supramolecular form/Localisation	% in normal human liver	% in cirrotic human liver
I	$\alpha1(I)_2\alpha2(I)$	Major interstitial Fibrils	40-50	60-70
III	$\alpha1(III)_3$	Major interstitial Fibrils	40-50	23-30
IV	$\alpha1(9)_2$ α2(9)	Basement membranes, space of Disse	1	1-2
V	$\alpha1(V)_2$ α2(V) α1(V)α2(V)α3(V) α1(V)3	Interstitial core fibrils, pericellular, intima of vasculature	2-5	5-10
VI	α1(VI)α2(VI) α3(VI)	Interstitial interfiber filaments	0.1	0.2

Table 1. Types I, III, IV, V, and VI collagens are major constituents of both the normal and fibrotic liver. Each collagen is made up of three identical or genetically different alpha chains.There are other more recently identified collagens that constitute the liver ECM in health and especially in disease (8,10).

Types I and III are fibril forming collagens, synthesized as triple helical precursor molecules - procollagens. These molecules pack together to form long thin fibrils of similar structure. Collagen type IV it is the major collagen found in basement membranes. In contrast, it is structurally quite distinct from the fibrillar collagens: forms a two-dimensional network-like sheet. Collagen type V is fibril-forming collagen, found as an exocytoskeleton around smooth muscle cells. In liver fibrosis hepatocytes become encased by a layer of type V collagen (8). Microfibrillar collagen VI is ubiquitously expressed in the interstitial ECM of liver, displaying prominent pericellular localization and showing interactions with other ECM components (6).

It is now known 28 different collagen types. Each type is comprised of homotrimers or heterotrimers that are formed by three polypeptide chains. Polypeptide chain is characterized by amino- and carboxy-terminal propeptide sequences, which flank a

series of Gly-X-Y repeats, where X and Y are frequently proline and hydroxyproline. These prolines and hydroxyproline amino acids can comprise 20% of the molecule, contributing to triple helix stabilization through hydrogen bonds N–H(Gly)···O=C(Xaa) (prolin) (Figure 2).

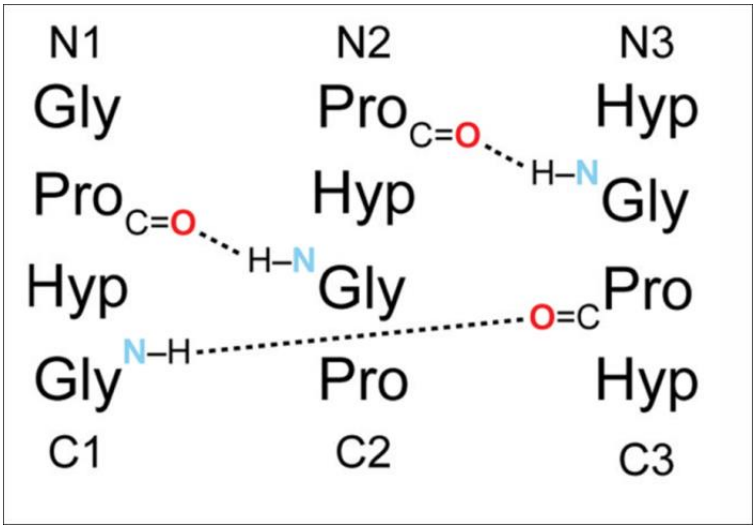

Figure 2. Hydrogen bonds of the collagen triple helix. From (11).

After lysyl and prolyl hydroxylation within the endoplasmic reticulum peptide chains self-assemble to form procollagen triple helix what is initiated by the C-terminal domain. Procollagen is secreted by cells into the extracellular space where enzymes (procollagen propeptidases) cleave propeptides form the interstitial (fibrillar) collagens (Figure 3) (7).

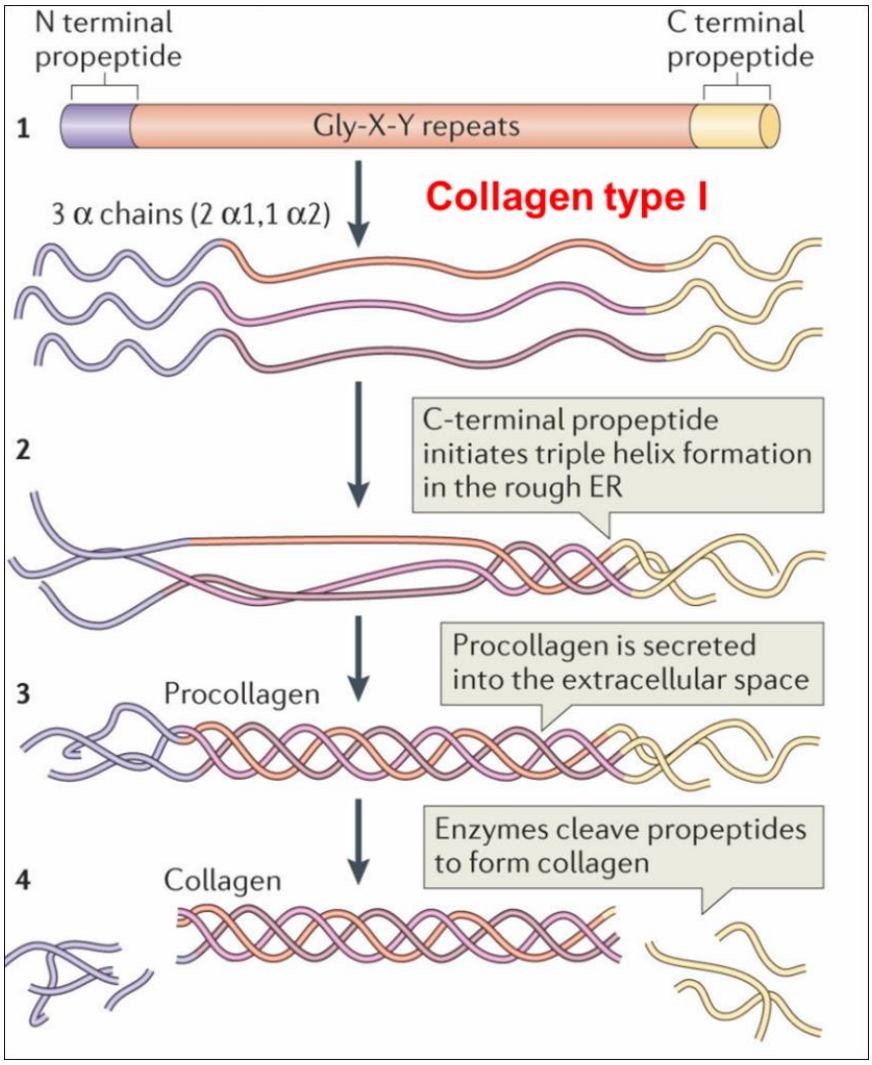

Figure 3. Collagen structure. 1.The standard fibrillar collagen molecule is characterized by amino- and carboxy-terminal propeptide sequences, which flank a series of Gly-X-Y repeats. 2.Three α-chains (the illustration shows two α1-chains and one α2-chain, which is representative of type I collagen) are intracellularly assembled into the triple helix following initiation of this process by the C-terminal domain. 3.Procollagen is secreted by cells into the extracellular space. 4. Conversion into fibrillar collagen by the removal of the N- and C-propeptides via ADAM-TS (a disintegrin and metalloproteinase-thrombospondin like secreted) and bone morphogenetic protein related enzymes. Modified from (7).

After cleavage of procollagen into collagen, initial fibril formation events occur at the cell surface. To form mature collagen fibres, further modifications are made during the assembly of collagen fibril aggregates. In the final step of collagen biosynthesis, covalent crosslinks are introduced into the supramolecular assembly to provide stability and enhanced mechanical properties (7).

Type I collagen is the most abundant and best studied collagen. It forms more than 90% of the organic mass of bone and is the major collagen of tendons, skin, ligaments, cornea, and many interstitial connective tissues. The collagen type I triple helix is

formed as a heterotrimer by two identical α1(I)-chains and one α2(I)-chain. A single molecule of type I collagen has a molecular mass of 285kDa, a width of 1.5nm and a length of 300nm.

Collagens type I is the main ECM protein accumulated in the fibrotic liver, and therefore, as the most “downstream” effector of fibrosis, an important target of anti-fibrotic therapy and drug development.

1.4. RNA interference (RNAi)

RNA interference (RNAi) is an evolutionarily conserved mechanism for silencing gene expression. The functions of RNAi are protection of the genome against invasion by mobile genetic elements such as viruses and transposons as well as regulation of the developmental programs of eukaryotic organisms. Double-stranded small RNAs (dsRNAs) have been shown to inhibit gene expression in a sequence-specific manner (9,12).

RNAi is initiated by the production of small non-coding RNAs (~20–30 nucleotides containing two nucleotides 3' end overhangs) with sequences that are complementary to the transcripts that they regulate. The RNAse III enzyme Dicer cleaves double-stranded RNA precursors, generating short interfering RNAs (siRNAs) or microRNAs (miRNAs) in the cytoplasm (13).

The siRNAs are derived from long double-stranded RNA (dsRNA) molecules that result from RNA virus replication, convergent transcription of cellular genes or mobile genetic elements, self-annealing transcripts or experimental transfection (13).

RNAi is mediated by the RNA-induced silencing complex (RISC) which recognizes mRNA containing a sequence homologous to the siRNA and cleaves the mRNA at a site located approximately in the middle of the homologous region (14) (Figure 4).
The endonuclease Argonaute 2 (Ago2) is responsible for the cleavage mechanism of RISC. One strand of the siRNA duplex (the guide strand) is loaded onto Ago2 at the core of RISC. During loading, the non-guide (passenger) strand is cleaved by theAgo2 and ejected. The Ago2 then uses the guide siRNA to associate with target RNAs that contain perfectly complementary sequence and then catalyses the slicing of these

targets. After slicing, the cleaved target RNA is released by cellular exonucleases, and the RISC is recycled for another round of slicing (13).

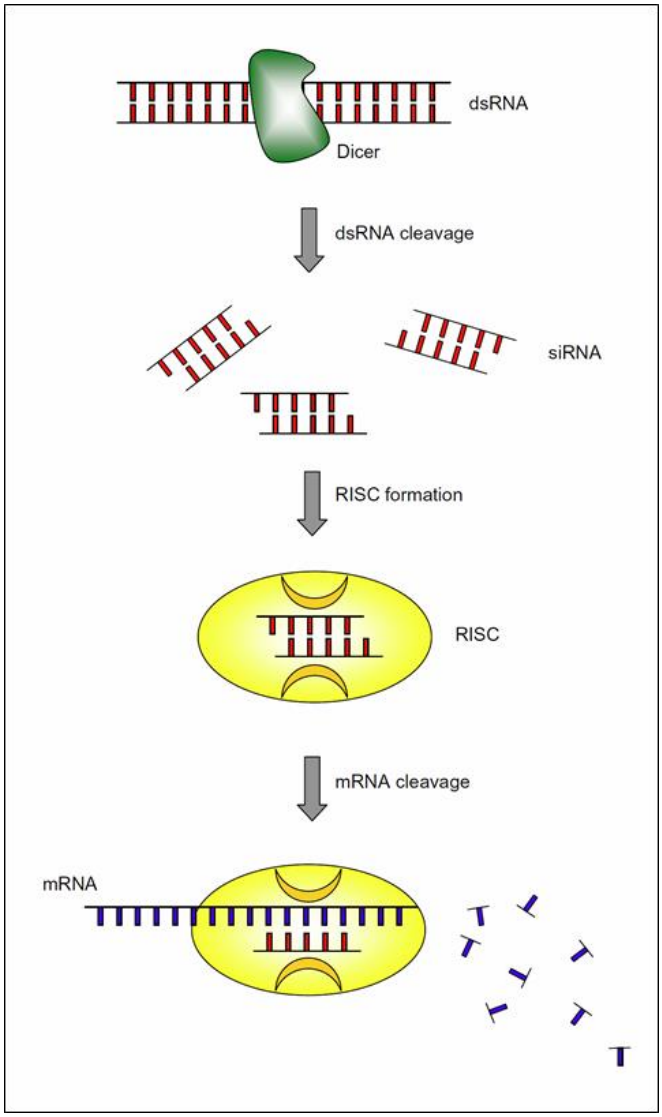

Figure 4. Mechanism of RNA interference (RNAi). The cellular enzyme Dicer binds to the (viral) dsRNA and cleaves it into short pieces of ~20 nucleotide pairs in length known as small interfering RNA (siRNA). These RNA pairs bind to the cellular enzyme called RNA-induced silencing complex (RISC) that uses one strand of the siRNA to bind to single stranded RNA molecules (mRNA) of complementary sequence. The nuclease activity of RISC then degrades the mRNA, thus silencing expression of the viral gene. From (14).

MiRNAs are encoded exclusively in the host genome and are generated from endogenous transcripts (13). They are major players in gene regulation at the post-transcriptional level (15).

Primary miRNAs (pri-miRNA) are expressed mostly as protein-coding genes from RNA polymerase II (Pol II) promoters. They are then processed by RNase III endonuclease

Drosha into stem-loop structures of pre-miRNAs. These pre-miRNAs are then exported to the cytoplasm by Exportin-5 and cleaved into small RNA duplexes of approximately 22 nucleotides by Dicer. Mature duplexes are loaded into RISC and serve as specificity determinants for the recognition of complementary targets (16) (Figure 5).

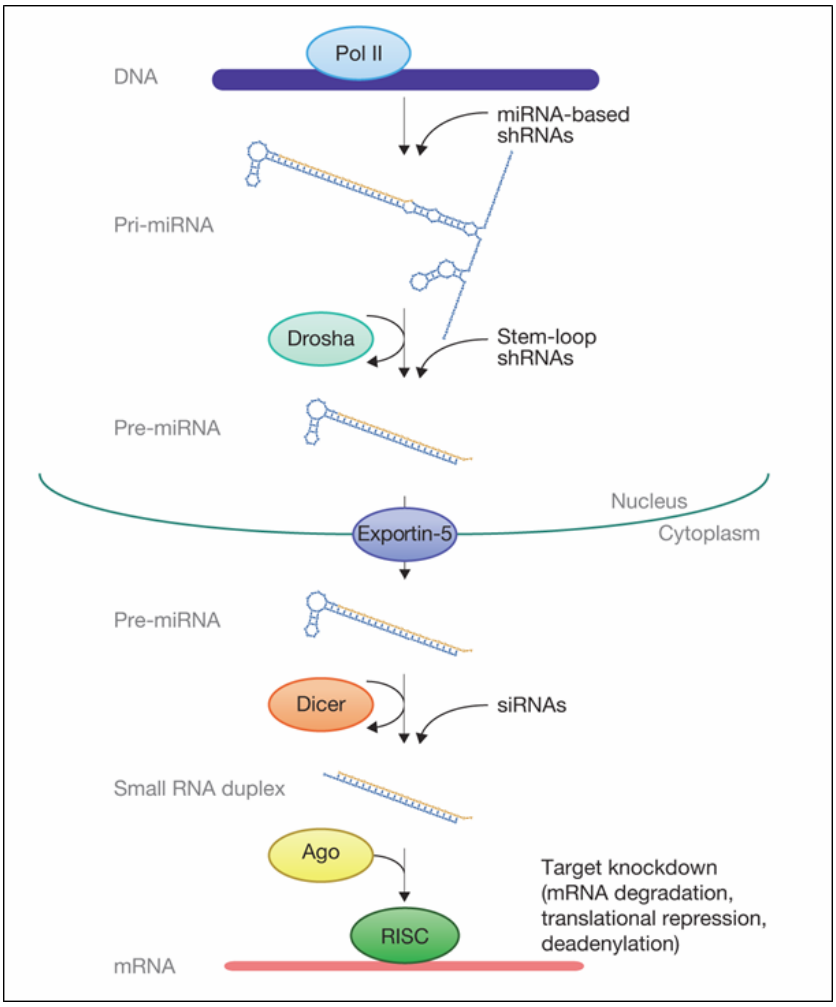

Figure 5. Endogenous RNAi pathways and their use as tools for gene silencing (16).

Genomic integration of vectors stably expressing stem-loop short hairpin RNAs (shRNAs) that mimic pre-miRNAs provides a continuous and heritable source of RNAi (Figure 5). Moreover, using a natural miRNA backbone also enables stable and regulated expression from Pol II promoters, as well as the construction of polycistronic 'tandem' shRNA vectors and their linking to fluorescent reporters. Application of the natural RNAi pathway ensures efficient production of mature small RNA duplexes and reduces toxicity (17) (Figure 6). The optimization of shRNA technology now enables

loss-of-function studies in mice; inducible shRNA transgenics can also expedite the evaluation of putative drug targets (16).

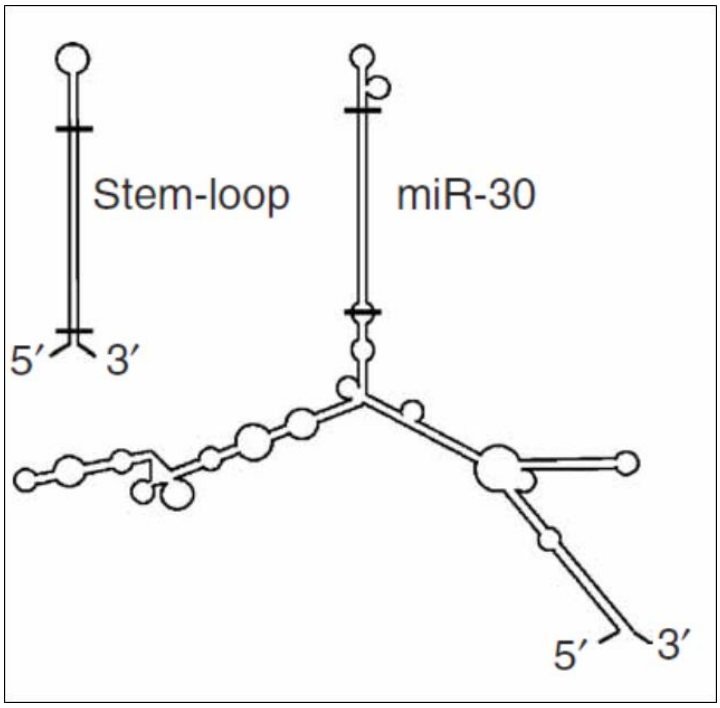

Figure 6. shRNA based on the scaffold of the miR-30 microRNA act as physiologic triggers of RNAi and can work more effectively at single copy in the genome than standard stem-loop shRNAs (17).

Post-transcriptional gene silencing by mRNA cleavage has been exploited as the method of choice for potential therapeutic applications of RNAi because of the potency of this catalytic gene-silencing pathway (18). Novel siRNA technologies have developed highly sophisticated RNA modifications and delivery systems into highly effective tools that can be used for different targets, most importantly for myeloid cell reprogramming in cancer (19).

1.5. Transgenic animals

Genetically engineered mice provide powerful tools for understanding mammalian gene function and development (20).

The creation of a transgenic mouse line can be achieved by a wide spectrum of technologies including random integration of a transgene via pronuclear injection, a more precise and predictable homologous recombination, or, as established in the last

decade, recombinase-mediated cassette exchange (RMCE) (21), by using zinc-finger nuclease (ZFN), Transcription Activator-like Effector Nuclease (TALEN) and most recently CRISPR/Cas technologies (22).

Employing these different technologies, the mouse genome can be altered towards heritable, tissue-specific and reversible overexpression of transgenes, disruption of single genes and knock-in of mutant alleles.

Conditional, i.e., inducible gene manipulation can be achieved using site specific recombination systems, including Cre/loxP and Flp/frt, or Tet regulatory system for temporally and spatially (cell type specific) controlled gene expression (23).
Recently established transgenic technologies allow rapid and efficient generation of mouse models for studying gene function in adult organisms as well as during development via a knock-in or knock-out of target genes.

1.6. Tet-system

The Tet regulatory system is a tetracycline-responsive binary system for temporally controlled gene expression in eukaryotes. It is applicable to cultured cells from mammals, plants, amphibians, and insects as well as to whole organisms including yeast, Drosophila, plants, mice, and rats (24). Currently, it is one of the most versatile and valuable tools for genetic manipulation of target genes in transgenic animals in vivo for assessing gene functions and for modelling human diseases.

“Tet switches” were established by Manfred Gossen and Hermann Bujard in 1992 as highly efficient regulatory systems in mammalian cells using control elements of the tetracycline-resistance operon encoded in Tn10 of *Escherichia coli* (25). As shown in the figure 7 the Tet repressor was fused with the activating domain of virion protein 16 of herpes simplex virus (which activates gene expression via the tetO) to generate the tetracycline-controlled transactivator (26). The transactivator is expressed constitutively in eukaryotic cells and induces transcription from the Tet operator sequences (tetO) fused to an engineered minimal promoter sequence (hCMV promoter). To facilitate specific binding, tetO was oligomerized up to seven times. When a tetracycline (usually doxycycline, Dox) is added to the cell cultures or injected into the transgenic animals, the transactivator is occupied and cannot activate gene

transcription via the oligomerized tetO. Thus, this Technology, known as the Tet-off system, promotes expression in the absence of tetracycline.

Over the following years the same group of scientists refined the original Tet expression system by the development of the "reverse tetracycline-controlled transactivator" (rtTA) system, where tetracycline acts as an inducer of transcription as well as the “recipient” tetracycline-controlled transactivator" (26) system, where the antibiotic prevents transcription activation (Figure 7) (27).

This original tetracycline-controlled transactivator was further improved to reduce residual binding to a responsive promoter in the absence of Dox and to increase its sensitivity to Dox. The more effective transactivator, rtTA2(S)-M2, operates at a 10-fold lower Dox concentration than rtTA, is more stable in eukaryotic cells, and has no background expression in the absence of Dox (28).

Thus, both the rtTA and the tTA systems provide valuable and tightly controlled genetic switches capable of quantitatively controlling individual gene activities in animals in a highly tissue- and/or cell-specific manner, opening broad perspectives for the study of gene function in mammalian organisms.

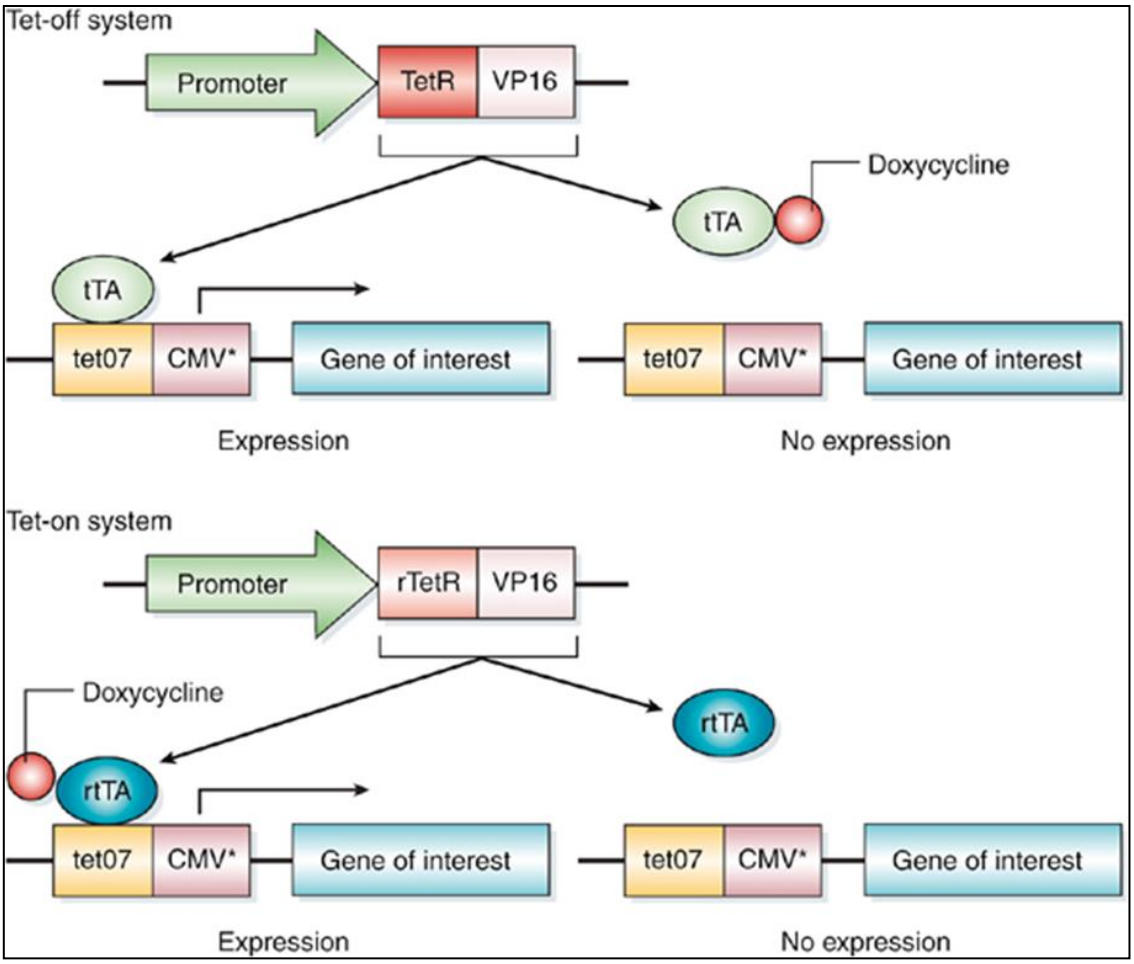

Figure 7. Tetracycline-regulated gene expression. In the tet-off system, the tetracycline transactivator protein (26) recognizes and binds to seven tetO domains (tetO7) connected to a minimally active CMV promoter (CMV*), resulting in gene activation. Doxycycline binds tTA and prevents gene activation. In the tet-on system, doxycycline binds to rtTA and activates the transcription (23).

1.7. Recombinase-mediated cassette exchange

Recombinase-mediated cassette exchange (RMCE) is a method that uses site-specific recombination (SSR) for modification of eukaryotic genomes by targeted integration. It can be achieved by precisely replacing a genomic target cassette by a compatible donor construct (21).

The best-studied and most commonly used SSRs in mammalian cell cultures exploit the bacteriophage P1-derived Cre, the Saccharomyces cerevisiae-derived Flp and the bacteriophage φC31-derived PhiC31 integrase. These recombinases recognize sequence-specific motifs termed as recombination target sites (29) (LoxP, FRT and

attB/attP, respectively) that catalyze efficient conservative DNA rearrangements (30). This recombinase system utilizes replacement or excision of gene cassettes flanked by two non-interacting RTs (Figure 8).

Flp and Cre recombinases recognize their specific target genomic sequences that are terminally tagged via loxP or FRT, respectively. This allows the incoming targeting vector carrying the tagged genomic sequence for replacement, to integrate this targeting vector sequence site-specifically.

The φC31 recombinase mediates recombination between the heterotypic attB and attP sites. A cassette flanked by two attB sequences is integrated into the genomic site and hybrid attL and attR sites are generated which are not compatible for any further recombination events.

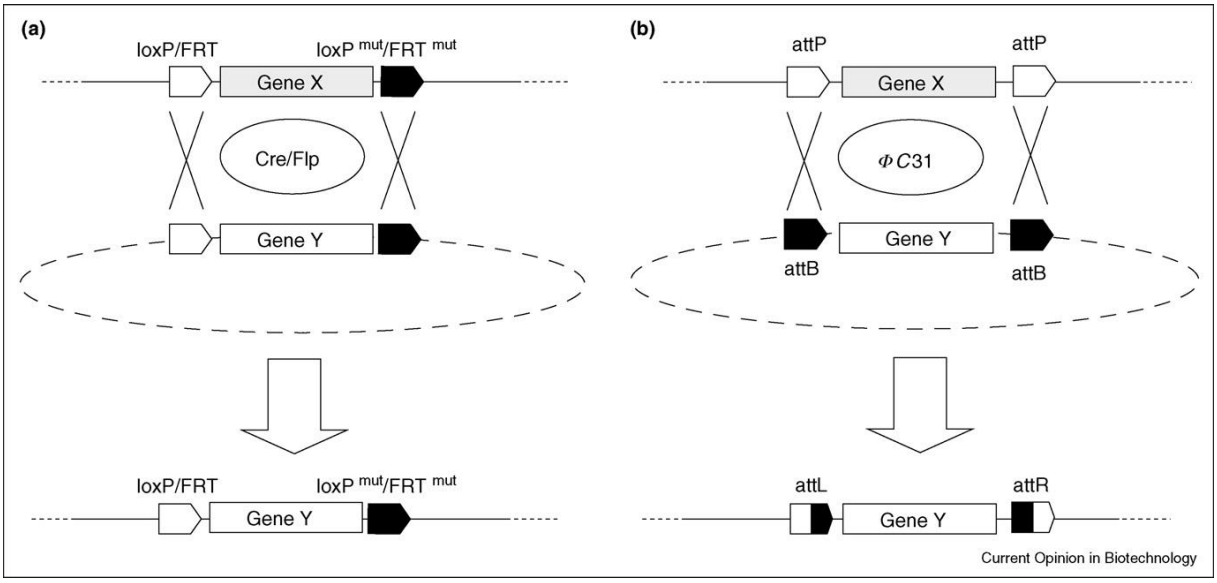

Figure 8. Principle of recombinase-mediated cassette exchange (RMCE). (a) via Cre or Flp recombinases; (b) Site-directed integration by φC31 (31).

Originally these systems were used for genome editing in cell culture and embryonic stem (ES) cells. Now RMCE is successfully applied for the generation of transgenic knock-out or knock-in mice and their further versatile genetic modification (32).

The RMCE strategy for generation of transgenic mice using a Flp recombinase and a frt homing site was refined by demonstrating feasibility of a “flp-in” strategy *in vivo* (33).

A plasmid was generated in which the frt homing site was added to a tetO-site. This DNA sequence then permitted the generation of tetracycline-inducible transgenes using RMCE technology in the presence of Flp recombinase (Figure 9). Furthermore, this lead to the development KH2 ES cells containing not only the frt-hygro-pA ‘‘homing’’ cassette downstream of the procollagen alpha 1 chain (ColA1) locus, but also the tetracycline-inducible M2rtTA transactivator driven from the endogenous Rosa26 promoter. This combination allows rapid production of ES cells and mice carrying tetracycline-inducible transgenes targeted to a specific locus to assure predictable temporal and spatial expression.

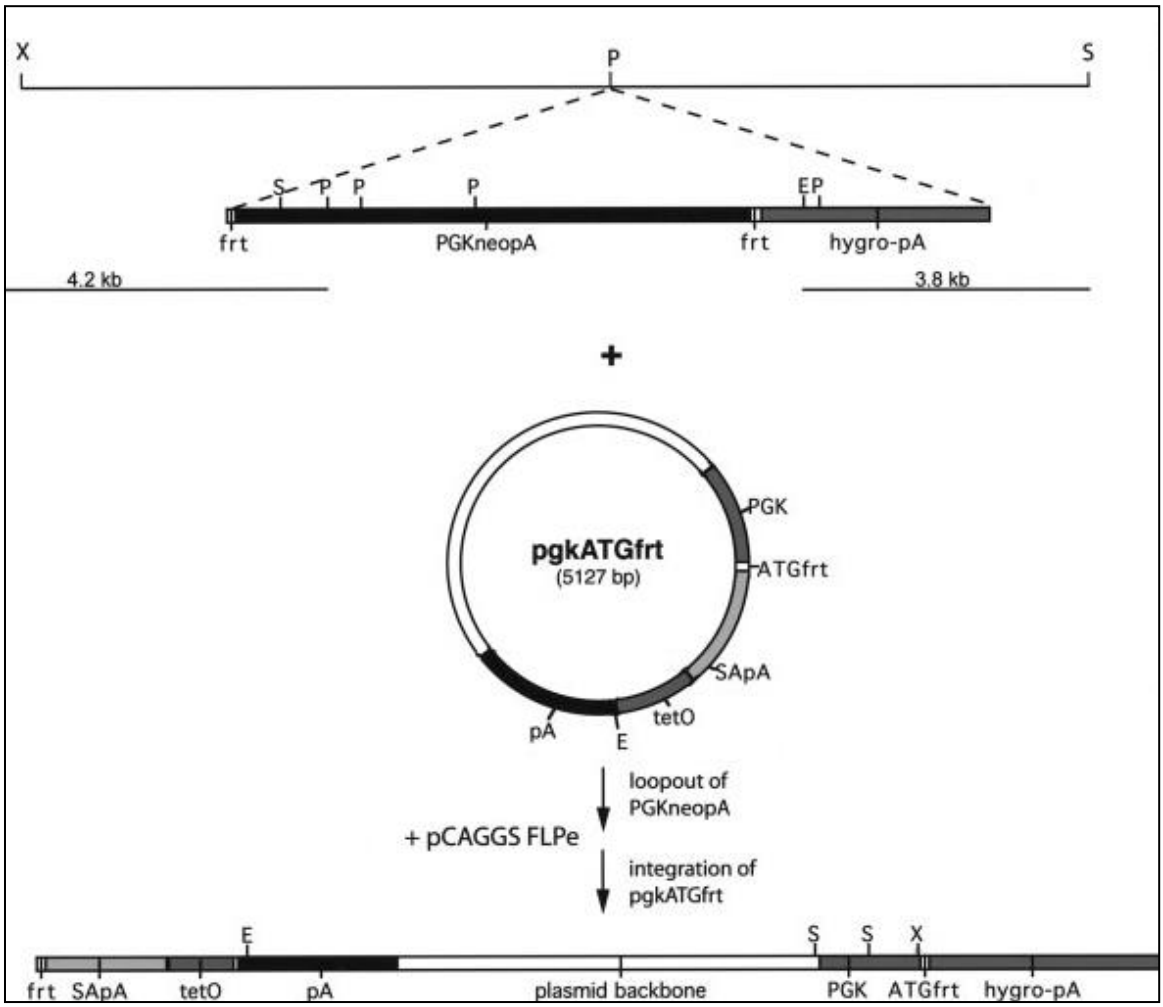

Figure 9. Strategy for FLPe-mediated recombination. Homologous recombination is used to place a frt-hygro-pA ‘‘homing’’ cassette downstream of the Col1A1 locus. A gene of interest is then targeted to the modified locus by co-electroporation of the pgkATGfrt vector carrying this gene and an Flpe transient expression vector. Inter- and intra-chromosomal recombination at the frt sites results in loss of the PGKneopA cassette and insertion of the gene of interest and the pgkATG cassette to restore and confer hygromycin resistance (33).

This Flp/FRT RMCE strategy to generate a system for the production of single-copy, tet-regulatable shRNA transgenic ES cells and mice was combined with optimized fluorescence-coupled shRNA technology (34,35). This approach includes the use of a targeting construct as a recipient vector for any miR30-loop structure-based shRNA (17) and an expression cassette whereby shRNA expression is linked to a fluorescent reporter (EGFP).

1.8. Zinc-finger nuclease (ZFN)

Zinc-finger nuclease (ZFN) is one of the programmable nucleases that have been used only for the last five years for targeted genome engineering. ZFNs are hybrid restriction enzymes composed of a customizable zinc-finger protein DNA-binding domain fused to the cleavage domain of the FokI endonuclease (from *Flavobacterium okeanokoites*) (Figure 10). Each zinc finger of the DNA-binding unit interacts with a triplet within the DNA substrate and makes its own unique contribution to DNA binding affinity and specificity. The modular structure of the DNA-binding domain usually consisting of 4-6 zinc finger proteins enables to design peptides that will bind DNA at predetermined nucleotide sequences (36). Cleavage is induced when two custom-designed ZFNs heterodimerize upon binding DNA to form a catalytically active nuclease complex. As the zinc-finger protein DNA-binding domain can be engineered to bind with high specificity to an investigator's base chosen sequence, ZFNs enable a DNA cleavage event to be targeted to effectively any genomic location (37).

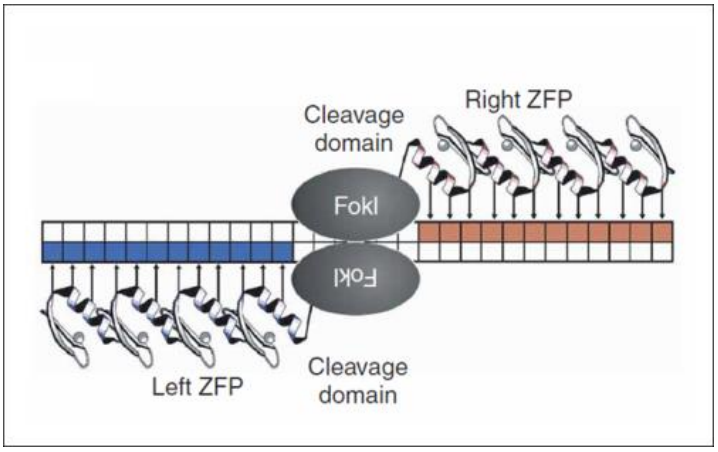

Figure 10. DNA recognition and cleavage by zinc-finger nucleases. ZFP- zinc-finger protein DNA-binding domain; FokI - cleavage domain (38).

Programmable ZFNs produce site-specific DNA double-strand breaks (DSBs), which enhance the efficiency of homologous recombination in the presents of a donor DNA or trigger error-prone nonhomologous end-joining (NHEJ), which leads to targeted mutagenesis (Figure 11). Plasmid DNA is often used to insert a gene of interest into the genome. Engineered nucleases enhance the efficiency of homologous recombination in a site-specific manner, which allows the targeted insertion of genes into genomic 'safe harbours' or pre-determined sites in the genome. To achieve this, the nuclease is co-transfected with a targeting vector, in which the genetic segment to be incorporated is flanked by homology arms with sequences that are identical to those near the target region (22).

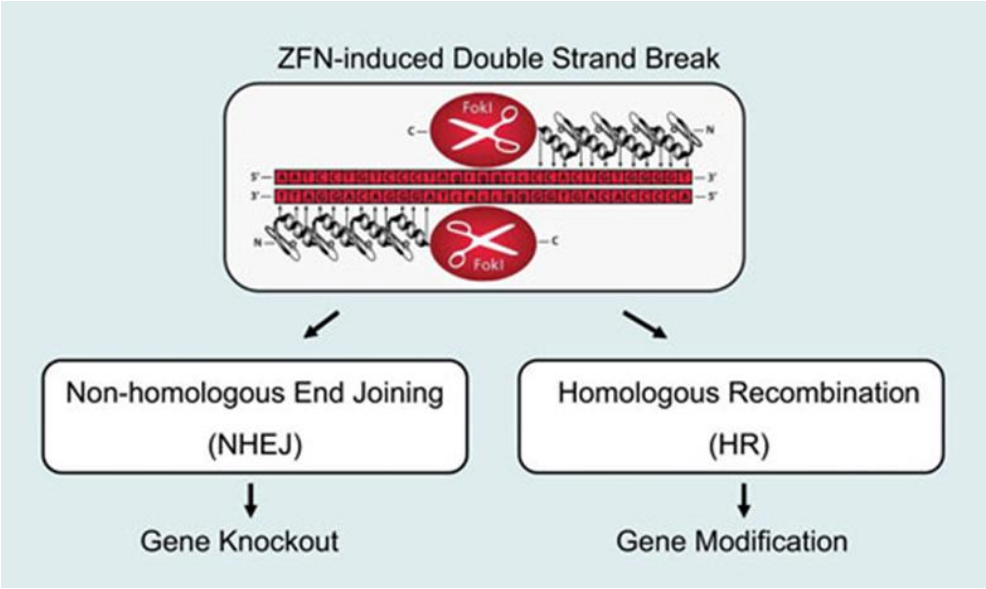

Figure 11. ZFN produces site-specific DNA double-strand breaks (DSBs), which leads to targeted mutagenesis or to gene modification by homologous recombination (adapted from Sigma-Aldrich St.Louis, USA).

1.9. Transgenic mice models to study liver fibrosis

Transgenic mice with the Col1a1 promoter driving the GFP reporter gene were generated (39) and used to study bone marrow-derived fibrocytes in liver fibrosis development (40), the fate of myofibroblasts during regression of liver fibrosis (41), collagen expressing (myo-) fibroblasts in conjunction with a reporter mouse for the expression of alpha smooth muscle actin (α-SMA) linked to red fluorescent protein (42).

In line with the human disease, spontaneous mutations in the pro-alpha2 chain of type I collagen mice are associated with osteogenesis imperfecta and identified at birth by hemorrhages into joint cavities, sides of the body or around the scapulas; breaks in the long bones and tail (43). Due to the several general and bone manifestations this strain is difficult to use for studying collagen matrix biology.

A transgenic α-SMA-Cre-ERT2 mouse line in which the expression of the Tamoxifen-dependent Cre-ERT2 recombinase is under the control of a large genomic DNA segment of the mouse smooth muscle α-actin (α-SMA) gene allowed efficient, temporally-controlled ablation of floxed DNA segments restricted to smooth muscle cells that express α-SMA (44).

Pdgfrb (Beta-type platelet-derived growth factor receptor)-Cre transgenic mice (45) were initially validated as a model to study and track tissue pericytes or myofibroblasts by crossing them with dual mTmG-GFP mice that expresses membrane-targeted Tomato prior to Cre-mediated excision and membrane-targeted green fluorescent protein after excision (46) and used for investigation whether β integrin chains that are associated with the αV integrin chain affected experimental liver fibrosis. Here it could be shown that genetic deletion of the αV-integrins carrying the β3, 5, 6, or 8 chains did not confer protection against CCl4-induced murine liver fibrosis (47,48) (Figure 12).

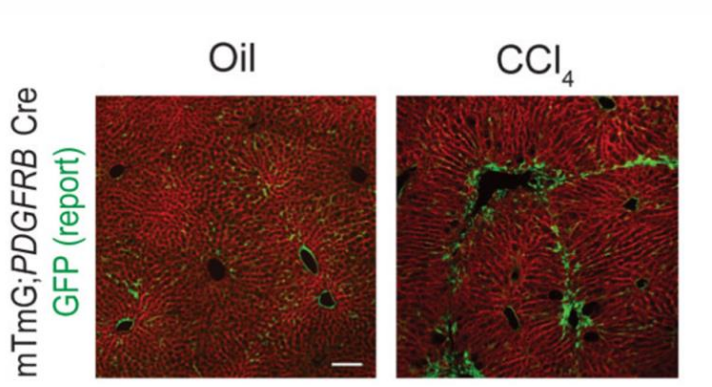

Figure 12. Pdgfrb-Cre effectively targets recombination in quiescent and activated hepatic stellate cells. Immunofluorescence micrographs of liver sections harvested from control (olive oil treated) or chronic CCl4 treated (x2 injections / week for six weeks) mTmG; Pdgfrb-Cre reporter mice (47).

As another project I have generated an activated myofibroblast specific inducible Col3a1-CreERT2 mouse model. The model showed high efficient recombination in the target tissue and was used for conditional knock-out of TGFßRII in activated HSC (own unpublished data, Figure 13).

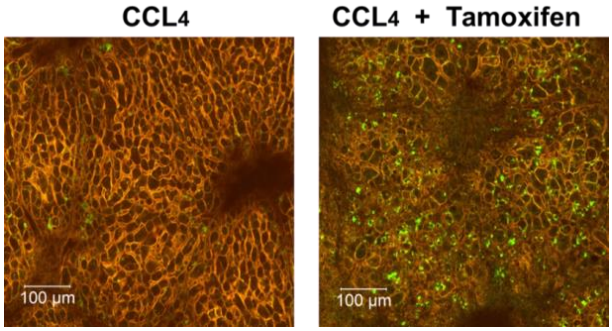

Figure 13. Bi-transgenic Col3a1-CreERT2/mTmG mice (n=4) were treated with CCl4 for three weeks, to induce liver fibrosis, and with tamoxifen for the last five days, to induce Cre recombination. Thereafter, mice were analyzed in vivo using confocal laser scanning microscopy showing a massive GFP signal in the liver compared to control animals without tamoxifen treatment (AG Prof.Schuppan, Institute of Translational Immunology, University Medical Center Mainz, Germany)

1.10. Aims

The aims of this thesis were:

1. To establish an inducible mouse model for the conditional knockdown of the Col1a1 gene that is rate limiting for collagen type I expression and deposition.

2. To establish and compare RMCE and ZFN based methods of transgenic inducible Col1a1 knockout mouse generation.

3. To study the development of hepatic fibrosis in these transgenic mouse models by conditional Tet-regulated RNAi-induced down-regulation of the Col1a1 gene.

4. To assess the effect of inducible procollagen alpha1(I) gene deletion on liver fibrosis, general matrix metabolism and inflammation.

2. Materials and methods

2.1. Materials

2.1.1. Instrumentation

Name	Manufacturer
A&B applied biosystems step one plus realtime PCR system	Life technologies GmbH, Darmstadt, Germany
Balance Sartorious AX2202	PK Elektronik Ettlingen, Germany
Balance Sartorious AX124	PK Elektronik Ettlingen, Germany
Bio-Rad T100™ thermal cycler	Bio-Rad, Munich, Germany
Bio Rad Powerpac basic	Bio-Rad, Munich, Germany
Bio Rad Powerpac HC	Bio-Rad, Munich, Germany
Centrifuge 5702	Eppendorf, Hamburg, Germany
Centrifuge HeraeusFresco21	Thermoscientific, Schwerte, Germany
ChemiDoc™ XRS+ System	Bio Rad, Munich, Germany
Electroporator	Bio Rad, Munich, Germany
Eppendorf centrifuge 5804R	Eppendorf, Hamburg, Germany
Eppendorf centrifuge 5415R	Eppendorf, Hamburg, Germany
Eppendorf Pipette 1000ul	Eppendorf, Hamburg, Germany
Eppendorf Pipette 100ul	Eppendorf, Hamburg, Germany
Eppendorf Pipette 10ul	Eppendorf, Hamburg, Germany
Ergone Pipette 20ul	Starlab GmbH, Hamburg, Germany
Ergone Pipette 10ul	Starlab GmbH, Hamburg, Germany
Ergone Pipette 2,5ul	Starlab GmbH, Hamburg, Germany
Gel chamber for agarose	NeoLab, Heidelberg, Germany
Gilson Pipette 1000ul	NeoLab, Heidelberg, Germany
Gilson Pipette 200ul	NeoLab, Heidelberg, Germany
Gilson Pipette 20ul	Starlab GmbH, Hamburg, Germany
Herasafe KS Biological Safety Cabinets	Thermoscientific, Schwerte, Germany
Heracell™ 240i CO2 Incubator	Thermoscientific, Schwerte, Germany
HeraeusMultifuge X3R centrifuge	Thermoscientific, Schwerte, Germany
LAUDA Aqualine AL 5	LAUDA, Lauda-Königshofen Deutschland
Leica EG 1150c	Leica, Wetzlar, Germany
Leica TP1020	Leica, Wetzlar, Germany
Leica CM1950 Cryostat	Leica, Wetzlar, Germany
Leica HI1210 water bath	Leica, Wetzlar, Germany
Microtome Leica RM2255	Leica, Wetzlar, Germany
Microtome blade MX35 premier 34°/80mm	Thermoscientific, Schwerte,Germany
Motorized inverted research microscope olympus ix81	Shinjuku, Präfektur Tokio, Japan
MulticalPH meter pH 538	WTW, Weilheim, Germany
Pipetus	Hirschmann, Eberstadt, Germany
Rocking platform	VWR International, Darmstadt, Germany

Rotamax 120	Heidolph Instruments, Schwabach, Germany
Shaker incubator	Thermoscientific, Schwerte, Germany
TECAN infinite M 200Pro	Tecan, Männedorf, Germany
TissueLyser II	Qiagen, Hilden, Germany
Vortex-Genie 2	Scientific Industries, New York, USA
Zeiss microscope AX10	Carl Zeiss, Munich, Germany
Zeiss microscope 40 CFL	Carl Zeiss, Munich, Germany

2.1.2. Consumables

Name	**Manufacturer**
1000µl Tips	Starlab GmbH, Ahrensburg, Germany
200µl Tips	Starlab GmbH, Ahrensburg, Germany
0,1-20µl GradanteTips	Starlab GmbH, Ahrensburg, Germany
6- well plates	Greiner Bio-One, Frickenhausen, Germany
12- well plates	Greiner Bio-One, Frickenhausen, Germany
24- well plates	Greiner Bio-One, Frickenhausen, Germany
96 well plates flat bottomed	Greiner Bio-One, Frickenhausen, Germany
96-well fast thermal cycling	Life technologies GmbH, Darmstadt, Germany
Cell culture flasks	Greiner Bio-One, Frickenhausen, Germany
Cellstar tubes (15ml and 50ml)	Greiner Bio-One, Frickenhausen, Germany
Cell strainer 100nm	BD Bioscience, Heidelberg, Germany
Cell strainer (100µm)	BD Bioscience, Heidelberg, Germany
Cyro tubes	Greiner Bio-One, Frickenhausen, Germany
DAKO Pen	Dako Deutschland GmbH, Hamburg, Germany
Disposal bags	Carl Roth, Karlsruhe, Germany
Filter paper	Whatman, Dassel, Germany
FILTER-TIP, 1000 µL	Greiner Bio-One, Frickenhausen, Germany
FILTER TIP, 200 µL	Greiner Bio-One, Frickenhausen, Germany
FILTER TIP, 100 µL	Greiner Bio-One, Frickenhausen, Germany
MICRO CRYSTAL FILTER TIP	Greiner Bio-One, Frickenhausen, Germany
Histosette tissue processing/embedding cassettes	Simport, Hague, Netherlands
Injekt-F (single use injection) 1ml	B.Braun, Melsungen, Germany

Knittel glass cover slips 24*50mm	Iss, Bradford, United Kingdom
Micrscope coverslips	Life technologies GmbH, Darmstadt, Germany
PCR tubes 0.2 ml Flat cap	Greiner Bio-One, Frickenhausen, Germany
Polysine slides	Thermoscientific, Braunschweig, Germany
Safe-lock tubes 2.0 ml	Eppendorf, Hamburg, Germany
Safe-lock tubes 1.5 ml	Eppendorf, Hamburg, Germany
Serological pipette, sterile (5,10,25 ml)	Greiner Bio-One, Frickenhausen, Germany
Superfrostultraplus slides	Thermoscientific, Braunschweig, Germany

2.1.3. Reagents

Name	**Manufacturer**
1-Propanol pure	Applichem, Darmstadt, Germany
2-Propanol pure	Applichem, Darmstadt, Germany
30% Acrylamide	Carl Roth GmbH, Karlsruhe, Germany
4-(Dimethylamino) benzaldehyde	Sigma Aldrich, Steinheim, Germany
Accutase cell detachment solution	Millipor, Darmstadt, Germany
DMSO	Sigma Aldrich, Steinheim, Germany
70% Ethanol	Carl Roth GmbH, Karlsruhe, Germany
Albumin from bovine serum	Sigma Aldrich, Steinheim, Germany
Borsäure	Carl Roth GmbH, Karlsruhe, Germany
Bovine serum albumin(BSA)	Sigma Aldrich, Steinheim, Germany
Bromophenole Blue	Sigma Aldrich, Steinheim, Germany
Chloroform	Applichem, Darmstadt, Germany
Collagenase Type I from Clostridium histolyticum	Sigma Aldrich, Steinheim, Germany
Collagenase from Clostridium histolyticum Type IA	Sigma-Aldrich, Steinheim, Germany
DAPI (4′,6-Diamidine-2′-phenylindole dihydrochloride)	Sigma-Aldrich, Steinheim, Germany
DEPC treated water	Life technologies GmbH, Darmstadt,Germany
EmbryoMax® 0.1% Gelatin Solution	Merck Millipore, Darmstadt, Germany
Ethanol absolute	VWR chemicals, Fontenay-sous-bois, France
Ethylenediaminetetraacetic acid (EDTA)	Sigma Aldrich, Steinheim, Germany
Fetal calf serum(FCS)	Invitrogen, San Diego, USA
Formaldehyde 4%	Carl Roth GmbH, Karlsruhe, Germany
FuGENE® HD Transfection Reagent	Promega, Madison, USA
GelRedTM Nucleic Acid Gel Stain	Biotium (Biotrend), Köln, Germany
Glycerol minimum 99%	Sigma Aldrich, Steinheim, Germany
Hematoxylin	Merck, Darmstadt, Germany
HiPerFect Transfection Reagent	Qiagen, Hilden, Germany

Hydrochloric acid 6N	VWR, Darmstadt, Germany
Hydrogen peroxide 30%	Carl Roth GmbH, Karlsruhe, Germany
Ketamin Hameln 50mg/ml	Hameln pharmaceuticals, Hameln, Germany
L-Hydroxyproline	Merck KGaA, Hessen, Germany
ESGRO (LIF)	Millipor, Darmstadt, Germany
Methanol Technical grade	Applichem, Darmstadt, Germany
OCT compound embedding medium for frozen tissue specimens	Sakura, Torrance, USA
Penicillin/Streptomycin	Gibco, New York, USA
Perchloric acid 70%	Sigma Aldrich, Steinheim, Germany
Picric acid	Sigma Aldrich, Steinheim, Germany
Potassium chloride	Carl Roth GmbH, Karlsruhe, Germany
Potassium phosphate monobasic	Sigma Aldrich, Steinheim, Germany
Ribozol	Ampresco, Solon, USA
Rompun 2%	Bayer vital GmbH, Leverkusen, Germany
Roti®-ImmunoBlock	Carl Roth, Karlsruhe, Germany
Sodium chloride	Carl Roth GmbH, Karlsruhe, Germany
Sodium phosphate dibasic	Carl Roth GmbH, Karlsruhe, Germany
Sodium citrate dihydrate	Fisher- scientific NewJersey, USA
Sodium dodecyl sulfate	Sigma Aldrich, Steinheim, Germany
StarPure Agarose	Starlab GmbH, Hamburg, Germany
SYBR Green PCR mix	Life technologies GmbH, Darmstadt, Germany
Taqman master mix	Life technologies GmbH, Darmstadt, Germany
Trypan Blue	Sigma Aldrich, Steinheim, Germany
Trypsin EDTA	Gibco, New York, USA
TRIS	Carl Roth GmbH, Karlsruhe, Germany
Triton™ X-100	Sigma Aldrich, Steinheim, Germany
Trizma base	Sigma Aldrich, Steinheim, Germany
TSA™ Cyanine 3 System	PerkinElmer
Tween 20	Merck KGaA,Darmstadt, Germany
VECTASTAIN ABC Systems	Vector Laboratories, Inc., Burlingame,USA
Xylene	Applichem, Darmstadt,Germany
Xylene Cyanol FF	Sigma Aldrich, Steinheim, Germany

2.1.4. Kits

Name	**Manufacturer**
Avidin/Biotin Blocking Kit	Vector laboratories, Burlingame, CA USA
DNeasy Blood and Tissue Kit	Qiagen, Hilden, Germany
Expand Long Rang, dNTPack	Roche, Basel, Schweiz

NucleoSpin® Extract II	Macherey-Nagel, Düren, Germany
peqGold Plasmid Miniprep Kit I	Peqlab, Erlangen, Germany
QIAfilter Plasmid Maxi Kit	Qiagen, Hilden, Germany
qScript cDNA SuperMix	Quantabio, Darmstadt, Germany
RNeasy Plus Mini Kit	Qiagen, Hilden, Germany
TSA™ Cyanine 3 System	PerkinElmer, Waltham, USA

2.1.5. Antibodies

Name	**Manufacturer**
anti α-Sma (E184)	Abcam plc, Cambridge, UK
anti-Collagen type III	Home made from D. Schuppan
anti-Mouse Collagen Type I Antibody	Merck Millipore, Darmstadt, Germany

2.1.6. Enzymes

Name	**Manufacturer**
Calf Intestinal Alkaline Phosphatase	Invitrogen, San Diego, USA
EcoRI	Thermo Fisher Scientific, Waltham, USA
Expand Long Range dNTPack	Roche-applied-science, Basel, Schweiz
NheI	NEB, Massachusetts, USA
T4 DNA Ligase	Thermo Fisher Scientific, Waltham, USA
Taq DNA Polymerase	Thermo Fisher Scientific, Waltham, USA
Pfx DNA Polymerase	Invitrogen, Carlsbad, USA
PstI	NEB, Massachusetts, USA
SbfI	NEB, Massachusetts, USA
XhoI	Thermo Fisher Scientific, Waltham, USA

2.1.7. Antibiotics

Name	**Manufacturer**
Ampicillin Natriumsalz	Carl Roth GmbH, Karlsruhe, Germany
Doxycycline hyclate	Sigma Aldrich, Steinheim, Germany
Hygromycin B Roche Applied Science	Roche Applied Science, Basel, Schweiz
Neomycin trisulfate salt hydrate	Sigma Aldrich, Steinheim, Germany
Spectinomycin dihydrochloride pentahydrate	Sigma Aldrich, Steinheim, Germany

2.1.8. General buffers, solutions and media

Acidified water	Glacial acetic acid 5ml dd H_2O 1000 ml
Annealing buffer 10X stock solution	1M TRIS pH 7.5 (500µl) 10M NaCl (500µl) 0.5M Na2EDTA (100µl) to 5ml dH2O
Antigen Unmasking Citrate buffer	2,94g sodium citrate trisodium salt dehydrate to 1L d H_2O Adjust pH to 6.0
Carbon tetrachloride (CCL4) working solutions	8.75% solution: 4.38ml Carbon tetrachloride (CCL4) to 50ml mineral oil 17.5% solution: 8.75ml Carbon tetrachloride (CCL4) to 50ml mineral oil
Citric Acetate buffer	5% citric acid (5 g) 7.24% sodium acetate (7.24 g) 3.4% NaOH (3.4g) 1.2% glacial acetic acid (1.2 ml) dissolve into 100 ml dH_2O adjust pH to 6.0.
Chloramine T	32 ml citric acetate buffer pH 6.0 4 ml distilled water 4 ml n-propanol 564 mg chloramine T hydrate Shake well to mix, heated around 50°C, then RT slightly in water bath to dissolve
Gel loading buffer (x6)	0,25g Bromophenol Blue, 0,25g Xylene Cyanol FF, 30 ml Glycerol to 100ml dH2O
Ehrlich's reagent	7.9 ml n-propanol 3.31 ml 70% perchloric acid 1.91mg 4-Dimethylaminobenyaldehyde Recommend to be prepared freshly just before. Cool down before experiment.
HEK 293 cells media	450 ml DMEM, FBS 50 ml, Penicillin/Streptomycin 2.5 ml
Mitomycin C	2 mg Mitomycin C, 2ml H2O
Mouse ear fibroblasts media	450 ml DMEM, FBS 50 ml, Penicillin/Streptomycin 7.5 ml
Na2EDTA 0.5M solution	14.6g Na2EDTA into 100ml d H2O Adjust pH to 8.0 with NaOH
NIH/3T3 cells media	450 ml DMEM, FBS 50 ml,

	Penicillin/Streptomycin 2.5 ml
Phosphate Buffered Saline(PBS) 10X stock solution	137mM NaCl (80g) 2.mM KCl (2g) 10 mM Na_2 HPO_4 (14.4g) 1.8 mM KH_2PO_4 (2.4g) to 1L dH_2O Adjust pH to 7.4 with HCl
Tris Buffered Saline(TBS) 10X stock solution	24,2g Trizma Base (C4H11NO3) 80g Sodium chloride (NaCl) to 1L Adjust pH to 7.6 with HCl
PBST 1X	100 ml 10X PBS stock solution 900 ml d H_2O, 1ml Tween 20
TBE 10X stock solution	890 mM TRIS Base (108g) 890 mM Boric Acid (55g) 20 mM 0.5M Na2EDTA (20mL) to 1L dH2O Adjust pH to 8.0 with NaOH
TBST 1X	100 ml 10X TBS stock solution 900 ml d H_2O, 1ml Tween 20
Sodium dodecyl sulfate10%	10g SDS into 100ml d H_2O
0.1% Sirius Red solution	Sirius Red 0.5 g saturated picric acid 500 ml

2.1.9. Eukaryotic cell lines and bacterial cells

Name	**Manufacturer**
KH2 ES cells	Thermo Scientific Open Biosystems, part of Thermo Fisher Scientific, Waltham, USA
DR4 MEF Feeder Cells, P2, untreated	Applied StemCell, Milpitas, USA
HEK cells	Prof.A.Reske-Kunz Lab, University Medical Center of the Johannes Gutenberg-University Mainz, Germany
NIH 3T3	Prof.A.Reske-Kunz Lab, University Medical Center of the Johannes Gutenberg-University Mainz, Germany
One Shot Top10 Chemically Competent E.coli	Invitrogen, Carlsbad, USA

2.1.10. Media

Name	**Manufacturer**
DMEM	Gibco, New York, USA
ESGRO-2i Medium	Merck Millipore, Darmstadt, Germany
LB-Agar (Luria/Miller)	Carl Roth GmbH, Karlsruhe, Germany

LB-Medium (Luria/Miller)	Carl Roth GmbH, Karlsruhe, Germany
ESGRO Complete PLUS Clonal Grade Medium	Merck Millipore, Darmstadt, Germany

2.1.11. Amino acids and nucleotides

Name	**Manufacturer**
AllStars Cell Death Control siRNA	Qiagen, Hilden, Germany
AllStars Negative Controls siRNA	Qiagen, Hilden, Germany
MAPK1 siRNA	Qiagen, Hilden, Germany
dNTP Set	Thermo Fisher Scientific, Waltham, USA
GeneRuler 1kb DNA Ladder	Thermo Fisher Scientific, Waltham, USA
GeneRuler 100pb DNA Ladder	Thermo Fisher Scientific, Waltham, USA
CompoZr Custom Zinc Finger Nucleases, Target Gene: Col1a1a PZFN1, PZFN2, ZFN mRNA	Sigma Aldrich, St.Louis, USA
ColA1_Target_Vector	Life Technologies, Carlsbad, USA
pCAGGS-flpE-puro vector	Addgene, Cambridge, UK
pCol-TGM vector	Prof.Lowe Lab, Memorial Sloan Kettering Cancer Center, New York, USA
pUHrT 62-1 vector	H. Bujard, ZMBH, Heidelberg University, Germany

2.1.12. Top eight DSIR-scoring 21-mer siRNA sequence predictions that pass the Sensor criteria

N	**Name**	**Target sequence (5'-3')**	**Sense strand (5'-3')**	**Antisense strand (5'-3')**
1	Col1a1.1417	CCCGGTGCTACTGGAGTTCAA	CGGUGCUACUGGAGUUCAAUU	UUGAACUCCAGUAGCACCGGG
2	Col1a1.69	CGCAAAGAGTCTACATGTCTA	CAAAGAGUCUACAUGUCUAUU	UAGACAUGUAGACUCUUUGCG
3	Col1a1.2551	CCTGGTGATACTGGTGTTAAA	UGGUGAUACUGGUGUUAAAUU	UUUAACACCAGUAUCACCAGG
4	Col1a1.236	CCGAGGTATGCTTGATCTGTA	GAGGUAUGCUUGAUCUGUAUU	UACAGAUCAAGCAUACCUCGG
5	Col1a1.359	CGGAAGAATACGTATCACCAA	GAAGAAUACGUAUCACCAAUU	UUGGUGAUACGUAUUCUUCCG
6	Col1a1.1351	CCCAAGGGTAACAGTGGTGAA	CAAGGGUAACAGUGGUGAAUU	UUCACCACUGUUACCCUUGGG
7	Col1a1.358	CCGGAAGAATACGTATCACCA	GGAAGAAUACGUAUCACCAUU	UGGUGAUACGUAUUCUUCCGG
8	Col1a1.373	TCACCAAACTCAGAAGATGTA	ACCAAACUCAGAAGAUGUAUU	UACAUCUUCUGAGUUUGGUGA

2.1.13. Custom siRNAs mimics (Qiagen, Hilden, Germany)

N	Name	View
1	Col1a1.1417	5'-CGGUGCUACUGGAGUUCAAd(TT)-3' ||||||||||||||||||| 3'-d(GG)GCCACGAUGACCUCAAGUU-5'
2	Col1a1.69	5'-CAAAGAGUCUACAUGUCUAd(TT)-3' ||||||||||||||||||| 3'-d(GC)GUUUCUCAGAUGUACAGAU-5'
3	Col1a1.2551	5'-UGGUGAUACUGGUGUUAAAd(TT)-3' ||||||||||||||||||| 3'-d(GG)ACCACUAUGACCACAAUUU-5'
4	Col1a1.236	5'-GAGGUAUGCUUGAUCUGUAd(TT)-3' ||||||||||||||||||| 3'-d(GG)CUCCAUACGAACUAGACAU-5
5	Col1a1.359	5'-GAAGAAUACGUAUCACCAAd(TT)-3' ||||||||||||||||||| 3'-d(GC)CUUCUUAUGCAUAGUGGUU-5'
6	Col1a1.1351	5'-CAAGGGUAACAGUGGUGAAd(TT)-3' ||||||||||||||||||| 3'-d(GG)GUUCCCAUUGUCACCACUU-5'
7	Col1a1.358	5'-GGAAGAAUACGUAUCACCAd(TT)-3' ||||||||||||||||||| 3'-d(GG)CCUUCUUAUGCAUAGUGGU-5'
8	Col1a1.373	5'-ACCAAACUCAGAAGAUGUAd(TT)-3' ||||||||||||||||||| 3'-d(AG)UGGUUUGAGUCUUCUACAU-5'

2.1.14. Animals

Wild-type mouse strains: C57Bl6/J, C57Bl6 Albino, CD1, FVB/N (f) x C57Bl6/J (m) F1

Mouse Line	Short description of genetic change	Reference
B6.Cg-Gt(ROSA)26Sor$^{tm1(rtTA*M2)Jae}$/J	Expression of an optimized form of reverse tetracycline controlled transactivator (rtTA-M2) downstream of the Gt(ROSA)26Sor promoter	Hochedlinger K, Yamada Y, Beard C, Jaenisch R. Ectopic expression of Oct-4 blocks progenitor-cell differentiation and causes dysplasia in epithelial tissues. Cell 2005; 121(49):465-77
Col1a1-ZFN-TGM-shRNA-4/Line1	The model has been generated via ZFN microinjections; contains	This work

	cassette TRE-EGFP-shRNA4	
Col1a1-RMCE-TGM-shRNA-7/Clone3	The model has been generated via modified (RMCE) KH2 ES cells; contains cassette TRE-EGFP-shRNA7	This work
Col1a1-RMCE-TGM-shRNA-7/Clone4	The model has been generated via modified (RMCE) KH2 ES cells; contains cassette TRE-EGFP-shRNA7	This work

2.1.15. Primers and oligos

Name	Use	Forward primer (5'-3')	Reverse primer (5'-3')
Col1a1.236(4)	Linker cloning	TACAATACTCGAGAAGGTATATTGCTGTTGACAGTGAGCGACCGAGGTATGCTTGATCTGTATAGTGAAGCCACAGATGTATACAGATCAAGCATACCTCGGGTGCCTACTGCCTCGGAATTCTTCTAAGT	ACTTAGAAGAATTCCGAGGCAGTAGGCACCCGAGGTATGCTTGATCTGTATACATCTGTGGCTTCACTATACAGATCAAGCATACCTCGGTCGCTCACTGTCAACAGCAATATACCTTCTCGAGTATTGTA
Col1a1.358(7)	Linker cloning	TACAATACTCGAGAAGGTATATTGCTGTTGACAGTGAGCGACCGGAAGAATACGTATCACCATAGTGAAGCCACAGATGTATGGTGATACGTATTCTTCCGGGTGCCTACTGCCTCGGAATTCTTCTAAGT	ACTTAGAAGAATTCCGAGGCAGTAGGCACCCGGAAGAATACGTATCACCATACATCTGTGGCTTCACTATGGTGATACGTATTCTTCCGGTCGCTCACTGTCAACAGCAATATACCTTCTCGAGTATTGTA
miR30seq	Sequencing	TGTTTGAATGAGGCTTCAGTAC	-
ColA1	Sequencing	AATCATCCCAGGTGCACAGCATTGCGG	CTTTGAGGGCTCATGAACCTCCCAGG
SAdpA	Sequencing	-	ATCAAGGAAACCCTGGACTACTGCG
TGM (ZFN)	Sequencing	CTGCCTATCAGAAGGTGGTG	GAGTCGCAGATCCAGACATG
Col1a1 (ZFN)	Sequencing	ACAGCAGACTGGAAACATCG	GACCTCTCTCACCATCTTGC
GFP	Genotyping	TTCAAGGACGACGGCAACTACAAG	CGGCGGCGGTCACGAACTCC
rtTA	Genotyping	CCATGTCTAGACTGGACAAGA	CTCCAGGCCACATATGATTAG
Hygro_rev	Sequencing	-	TGTAGGAGGGCGTGGATATGT

2.1.16. Real-time PCR primer for marker analysis

Target gene	Forward primer (5'-3')	TaqMan Probe	Reverse primer (5'-3')
α-Sma	ACAGCCCTCGCACCCA	CAAGATCATTGCCCCTCCAGAACGC	GCCACCGATCCAGACAGAGT
Col1a1	TCCGGCTCCTGCTCCTCTTA	TTCTTGGCCATGCGTCAGGAGGG	GTATGCAGCTGACTTCAGGGATGT

Col3a1	AATGGTGGCTTTCAGTTCAGCT	TGGAAAGAAGTCTGAGGAAGGCCAGCTG	TGTAATGTTCTGGGAGGCCC
Tgfß1	AGAGGTCACCCGCGTGCTAA	ACCGCAACAACGCCATCTATGAGAAAACCA	TCCCGAATGTCTGACGTATTGA
Timp-1	TCCTCTTGTTGCTATCACTGATAGCTT	TTCTGCAACTCGGACCTGGTCATAAGG	CGCTGGTATAAGGTGGTCTCGTT
Mmp13	GGAAGACCCTCTTCTTCTCT	TCTGGTTAACATCATCATAACTCCACACGT	TCATAGACAGCATCTACTTTGTT
TNF-α	CTCAGCCTCTTCTCATTC	CACCACGCTCTTCTGTCTACTGA	GCCATAGAACTGATGAGA
IFN-γ	CAGCAACAGCAAGGCGAAA	TCAAACTTGGCAATACTCATGAATGCATCCT	CTGGACCTGTGGGTTGTTGAC
GapDH TaqMan,	GAAGGTGAAGGTCGGAGT	CAAGCTTCCCGTTCTCAGCC	GAAGATGGTGATGGGATTTC
GapDH SYBR	AGGTCGGTGTGAACGGATTTG		GGGGTCGTTGATGGCAACA
MMP-3 SYBR	ACATGGAGACTTTGTCCCTTTTG		TTGGCTGAGTGGTAGAGTCCC
MMP-8 SYBR	TCTTCCTCCACACACAGCTTG		CTGCAACCATCGTGGCATTC
MMP-9 SYBR	CTGGACAGCCAGACACTAAAG		CTCGCGGCAAGTCTTCAGAG
IL1b SYBR	AAATACCTGTGGCCTTGGGC		CTTGGGATCCACACTCTCCAG
CD68 SYBR	ACCGCCATGTAGTCCAGGTA		ATCCCCACCTGTCTCTCTCA
Col4a1 SYBR	CACTGCTGAAAGGGGAGAGA		GTGGTCCAGTAAATCCCGGA
Col5a1 SYBR	GCTGTACCCTGAGTCTGGTT		TGGATGCCCTGCTCATTGTA
Col6a1 SYBR	TCCGACCAGCTCAATGTCAT		TGGTTTCGAAGTTGTGGCTG
Col6a3 SYBR	GCAATGCATGAGACCCTCTG		ACTCAAGGCCCTTCTGACTC
GFP SYBR	ACGACGGCAACTACAAGACC		CTTGATGCCGTTCTTCTGCT
MAPK1 SYBR	Qiagen, Hilden, Germany Cat. no.QT01050056		

2.2. Methods

2.2.1. Molecular cloning

2.2.1.1. DNA digestion with type II restriction endonuclease

DNA was digested with the suggested amount of type II restriction endonuclease depending on the company. The standard for a restriction digest is normally 1 unit of the type II restriction endonuclease digests for 1 µg of DNA at 37°C for 1-3 hour. Normal volumes of digestion were 30-50 µl.

2.2.1.2. 5’ Dephosphorylation with calf-intestinal-phosphatase (CIP) reaction

Alkaline phosphatase catalyzes the removal of 5’ phosphate groups from DNA. In order to prevent the re-ligation of vectors, the 5’ phosphate group of the vector was removed using CIP prior to ligation. 5.0 µg of previously digested vector DNA was dephosphorylated at 37°C for 30 min in a 50 µl reaction containing of 1U of CIP and immediately was put on a placed for the extraction.

2.2.1.3. Cloning from oligonucleotides

For the generation of new multiple cloning sequences in the pCol-TGM, biomers.net GmbH synthesized oligonucleotides with the desired proper order. The oligonucleotides were allowed to anneal with each other by placing the sense and the anti-sense in the annealing buffer. The reaction was then placed in the thermocycler for the annealing program.

Thermocycler program

Step	Number of cycle	Temperature	Time
1	1	95°C	5 min
2	70	95°C (-1°C/cycle)	1 min
3		4°	HOLD

After purification and restriction with appropriated enzymes the annealed products were used to ligate into the cut dephosphorylated vector plasmid.

2.2.1.4. DNA ligation

Digested DNA fragments were ligated with T4 ligase in a 10µl volume overnight at 4°C. The vector: insert concentration was in a molar ratio of 1:3.

X µl of vector-DNA
x µl of DNA fragment
1 µl of T4 DNA Ligase Buffer (10x)
1 µl of T4 DNA Ligase (5U)
Fill to a final volume of 10 µl with H2O

2.2.1.5 Transformation of bacteria

An aliquot containing 50µl of the competent cells E.coli One Shot Top10 were thawed from –80°C on ice. 3µl of the ligation mix was placed into the tube and then placed on ice for 30 minutes to allow the bacteria to pick up the plasmid. The tube containing the bacteria and the ligation mix were heat shocked in a hot water bath set to 42°C for 30 seconds. The mixture was placed on ice for 2 minutes. After the ice incubation, 250µl of warmed SOC media (a rich media used primarily in the recovery step of Escherichia coli competent cell transformations) was added to the bacteria/ligation mixture and shaken horizontally at 37°C for 1 hour at 225 rpm in the shaking incubator. During this period LB agar plates were prepared for plating out the bacteria. The bacteria, was then plated out at different concentrations. The plates were placed overnight at 37°C and on the next day bacterial clones were picked for further processing of the plasmid.

2.2.2 Preparation and analyses of DNA

2.2.2.1 Mini-preparation of plasmid DNA

For the preparation of the plasmid from bacteria, a kit from Peqlab was used. Clones were picked from bacterial plates that were grown overnight. The clones were then grown overnight in 5 ml of LB media containing appropriate antibiotics. On the next day the bacterial suspension was centrifuged at 10.000xg for 1 minute in 2.0 ml tubes and the bacterial pellet was resuspended in 250µl of buffer I/RNase A. 250 ml buffer II was added to lyse the cells, mixed gently and 350 ml buffer III was added to neutralize the mixture. The mixture was centrifuged at 10.000xg for 10 minutes to separate the

cell debris. After this step the supernatant was taken and placed on a special Perfect Bind DNA Column trap to isolate the plasmid DNA. The column was then washed with washing buffers that were provided in the kit and centrifuged at 10.000xg for 2 minutes to dry the DNA. Then the plasmid DNA was eluted with elution buffer.

2.2.2.2 Maxi-preparation of plasmid DNA (Qiagen kit)

The Qiagen plasmid maxi-kit method uses an alkaline lysis. A 200ml bacterial suspension was grown to high density overnight in 37°C incubator with shaking at 225 rpm. The resultant high density bacterial suspension was centrifuged at 4000rpm for 20 min and the pellet was resuspended in 20 ml of buffer 1 (resuspension buffer). To this suspension 20 ml of buffer P2 (lysis buffer) was added, mixed gently and incubated at RT for 5 min. Then 20 ml of prechilled buffer P3 (neutralization buffer) was added and incubated at 4°C for 20 min to neutralize the reaction. To remove unwanted bacterial debris the mix was passed through glass wool using QIAfilter Cartridge. The precleared DNA solution was then applied to an equilibrated QIAGEN-tip 500 with 20 ml of QBT buffer (equilibration buffer). At this point the DNA was bound to the resin by gravitational pull. The QIAGEN-tip resin was cleaned of any remaining debris by washing twice with 30 ml buffer QC (washing buffer). Plasmid DNA was eluted with 15 ml buffer QF (elution buffer). The flow through contained the DNA in solution, to allow for precipitation of the DNA 0.7 volumes of isopropanol (10.5 ml) was added and the solution centrifuged for a further 10,000 rpm for 1 hour at 4°C. The DNA pellet was washed with 70% ethanol and followed by air-drying at RT and resuspended in ddH_2O.

2.2.2.3 Preparation of genomic DNA from tissue

Genomic DNA was prepared out of 0.3 cm fragments of mouse tails. DNeasy Blood and Tissue Kit from Qiagen was used to extract the tails. Tails were digested overnight at 56°C in the ALT buffer (tissue lysis buffer) with proteinase K. On the next day 200 µl of AL buffer (lysis buffer) and 200 µl of 100% ethanol were added. The mixture was placed over a DNeasy Mini spin column and centrifuged at 6.000xg for 1 minute. The column was then washed with washing buffers that were provided in the kit. Then the genomic DNA was eluted with elution AE buffer. After the tails were ready, they were stored at 4°C. For PCR use 1-3µl of the genomic DNA was used.

2.2.2.4. Measuring DNA concentration

DNA concentration was assessed by 260/280 nm OD measurements with the help of TECAN infinite M 200Pro using NanoQuant Plate.

2.2.2.5. Agarose gel electrophoresis of DNA

For the visualization of DNA fragments between an agarose gel between 1% and 2% was used. The agarose was boiled in 1 X TAE buffer to allow it to dissolve. GelRed 10,000X stock reagent was diluted into the molten agarose gel solution at 1: 10,000 and mixed thoroughly. The mixture was poured into a gel chamber containing a comb for the DNA pockets to polymerize. After the agarose gel polymerized, it was submerged in a chamber containing 1 X TAE buffer. Before loading the probes, 0.15 volume of gel loading buffer was added. The probes were then loaded into the agarose pockets. The DNA fragments were separated in an electric field at 100V, 400mA, and DNA was visualized using the ChemiDoc™ XRS+ System under UV light. Molecular weight marker was loaded next to the DNA probe to determine proper sizes, and a photograph was taken to document the results.

2.2.2.6. Elution of DNA from agarose

The DNA bands on the agarose gel were as visualized under a UV light, and the desired DNA fragment was cut out with a disposable scalpel. The fragment was placed into an Eppendorf tube and incubated at 52°C for 20 minutes with 2x NT buffer. The sample was vortexed every 2-3 minutes until the gel slice was completely dissolved. Then the sample was loaded into a NucleoSpin® Extract II column and centrifuged at 11.000xg for 1 minute. The silica matrix was washed two times with 700 µl NT3 buffer, dried by centrifugation at 11.000xg for 2 minutes and the DNA was eluted with 25 µl NE buffer.

2.2.2.7. Polymerase chain reaction (PCR)

PCR is the method of choice for in vitro amplification of DNA (50), utilizing oligonucleotides (primers), to amplify particular DNA sequences. It is basically a cyclic reaction chain consisting of three steps: 1. denaturation of dsDNA, 2. primer annealing, 3. synthesis of new DNA strands by DNA polymerase (primer extension).

The standard PCR protocol for a final volume of 25 µl was:

Reaction mix:

2.5 µl 10x PCR buffer ($MgCl_2$), 1 µl dNTP mix (25 mM each dNTP), 1 µl sense primer (10 pM), 1 µl anti-sense primer (10 pM), 3-6µl $MgCl_2$, (25 mM), 1-3 µl template DNA, 0.5 µl Taq polymerase (2.5 U), made up to 25 µl with ddH_2O.

The temperature protocol was:

Step	Temperature	Time	Cycle
Initial denaturation	94°C	4 min	1x
Denaturation Annealing Elongation	94°C 60°C 72°C	1 min 1 min 1 min	30x
Final elongation	72°C	7 min	1x
Cooling	4°C	∞	

The PCR product was then visualized using gel electrophoresis as described in section 2.2.2.5 (Agarose gel electrophoresis of DNA).

2.2.2.8 Long rang polymerase chain reaction

Long Rang PCR was used to efficiently amplify large genomic DNA fragments up to 1-2 kb with a threefold higher fidelity then Taq DNA polymerase for the following DNA sequencing.

The Long Rang PCR protocol for a final volume of 50 µl was:
Reaction mix:
10 µl 5x PCR buffer with $MgCl_2$, 2.5 µl dNTP mix (10 mM each dNTP), 2 µl sense primer (10 pM), 2 µl anti-sense primer (10 pM), 2-5 µl 100% DMSO, 1 µl template DNA, 0.7 µl Expand Long Rang Enzyme mix (3.5 U), made up to 50 µl with ddH_2O.

The temperature protocol was:

Step	Temperature	Time	Cycle
Initial denaturation	92°C	2 min	1x
Denaturation Annealing Elongation	92°C 45 to 65°C 68°C	10 s 15 s 60s/kb	10x
Denaturation Annealing Elongation	92°C 45 to 65°C 68°C	10 s 15 s 60s/kb + 20 s cycle elongation for each successive cycle	25x
Final elongation	68°C	7 min	1x
Cooling	8°C	∞	

The PCR product was then visualized using gel electrophoresis as described in section 2.2.2.5.

2.2.2.9. DNA sequencing

DNA sequencing analysis was done by StarSEQ (Mainz) using an ABI 3730 capillary sequencer.

2.2.3. Preparation and analyses of RNA

2.2.3.1. RNA extraction with TRIzol

Total liver RNA was isolated using TRIzol reagent (Invitrogen). 1 ml TRIzol reagent was added to each sample. The samples were then lysed using a TissueLyser II (Qiagen). 200 µl chloroform and 700 µl TRIzol reagent were added to 300 µl of the homogenate, vigorously mixed and centrifuged at 12.000xg for 15 minutes at 4°C. Three phases were separated: the lower red phenol-chloroform layer, the interphase and the colorless upper RNA containing aqueous phase. For RNA precipitation 200 µl of the aqueous phase was transferred to a new tube, containing 500 µl isopropanol and 200 µl DEPC-water, mixed, incubated for 10 minutes and centrifuged at 12.000xg

for 10 minutes at 4°C. The RNA pellet was washed two times with 70% ethanol, air dried and dissolved in 100-200 µl DEPC-water.

2.2.3.2. RNA isolation from mouse ear fibroblasts (MEF)

MEFs were grown to 80% confluence on 60 mm cell culture plates, washed with PBS and lysed with 350 µl RTL buffer, placed in a gDNA Eliminator spin column (RNeasy Plus Mini Kit, Qiagen) and centrifuged at 10.000xg for 1 minute. 350 µl 70% ethanol was added to the flow-through and mixed by pipetting. Than the mixture was transferred to an RNeasy spin column and column and centrifuged at 10.000xg for 1 minute. The matrix with bound RNA was washed once with 700 RW1 buffer and two times with 500 µl RPE buffer. RNA was eluted with 40 µl RNase-free water.

2.2.3.3. Quantitative real-time PCR

cDNA synthesis was performed with the qScript cDNA SuperMix kit (Quantabio, Darmstadt, Germany). TaqMan probes and primers were designed using the Primer Express software (Perkin Elmer, Foster City, CA). All sequences are summarized in 2.1.15. qPCR reactions were run on an A&B step one plus real time PCR thermocycler (Applied Biosystems). RNA levels were normalized against the transcription levels of GAPDH using the relative standard curve method (Sequence Detection Systems software version 2.2.2 (Applied Biosystems).

2.2.4. Cell Culture Methods

2.2.4.1. Transfection of NIH/3T3 cells with siRNA

Shortly before transfection $1.5x10^5$ cells were seeded per 60 mm culture dish in 4000µl DMEM culture medium, containing 10% FCS and 1% Penicillin/Streptomycin antibiotics and incubated overnight under normal growth conditions (37°C an 5 % CO_2). 1 µg siRNA was diluted in 100µl culture medium without serum and 20 µl HiPerFect Transfection Reagent (Qiagen) was added and vortexed (final siRNA concentration of 20nM after adding the complex to cells). Then the mixture was incubated for 10 min at room temperature to allow the formation of transfection complex. The complex was added drop-wise onto the cells. After 72 hours the cells were harvested for RT-PCR.

2.2.4.2. Mouse ear fibroblasts culture

Mouse ears were cut, rinse briefly (1 min) in 70% EtOH, washed with PBS, cut into small pieces with a clean scalpel and put in a 6-well-plate covered the with 2 ml of DMEM containing 20% FCS, 3% Penicillin/Streptomycin and 1 mg/ml collagenase Type I. After overnight incubation under normal growth conditions (37°C an 5 % CO2) the solution containing tissue fragments was pipetted up and down to break clumps. Then it was transferred into a 15ml tube containing 10 ml medium and centrifuged at 1.500 x rpm for 5 min. The cell pellet was suspended in 2 mL medium and seeded in a 6-well-plate. After 24 hours the cells were washed with PBS ant the medium was changed. After one week cultivation the cells were used for further experiments.

2.2.4.3. Transfection of HEK 293 cells with modified pCol-TGM vector

$1.5x10^5$ HEK 293 cells were seeded per 60 mm dish in 1000µl DMEM culture medium without serum and antibiotics. 8 µl FuGENE® HD Transfection Reagent (Pomega, Madison, USA), 2 µg modified pCol-TGM vector and 2 µg pUHrT 62-1 vector were mixed with 100 µl DMEM culture medium without serum and antibiotics. The mixture was incubated for 10 min at room temperature and transferred to the cells. After 4 hours 1 ml DMEM culture medium, containing 10% FCS and 1% Penicillin/Streptomycin antibiotics was added. 1µg/ml doxycycline was added to experimental wells. After four days the cells expressing GFP were visualized with a Olympus Motorized Inverted Research Microscope Model IX81.

2.2.4.4. DR4 Mouse embryonic fibroblasts feeder cells culture

Mouse Embryonic Fibroblasts (MEF) (Applied StemCell, Milpitas, USA) (51) were grown to 80% confluence on 100 mm dishes in 10 ml DMEM medium with 10% FCS and 1% Penicillin/Streptomycin. For passaging cells were washed with PBS 3 times. 2 ml of trypsin was added to the dish, which was then placed at 37°C for 2 min. Trypsin activity was stopped by adding 2 x the volume of medium. The cells were then centrifuged at 1000 rpm for 10 min, resuspended and expanded at a 1:4 ratio. For freezing, cells were counted and concentrated to 1×10^7 cells/ml, to be stored in liquid N_2.

2.2.4.5. Preparation of Mitomycin C treated MEF for ES cell plating

1 cryo tube was thawed and 5 x 10^6 MEF feeder cells were plated on four 10 cm tissue culture dishes. The cells were expanded after 3-4 days of culture. The embryonic feeders were treated with Mitomycin C (10 µg/ml) in the medium 2 hours, and aliquots were then frozen (5 x 10^6cells/ml). The cells were thawed and plated for one week before plating ES cells on top.

2.2.4.6. Growing, passaging, and freezing of KH2 embryonic stem (ES) cells

ES cells were seeded onto MEFs that were treated with mitomycin C in ESGRO Complete PLUS Clonal Grade Medium at high density. After a maxim of three day in culture the ES cells reached 80% subconfluence. The ES cells were then expanded at 1:3-5 ratio. Every day the medium was changed. For freezing, the cells were plated onto a 24 well plate in freezing medium. The dish was then placed on ice and 250 µl of cold freezing medium was added. The plate was then wrapped tightly with parafilm and placed at –20°C for 2 hours, to be stored for longer periods of time at –80°C.

2.2.4.7. Electroporation and antibiotic selection of KH2 ES cells

1-2 hours before the electroporation, the medium of the ES cells (70% confluent) was changed, before removing the ES cells (passage 12) from the fibroblasts. The ES cells and the fibroblasts were first washed with PBS. Accutase was added and the cells were suspended into a single cell suspension. The cell suspension was centrifuged at 1000 rpms for 5 min, the supernatant was removed and the cells were washed with PBS and centrifuged at 1000 rpms for another 5 min. Then the cells were suspended in 1 ml fresh ES cell medium, and 25 µg (2 mg/ml) of modified pCol-TGM containing the desired DNA construct, 50 µg pCAGGS-flpE-puro vector and 5x10^6 (in 900 µl PBS) KH2 ES cells were put in a 1.5 ml microcentrifuge tube, mixed gently, transferred to an ice-cold 0.4-cm cuvette and incubated on ice for 5 min. The mixture was electroporated with one pulse at 250V (500 µF) in a Bio-Rad Gene Pulser and the cuvette was immediately returned to ice for 10 min. After that 1 ml of ES cell medium was added to the cuvette, mixed gently and transferred to a 10-cm cell culture plate containing MEF feeders and 8 ml of ES cell medium. 48 hours after the electroporation the selection of the positive ES cell clones was started by adding fresh medium containing 140µg/ml of hygromycin B. The cells were selected in hygromycin B – containing medium for 12

days, refreshing the medium every day. Clones were then picked, starting day 12 of selection.

2.2.4.8. Isolation and analysis of Hygromycin B resistant ES cell clones

In a time period between 10-12 days of selecting ES cells with Hygromycin B, macroscopic colonies could be seen on the dish. The colonies were washed 3 times with PBS and then the final wash was done in PBS containing Penillin/Streptomycin. The cells were kept in this final buffer for picking. The ES colonies were picked under a microscope with a yellow tip of a Gilson pipette from the bottom of the dish in 10ml of PBS by scraping the colony with the tip. The colony that was picked was then dissociated in a round bottom 96 well dish containing 15µl of PBS/Accutase mixture (5µl/10µl) per well. The colony was checked to make sure it was dissociated under the microscope. Once a clone was isolated, it was expanded in wells of a flat bottom 24 well dish containing ES cell medium. Once the cell density in these wells had reached 80% the ES cell clone was further expanded in a 6 well dish. At this point 1/3 of the positive clones were frozen for back up. From the 6 well dish the ES cell clones were used for DNA isolation and Long Rang PCR.

2.2.5. Microinjections to generate transgenic mice

2.2.5.1. Injection of blastocysts and embryo transfer

To prepare ES cell clones for microinjection, the MEFs were first separated from the ES cell clone. This was done as described in the *electroporation section* of Material and Methods. Suspension of ES cells and MEFs were plated onto previously gelatinized tissue culture dishes for 45 min. Since the MEF require only a short time to adhere, this method is a quick and easy way of getting the ES cells MEF free. Then not attached ES cells collected from the plate with normal medium and gently centrifuged at 1000 rpm for 5 min. The pellet was resuspended in ES culture medium at a concentration of (1 X 10^3 cells/ml). 10-15 ES cells were injected into one blastocyst of B6 albino mice line (3.5 days post coitus - dpc). The blastocysts were then transferred to the oviduct pseudo pregnant CD1 foster mouse (0,5 dpc). The KH2 ES cells originate from a C57BL/6 x129/SV F1 background. The injection and embryo transfer were performed by Dr. Leonid Eshkind and Svetlana Ohngemach, Transgenic

Facility Mainz (TFM) at the University Medical Center of the Johannes Gutenberg University.

2.2.5.2. Preparation of DNA injection aliquots and oocyte injection

The plasmid DNA for oocyte microinjection was prepared using the QIAfilter Plasmid Maxi Kit (Qiagen, Hilden, Germany). For the generation of knock-in mutants using ZFNs, injection aliquots with 2.5 ng/µl of each ZFN mRNA and 8 ng/µl targeting circular plasmid DNA were prepared. For the preparation of the mix ZFNs mRNA/ plasmid DNA solution, the purified mRNA and plasmid DNA sample were mixed and the concentration was adjusted using injection buffer (10mM TRIS-HCl pH 7.4, 0.1mM EDTA) to prepare single-use aliquots of 50 µl for each day of microinjection. The aliquots were stored at −80 °C until usage. For microinjections, zygotes were obtained by mating of C57BL/6J males with super-ovulated FVB/N females. Zygotes were microinjected into one pronuclear. Injected zygotes were transferred into the oviducts of pseudo-pregnant CD1 female mice to obtain live pups. Mice were handled according to institutional guidelines and all experiments were performed under registration and ethical approvement (Registration No. 23 177-07/G12-1-001) by the Landesuntersuchungsamt of Rheinland Pfalz (Mainzer Str. 112, 56068 Koblenz, Germany). Mice were housed in individually ventilated cages (IVC, Tecniplast) in a specific pathogen-free facility on 12 h light/dark cycles with ad libitum access to food and water. Injections and transfers were performed by Dr. Leonid Eshkind and Svetlana Ohngemach, Transgenic Facility Mainz (TFM) at the University Medical Center of the Johannes Gutenberg University.

2.2.6. Histological and immunohistochemical methods

2.2.6.1. Immunofluorescence staining with anti-collagen type I antibodies

Biopsies were embedded in OCT (Sakura, Torrance, USA), 7 micrometer sections were prepared using Leica CM1950 Cryostat (Leica, Wetzlar, Germany) and fixed in 4% formaldehyde for 20 min. Endogenous peroxidase was quenched using 3% H_2O_2 in deionized water. After washing sections were blocked with avidin and incubated with biotin (Vector laboratories, Burlingame, CA USA). Sections blocked with Roti®-ImmunoBlock (Carl Roth, Karlsruhe, Germany) and incubated with rabbit anti-mouse collagen type I antibodies (1:1000, Merck Millipore, Darmstadt, Germany) diluted in

TBS Tween 0.05% (TBST) +2% BSA overnight at 4°C. After washing with TBST, biotinylated secondary antibody (1:1000, Dianova) was added for 30 minutes at room temperature followed by three washes in TBST. Sections were revealed using the TSA™ Cyanine 3 System (PerkinElmer, Waltham, USA). Tissues were visualized in a Zeiss Axio Imager AX10 Microscope with the appropriate filters. Representative images were taken with an AxioCamMRc 5 camera. A series of images covering >90% of the total tissue section were generated at uniform settings of magnification, light, and exposure time. Quantitative analysis was performed using Image J software.

2.2.6.2. Immunofluorescence staining anti-procollagen type III antibodies

Sections as prepared above were stained with rabbit anti-mouse procollagen type III antibodies (1:800, produced in-house) diluted in 1X PBS plus 1% BSA/ 0.3% Triton™ X-100 and incubated overnight at 4 °C. After washing three times in PBS, sections were incubated with Alexa Fluor 488-conjugated anti-rabbit immunoglobulin as secondary antibody (1:500 diluted in PBS, Life technologies, A-11008) for 2 hours at room temperature and counterstained with DAPI. For the staining a minimum of 10 randomly selected fields were quantitated and positive cells were scored in each individual field. Quantitative analysis was performed using the Image J software (National Institute of Health, Bethesda, Maryland, USA).

2.2.6.3. Immunohistochemical staining for αSMA

Formalin fixed, paraffin-embedded sections were deparaffinized, rehydrated and antigen retrieved by heating to 100^{o}C in 0.01 M sodium citrate buffer (pH 6.0) for 30 min. Endogenous peroxidase was quenched using 3% H_2O_2 in deionized water. After washing sections were blocked with 2.5% horse serum. Rabbit anti-mouse αSMA (1:500, Abcam, E184) antibodies were diluted in antibody diluent (Dako) and incubated overnight at 4°C. After washing three times in TBS a biotinylated secondary antibody (1:500, Vector Labs, BA-1000) was added for 30 minutes at room temperature followed by three washes in TBS. Sections were revealed using the Vectastain ABC kit (Vector Laboratories) and the DAB substrate kit (Vector Laboratories) and counterstained with hematoxylin. Tissues were visualized in a Zeiss Axio Imager AX10 Microscope with the appropriate filters. Representative images were taken with AxioCamMRc 5 camera. A series of images covering >90% of the total tissue section were generated

at uniform settings of magnification, light, and exposure time. Quantitative analysis was performed using Image J software.

2.2.6.4. Sirius red staining

The formalin-fixed tissue sections were deparaffinized and rinsed twice for 5 min in distilled water. Excess moisture from the slides was removed and sections were incubated in 0.1% Sirius red dissolved in saturated picric acid for 30 min. Excess stain was removed by rinsing twice in 0.05% acetic acid for 5 min, followed by distilled water and dehydration by dipping a few times in 70% Isopropyl alcohol and twice in 95% and 100% Isopropyl alcohol followed by twice addition of xylene for 5 min. The slides were mounted with resinous medium and visualized in a Zeiss Axio Imager AX10 Microscope with the appropriate filters. Representative images were taken with AxioCamMRc 5 camera. A minimum of 10 random high-power fields was quantitated for each section. Quantitative analysis was performed using Image J software (National Institute of Health, Bethesda, Maryland, USA).

2.2.7. Hydroxyproline (HYP) assay

Two snap-frozen liver pieces from the left and right liver lobe (150–160 mg each) were hydrolyzed in 5 ml 6N HCL at 110°C for 16 hours. 5µl hydroxyproline sequentially diluted standards (Merck), liver hydrolysate samples and blanks were added into wells of a 96 well plate. 50µl citrate-acetate (Fisher-scientific) (section 2.1.8.) buffer and 100µl chloramine T (Sigma) solutions (section 2.1.8.) were separately added to the hydrolyzed samples and hydroxyproline standards. After incubation on an orbital shaker at room temperature for 30 min, the samples were incubated in a solution containing of 4-dimethylaminobenzaldehyde (Sigma) dissolved in 70% perchloric acid (Sigma) and 1-isopropanol (Applichen) (Ehrlich’s reagent, section 2.1.8.) for 30 minutes at 65°C. The absorbance of the solution was measured at 550 nm and the amount of HYP per milligram of liver tissue was calorimetrically quantified and calculated using the standard curve of the serial dilution of HYP (Merck). Total hepatic HYP content was calculated by multiplying the above determined liver weights with the relative hepatic HYP concentration as described (52).

2.2.8. Treatment of transgenic mouse lines

2.2.8.1. Treatment with CCL_4

CCL_4 was given in mineral oil via oral gavage 3 times a week for up to 3 weeks according to an escalating dose protocol (first dose, 0.875 mL/kg; week 1–3, 1.75 mL/kg) (52). Mice were always sacrificed 3 days after the last dose of CCL_4. Livers and spleens were weighed at sacrifice and livers snap-frozen or formalin-fixed for further analysis.

2.2.8.2. Treatment with doxycycline (Dox)

Doxycycline treatment was used to induce the expression of the tetracycline transactivator. To process this activation mouse chow containing 625 mg/kg doxycycline (ssniff Spezialdiäten GmbH, Soest, Germany) was given for 3 weeks during CCL_4 treatment.

2.2.9. In *Vivo* Imaging

After four days of the doxycycline diet chimeric and bi-transgenic mice were analyzed using the IVIS spectrum imaging system (Caliper LifeSciences). Mice were anesthetized using isoflurane and subjected to in vivo fluorescent imaging by a Xenogen Spectrum system (Caliper, Hopkinton, MA), using 465 and 520 nm of excitation and emission wavelengths, respectively, and 3 sec of imaging integration time. Afterwards, mice were sacrificed by cervical dislocation, and liver, lungs, spleen and kidneys removed for ex vivo imaging using the same system and settings as above. Total fluorescence signals were analyzed by Living Image in vivo imaging software (PerkinElmer, Hopkinton, MA) and represented as total Radiant Efficiency. The Imaging was done by Dr. Mustafa Diken, Institute of Translational Oncology (TRON), University Medical Center, Mainz, Germany.

2.2.10. Statistical analysis

All data points are expressed as mean values ±SEM (standard error of mean). Differences between two groups of normalized data were compared by the two-tailed unpaired Student’s t-test. Differences between more than two groups used ANOVA.

Differences were considered to be statistically significant at $p<0.05$. All statistical data was produced using GraphPad Prism 5.0 0 (GraphPad software).

3. Results

3.1. General strategy and siRNA identification and testing.

The aim of this study was to conditionally knock down the procollagen α1(I) gene (Col1a1) and potentially also other genes relevant for fibrosis by target specific expression of RNAi in transgenic mice during the development of liver fibrosis. In order to be able to conditionally express RNAi, the Tet on/off systems (25) were chosen. As a basis for the generation of transgenic mice conditionally expressing shRNA targeting Col1a1 the protocol detailed in “A pipeline for the generation of shRNA transgenic mice” (53) was used with modifications. The original vector pCol-TGM published in this paper was used as “starting material” and a kind gift by Dr. L.E. Dow, address, and is based on the pgkATGfrt vector (33).

Identification of shRNA sequences that induce potent gene silencing at a single gene copy level was one of the most central challenges and a crucial step in developing an effective shRNA system. For identification of an optimally effective shRNA a two-step in silico filter method was used (53).

To select a panel of shRNA sequences with a good knockdown potential for Col1a1, an online siRNA prediction tool was employed: ‘Designer of Small Interfering RNAs—DSIR’ (http://biodev.extra.cea.fr/DSIR/DSIR.html) (53,54) (Figure 14).

DSIR

Designer of **S**mall **I**nterfering **R**NA

Results for: Col1a1 mice

Current settings:

Score threshold : 90

Design : siRNA 21 nt

[End of page] [Home]

Select rows you want to export or search for in databanks. No selection means that all siRNA sequences will be exported.

siRNA_id	Position	SS Sequence	AS Sequence	Score	Corrected score
1	1417	CGGUGCUACUGGAGUUCAAGG	UUGAACUCCAGUAGCACCGGG	105.9	91.9
2	69	CAAAGAGUCUACAUGUCUAGG	UAGACAUGUAGACUCUUUGCG	99.7	99.7
3	2551	UGGUGAUACUGGUGUUAAAGG	UUUAACACCAGUAUCACCAGG	98.1	73.1
4	3352	GGGUGAGACAGGCGAACAAGG	UUGUUCGCCUGUCUCACCCUU	97.9	64.9
5	1225	CCCUGGUGCUGAUGGACAACC	UUGUCCAUCAGCACCAGGGUU	97.5	85.5
6	2848	CGGUCCUGCUGGUGAGAAAGG	UUUCUCACCAGCAGGACCGGG	97.3	69.3
7	2047	GGGUGUUCCUGGAGACCUUGG	AAGGUCUCCAGGAACACCCUG	96.2	76.2

Figure 14. Example of the siRNA prediction using DSIR algorithm. "Position": position site where the siRNA guide strand begins in the target sequence (from 5' to 3')."Score": predicted efficacy. "Corrected Score": previous efficacy score minored by the penalties from some intrinsic target features which have been shown to influence siRNA efficacy. The criteria for siRNA inclusion in the second round were: 80% extinction activity predicted by DSIR, location in the coding sequence (CDS) part of the target, no polynucleotide tracts and no potential off-targets allowed, an extended panel of target sites by complementary coverage of the overall transcript sequence with respect to the siRNA sequence designed for the first set (55).

As a second step a series of seven sensor exclusion were applied for the 21-mer ‘guide strand’ output from DSIR to further define effective shRNA sequences. “Sensor assay” was developed experimentally by analyzing of ~20,000 shRNA-Sensor constructs comprising every possible shRNA for 9 mammalian transcripts criteria (53,56). Most effective and specific shRNAs were predominantly A/U-rich and exhibit a strong thermodynamic asymmetry, low G/C content. Most of all top-scoring shRNAs carry U or A in guide position 1. Position 20 also shows a remarkable depletion of A. The top eight DSIR-scoring 21-mer guide strand predictions that pass the Sensor criteria (Table 2) have been chosen to test in vitro (section 2.1.12.).

Sensor exclusion criteria for the design of siRNAs	1.siRNA 1417	2.siRNA 69	3.siRNA 2551	4.siRNA 236	5.siRNA 359	6.siRNA 1351	7.siRNA 358	8.siRNA 373
1. A/U at position 1	YES	YES	YES	YES	YES	YES	YES	YES
2. 40-80% A/U content	YES (42%)	YES (57%)	YES (57%)	YES (52%)	YES (43%)	YES (52%)	YES (52%)	YES (57%)
3. >50% A/U content in pos. 1–14	YES (58%)	YES (64%)	YES (71%)	YES (62%)	YES (57%)	YES (64%)	YES (64%)	YES (64%)
4. (A/U% 1-14)/ (A/U% 15-21)> 1	YES	YES	YES	YES	YES	YES	YES	YES
5. No A at pos.- 20	YES	YES	YES	YES	YES	YES	YES	YES
6. A/U at pos. 13 or U at pos. 14	YES	YES	YES	YES	YES	YES	YES	YES
7. No 'AAAAAA' or 'TTTTT' or 'CCCC' or 'GGGG'	YES	YES	YES	YES	YES	YES	YES	YES

Table 2. The top eight DSIR-scoring 21-mer guide strand predictions that pass the Sensor criteria.

The eight siRNA mimics (section 2.1.13.) were transfected to NIH/3T3 fibroblasts as described in 2.2.4.1. After 72 hours the cells were harvested and Col1a1 down-regulation was quantified by quantitative real-time PCR, the experiment was repeated for two times; as the third experiment only, siRNA 4 and siRNA 7 were analyzed (Figure 15).

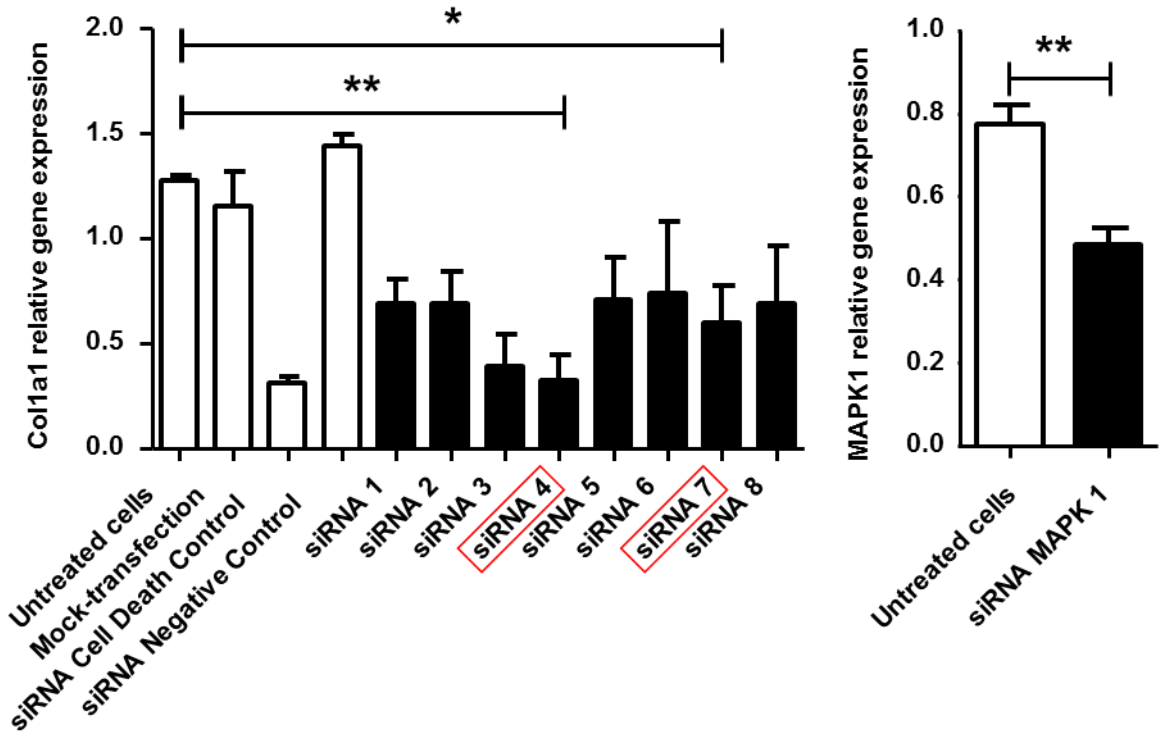

Figure 15. Col1a1 knock-down quantification for eight different preselected siRNAs targeting Col1a1 using the mouse 3T3 fibroblast cell line and quantitative real-time PCR for Col1a1 expression as efficacy readout 72h after transfection. HiPerFect Transfection Reagent (Qiagen) was used as transfection agent with 1 µg siRNA for1.5x10^5 cells in 60 mm dish. Transfection controls: 1. untreated cells; 2. mock-transfection: without siRNA; 3. control of transfection efficiency using a cell death inducing siRNA, a blend of highly potent siRNAs targeting ubiquitously expressed mouse/rat genes that are indispensable for cell survival; knock-down of these genes induces a high degree of cell death, which is visible by light microscopy (Qiagen); 4. negative control: siRNA without homology to any known mammalian gene (Qiagen); 5. positive control: siRNA targeting MAPK1 (Qiagen).

Finally, siRNA4 and siRNA7 were chosen for transgenic mouse generation.

3.2 ShRNA design and cloning

The target sequences of siRNA4 and siRNA7 were inserted into miR30 context of the pCol-TGM vector (53). This vector contains a targeting construct which provides robust tetracycline conditional expression (TRE) of the shRNA-mir and the fluorescent marker (GFP) (Figure 16).

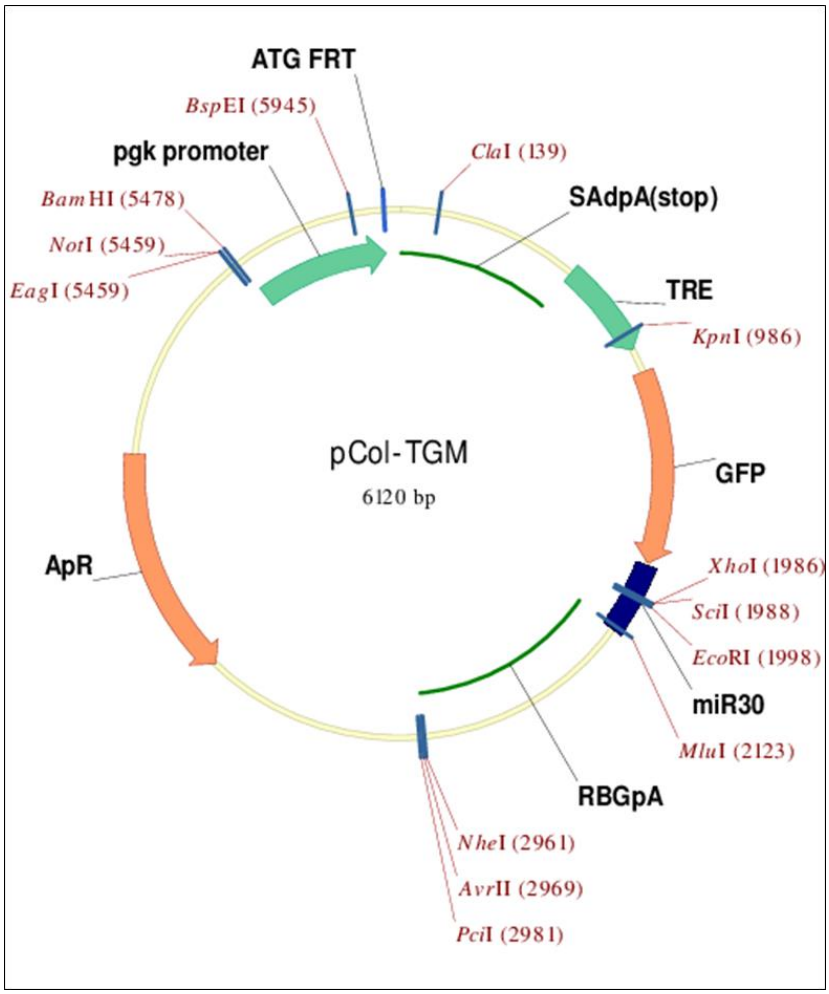

Figure 16. Schematic representation of the pCol-TGM vector (Dow LE et al., Nat Protocols, 2012). TRE - Tet responsive element, GFP - green fluorescent protein, PGK - phosphoglycerate kinase promoter, miR30 - microRNA precursor (17), XhoI/EcoRI – restriction sites for cloning into the miR30 context (Addgene).

To generate the appropriate shRNA-mir template, the nucleotide immediately 5′ to the 21-mer sense strand of siRNA4 and siRNA7 were adjusted according to the nucleotide 5′ to the 21-mer target site in the mRNA transcript (Figure 17); since the 5′ nucleotide in the mRNA is a C, the first base of the 22-mer sense strand becomes an A. This adjustment creates a mismatch at the base of the stem-loop that mimics the structure of endogenous miR30, thereby enabling more efficient processing by the RNAi machinery (16,53).

Figure 17. Schematic overview of the process to transform 21-mer guide strand predictions into miR30-based cloning templates for linker cloning. First, the 21-mer guide strand is reverse complemented to generate the 21-mer sense strand (or 21-mer target site). To generate the appropriate shRNAmir template, the nucleotide immediately 5′ to the 21-mer sense strand is changed according to the nucleotide 5′ to the 21-mer target site in the mRNA transcript; since the 5′ nucleotide in the mRNA is a C, the first base of the 22-mer sense strand becomes an A, to create a targeted mismatch.

The final 22-mer sense and antisense strands were then designed into the 131-mer linker cloning template (Figure 18).

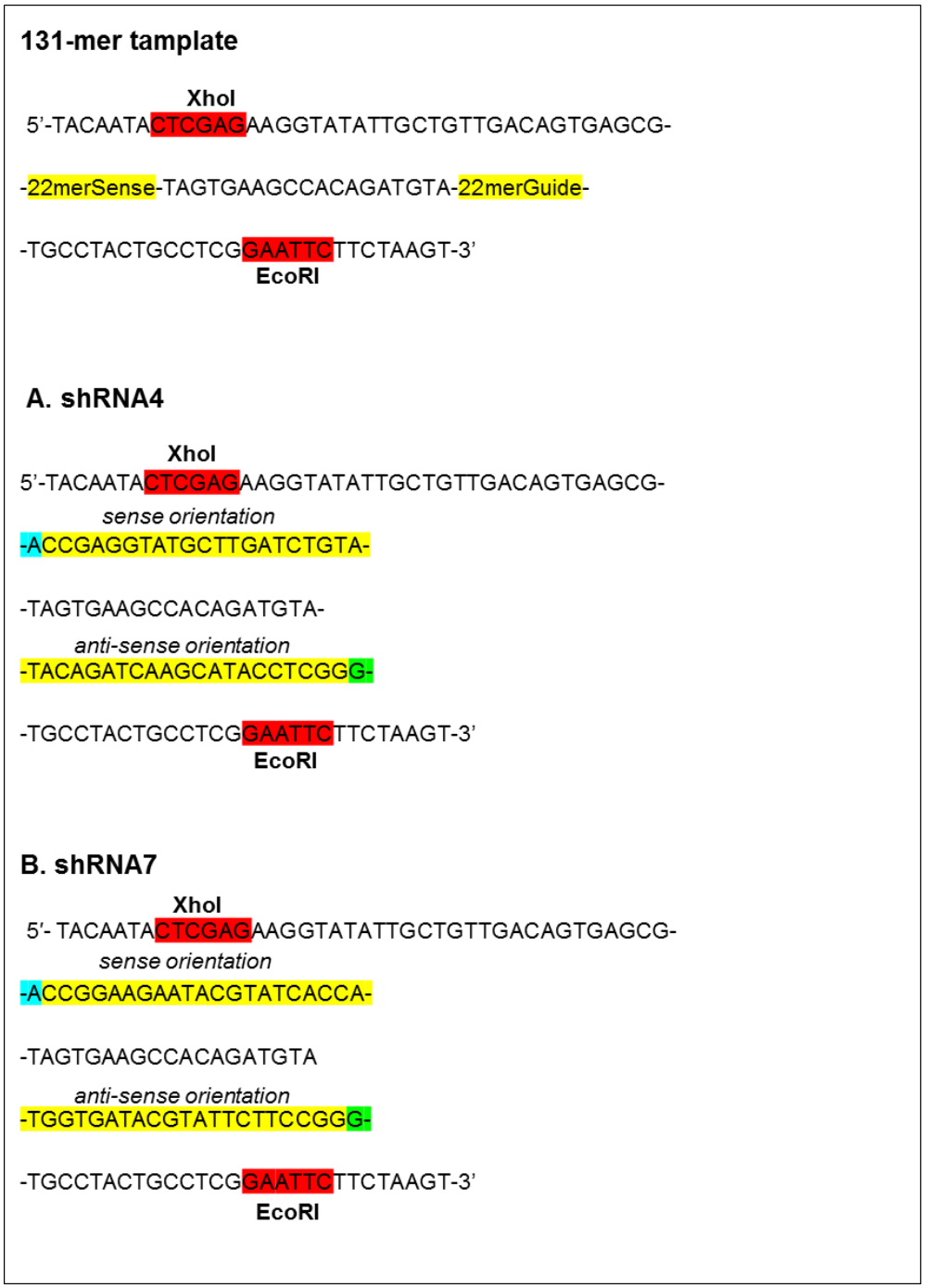

Figure 18. 131-mer oligos containing sense and antisense strands of shRNA4 (A) and shRNA7 (B) in miR30-based cloning templates. XhoI and EcoRI are restriction cloning sites.

The 131-mer oligonucleotides containing sense and antisense strands of shRNA4 and shRNA7 were annealed with their appropriate reverse transcribed complements (section 2.2.1.3) and digested with restriction enzymes XhoI and EcoRI. The sticky end fragments encoding the appropriate shRNAs were purified using 1% agarose gel electrophoresis and cloned into the XhoI and EcoRI sites of the pCol-TGM vector

enabling the doxycycline-regulated expression of fluorescent GFP linked to the shRNAs expression cassette embedded in miR30 context (Figure 19). The preparation and ligation were performed as described in section 2.2.1.1, 2.2.1.2, 2.2.1.4.

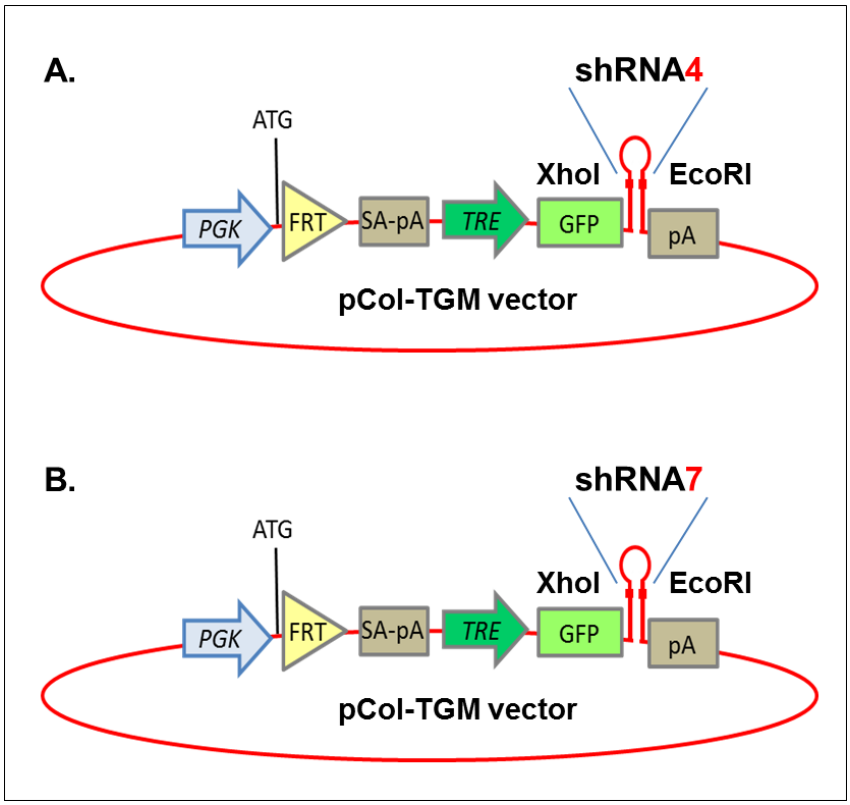

Figure 19. Cloning scheme for the pCol-TGM knock-down vector. A. shRNA4. B. shRNA7.

To confirm successful integration of the double stranded oligonucleotides into the pCol-TGM vector, different restriction digests were done. Then two modified vectors containing shRNA4 and shRNA7 were sent for sequencing to check for mutations. Sequencing confirmed correct integration without additional mutations.

To test the ability of the target cassette for expression, a transfection assay was performed. Vectors pCol-TGM-shRNA4 and pCol-TGM-shRNA7 were co-transfected with the rtTA expression pUHrT 62-1 vector (28) to HEK 293 cells (section 2.2.4.3). followed by addition of 1 µg/ml doxycycline to the experimental wells. After four days of incubation the transfection was visually analyzed under a fluorescent microscope for the expression of GFP. As expected the mock transfected HEK 293 cells and cells transfected without pUHrT 62-1 did not show any GFP expression and were

appropriate negative controls, while both Col1a1 targeting siRNA containing plasmids robustly expressed GFP. These results demonstrated that both of the modified vectors containing shRNA4 and shRNA7 downstream of GFP were fully functional and could be used for genomic integration.

3.3. Generation of the mouse line containing a TRE-GFP-shRNA-Col1a1 cassette in the Col1a1 locus using recombinase-mediated cassette exchange (RMCE) in KH2 ES cells.

To perform the integration of the targeting cassette TRE-GFP-shRNA7 in the 3'UTR Col1a1 locus, a recombinase-mediated cassette exchange (RMCE) in KH2 embryonic stem cell was performed. The KH2 ES cells (33) the Flp-RMCE recipient locus (homing cassette) downstream of the Col1a1 gene (Figure 19) that allows efficient FLPe recombinase-mediated integration of a transgenic cassette at single copy in a defined locus, here downstream of the Col1a1 gene (Figure 20).

Figure 19. Homing cassette in KH2 ES cells containing FRT - flp recognition target sites flanking the neomycin resistance gene under the control of the phosphoglycerate kinase promoter (PGK), the hygromycin resistance gene without promoter and an AGT initiation start codon (57).

The KH2 embryonic stem cell line with was co-electroporated with 25µg of targeting vector pCol-TGM-shRNA7 and 50µg of flp recombinase expression vector pCAGGS-flpE-puro (58) to achieve integration into the target locus as described in section 2.2.4.7.

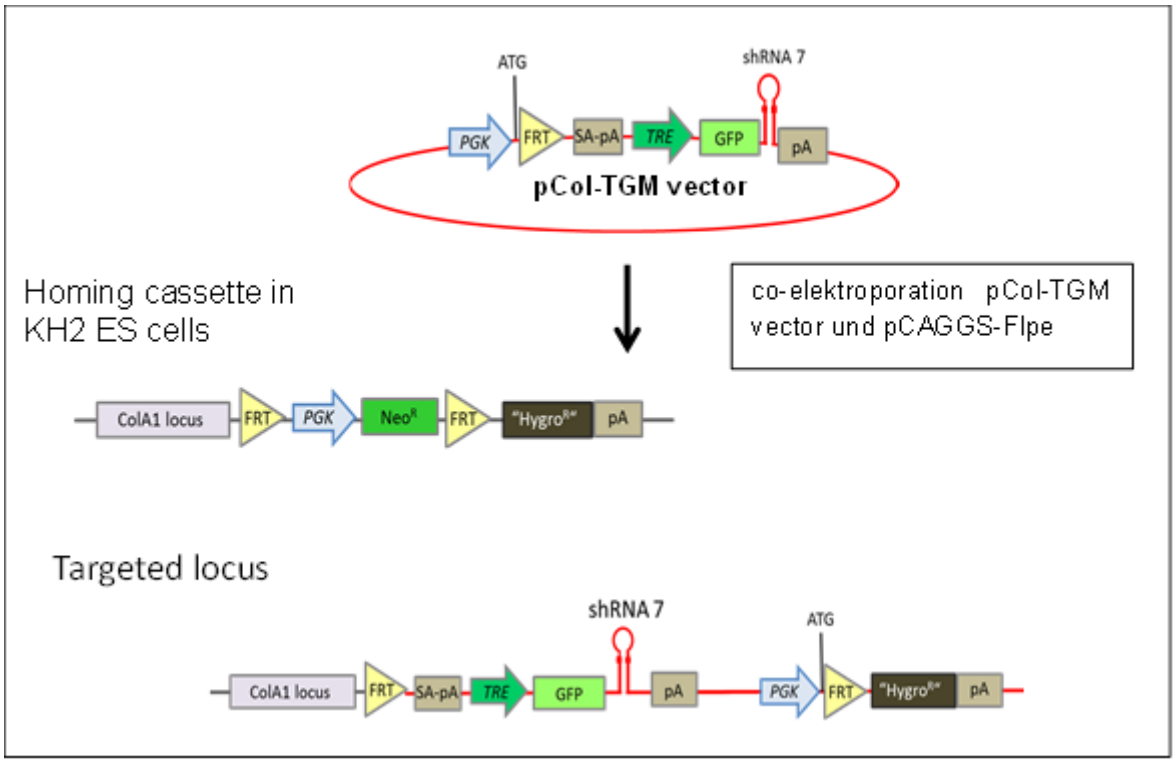

Figure 20. Integration of the target cassette downstream of the Col1a1 gene locus (Modified (57).

48 hours after electroporation, hygromycin selection was started and continued for eight days, with Hygromycin selection medium being changed every 24 hours. During the first three days of selection the embryonic stem cells were growing at a normal rate. Between days four to six massive cell death was observed among the embryonic stem cells indicating that most cells did not integrate the targeting vector carrying the resistance gene. In the time period between 6 - 8 days of hygromycin selection macroscopic ES cell colonies were seen. At day 10 five clones were picked and expanded as described in section 2.2.4.8. Then aliquots of all five clones were tested by incubation in neomycin selection medium, to exclude clones showing neomycin resistance due uncorrected integration of the targeting cassette. Finally, the two ES cell clones 3 and 4 that that survived only in the hygromycin selection medium but not in the presence of neomycin have were chosen for future experiments. ES cells of clones 3 and 4 expanded in 6 well dishes were used for DNA isolation and “Long range” PCR, and frozen aliquots conserved.

Long range PCR was performed as described in section 2.2.2.8 for two regions of the targeting construct:

1. From the first FRT sites in the Col1a1 locus outside of the targeting cassette to 3'-downstream of GFP inside the cassette using ColA1 forward and GFP reverse primers (Table 2.1.14) resulting in a 2061 bp DNA product.

2. From 5'-upstream of miR30 to 3'-downstream of the hygromycin resistance gene outside of the targeting cassette using miR30seq forward and Hygro reverse primers (Table 2.1.15) releasing in resulting in a 4470bp DNA product. The results of the agarose gel electrophoresis showed correct sizes of the DNA bands for both clones number 3 and 4 (Figure 21).

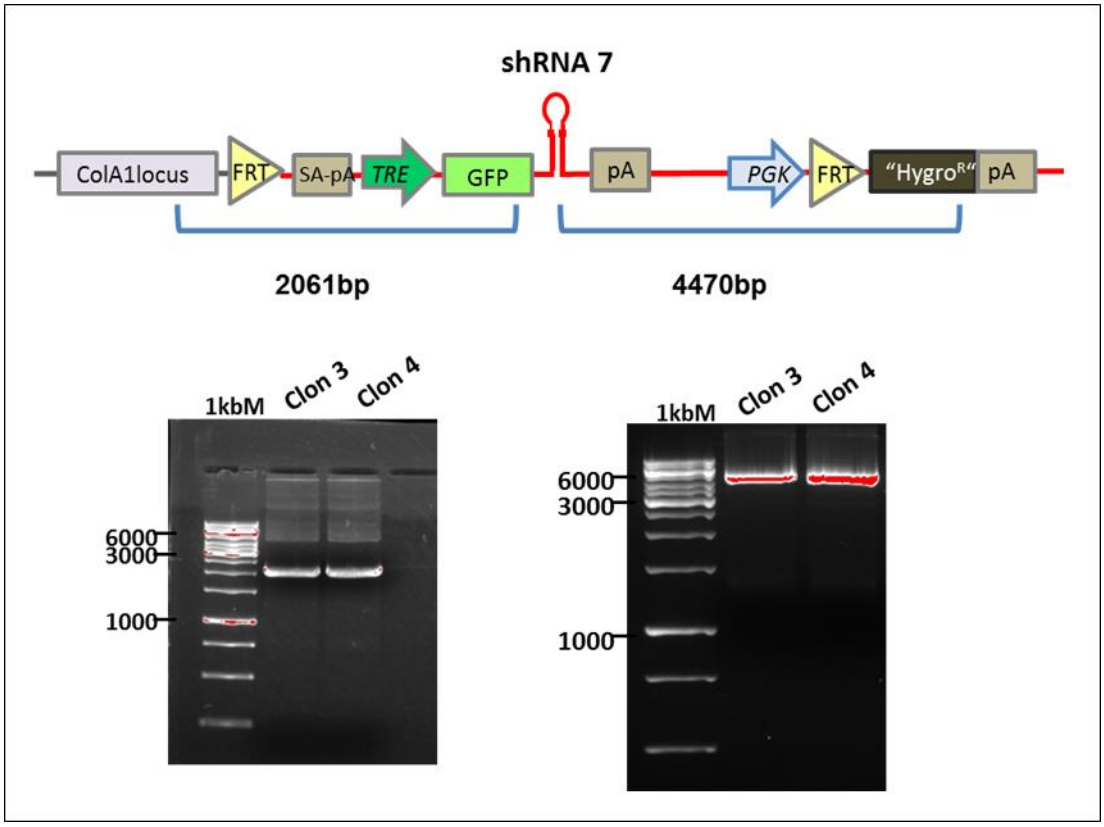

Figure 21. Agarose gel electrophoresis after long range PCR. Left: expected size of 2061bp for the 5'-region; right: expected size of 4470bp for the 3-'region.

Finally, DNA of clones 3 and 4 was further checked by sequencing which confirmed that the targeting cassette was correctly incorporated in the both cases, without

random mutations. The resultant embryonic stem cell clones were used for establishing the RMCE-shRNACol1a1-7 mouse lines.

To this aim the embryonic stem cell clones 3 and 4 were subsequently injected into blastocytes (3.5 days post coitum (dpc) from the C57BL6/N-albino mouse line (section 2.2.5.1). Microinjection was performed at the Transgenic Facility Mainz (TARC, University Medical Center, Mainz, Germany). After embryo transfer into a pseudo-pregnant CD1 foster mother chimeric mice were born. Almost all chimeric mice were males and have significantly high levels of chimerism, including 100% coat color chimerism. This opened the possibility to perform a first *in vivo* experiment to check the functionality of the transgene directly on chimeric mice.

The KH2 ES cells contain not only the Flp-RMCE homing site downstream of the Col1a1 gene but also a second-generation reverse tet-transactivator (rtTA2^{S}-M2) expressed from the Rosa26 promoter, yielding Rosa26-rtTA/RMCE-shRNACol1a1-7 mice, allowing immediate validation of regulated GFP-shRNAmir expression and gene silencing.

Chimeric mice from clones 3 and 4 were fed doxycycline (625 mg/kg in food pellets) for four days and then analyzed using *in vivo* fluorescence imaging (section 2.2.9), which demonstrated a massive GFP signal for both clone 3 and 4 in the whole body and in the isolated organs of the mice (Figure 22).

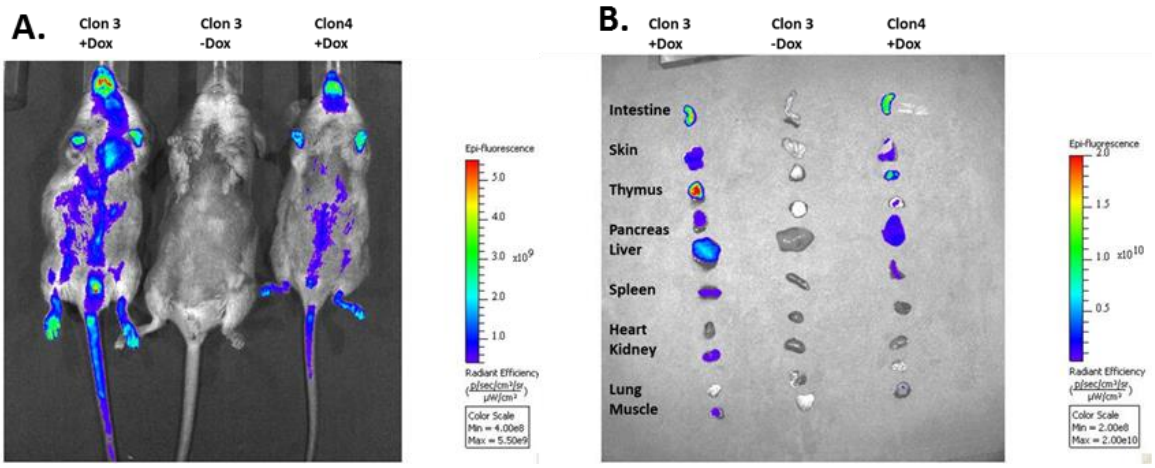

Figure 22. *In vivo* imaging analysis of chimeric mice. A. *In vivo* imaging of chimeric mice generated from KH2 ES cell clones 3 and 4 demonstrates a strong GFP signal in the whole body after four days of treatment with doxycycline (625 mg/kg food). B. GFP signal in the isolated organs: intestine, skin, thymus, pancreas, liver, spleen and in addition kidney, and muscle for clone 3.

The results of the *in vivo* imaging clearly showed the functionality of the transgenes derived from clones 3 and 4 in living chimeric mice and confirmed that the ubiquitous Rosa26 locus provided constitutive gene expression of rtTA and hence also of the inducible transgene in almost all organs.

To further check the functionality of the constructs, ear fibroblasts of chimeric mice were cultured as described in section 2.2.4.2 and cultivated without und with doxycycline (1 µg/ml) for four days. Col1a1 knock-down was quantified by quantitative real-time PCR. The results for both mice lines showed the same level of the down-regulation of Col1a1 by around 80% (Figure 23).

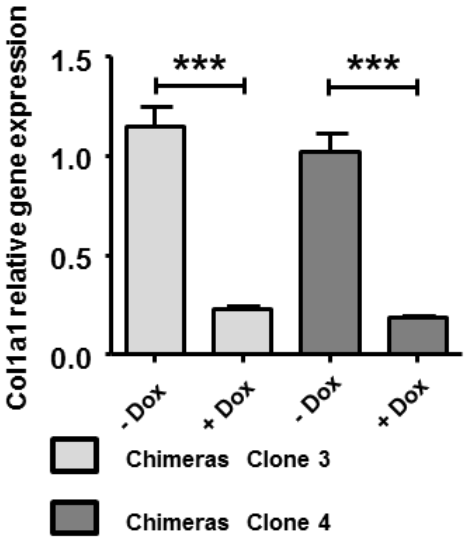

Figure 23. Relative Col1a1 gene expression in the culture of mice ear fibroblasts of chimeric mice without and with doxycycline (1 µg/ml). Data are means ± SEMs. Each group of the cells performed in triplicates. The target gene was relative to Gapdh mRNA.

Chimeric male mice were used for further breeding with C57BL6/N-albino female mice to establish transgenic mouse lines. Germline transmission was obtained for both ES cell clones, leading to the new mouse lines RMCE-shRNACol1a1-7/Clone3 and RMCE-shRNACol1a1-7/Clone4 (indicated below as RMCE-Clone3 and RMCE-Clone4), respectively.

3.4. Generation of a mouse line containing the targeting cassette TRE-GFP-shRNACol1a1 in Col1a1 locus using zinc finger nuclease (ZFN)

The generation of transgenic mouse lines using RMCE/KH2 ES cell technology is straightforward, but quite laborious and time consuming. A viable alternative would be the direct targeting of the Tet-inducible expression cassette to the Col1a1 locus in fertilized oocytes by DNA microinjection. Direct targeting without the possibility of a positive selection is a rare event but can be stimulated strongly by a double strand break in the target locus. To induce a double strand break we made use of the zinc finger nuclease (ZFN) technology, as described in the Introduction. The nuclease was custom-made by Sigma-Aldrich (Figure 24).

Zinc Finger Nuclease Binding/catting site

CCAGGTTGCTCCttggtcACACATGGAGGGGTA

Figure 24. The sequence of DNA binding (37)/catting (47) site used for generation of Zinc Finger Nuclease targeting Col1a1 locus.

This experiment was designed not only to speed up the generation of transgenic shRNA expressing mice, but also to compare efficiency of two different shRNAs, i.e., shRNA7 and shRNA4, targeting Col1a1. For direct comparison of both shRNAs the same target locus downstream of Col1a1 that was used for integration of the TRE-GFP-shRNA4 cassette was chosen. To enable the insertion of the targeting TRE-GFP-shRNA4 construct with help of the specific ZFN, first a donor/targeting vector containing two 1kb homology arms homologous to the targeting locus Col1a1 was designed. The vector was generated by DNA synthesis and obtained commercially (Life Technologies, Carlsbad, USA) (Figure 25).

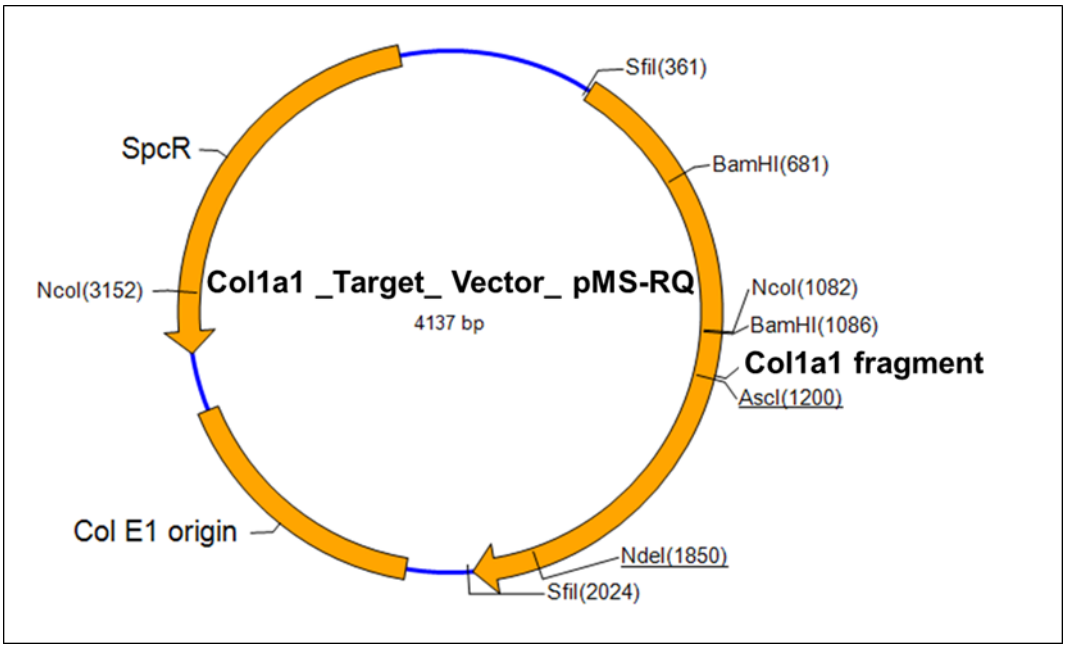

Figure 25. Col1a1 target vector. 2 kb fragment of locus downstream of Col1a1 was assembled from synthetic oligonucleotides and cloned into pMS-RQ plasmid using SfiI and SfiI cloning sites. SpcR - spectinomycin resistance; Col E1 origin - replication origin of ColE1 plasmid (*Escherichia coli* plasmid that carries a gene for colicin E1); NcoI, SfiI, BamHI, AscI, NdeI are restriction enzymes sites (Life Technologies, Carlsbad, USA).

For the generation of the final targeting vector, the TRE-GFP-shRNA4 expression cassette had to be inserted in the plasmid Col1a1_Target_Vector_ pMS-RQ. The respective DNA fragment was removed from the vector pCol-TGM-shRNA4 by PstI and NheI digestion. The Col1a1_Target_Vector_ pMS-RQ was linearized with SbfI and NheI and dephosphorylated. The sticky ends produced by SbfI and PstI are compatible to allow direct ligation of both agarose purified fragments. Purification and ligation was performed as described in sections 2.2.2.6 and 2.2.1.4, respectively (Figure 26).

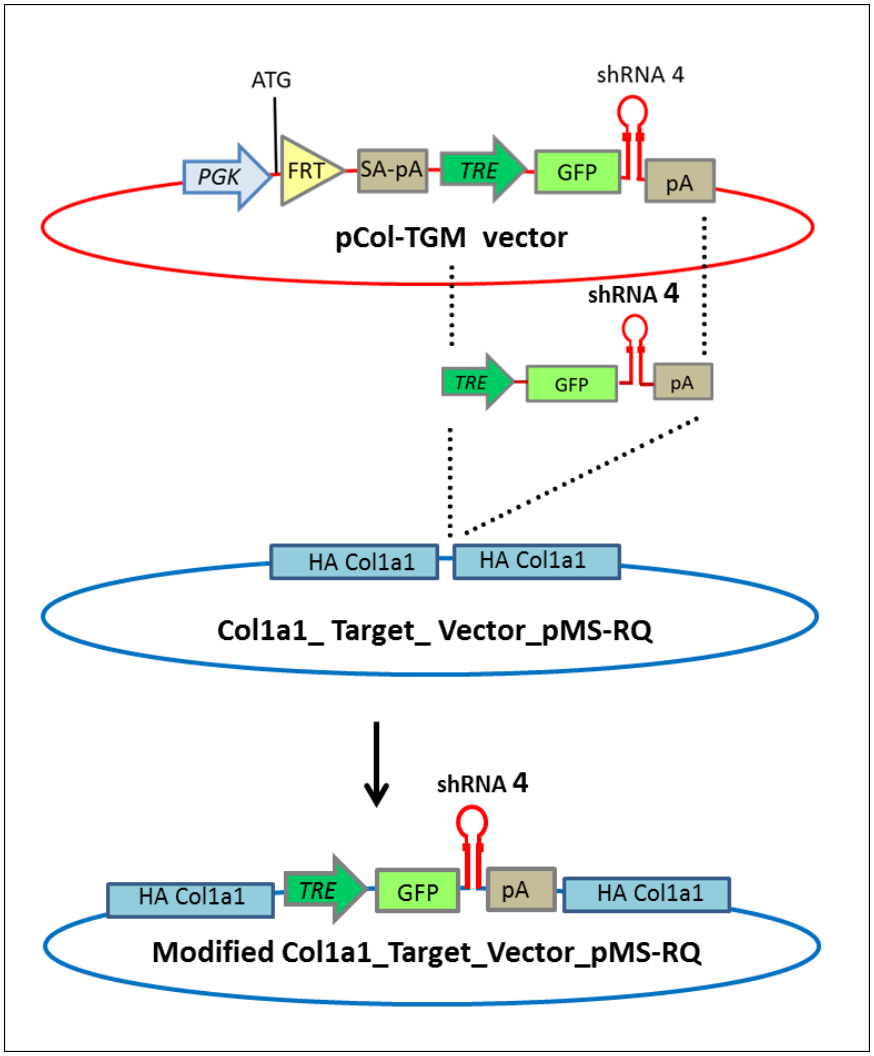

Figure 26. Cloning of the targeting cassette TRE-GFP-shRNA4 into the Col1a1_Target_Vector_pMS-RQ. HA Col1a1 – homology arms to locus downstream of Col1a1.

To confirm the correct ligation of the cassette TRE-GFP-shRNA4 into the Col1a1_Target_Vector_pMS-RQ some individual clones were digested with PstI/NdeI,

NcoI and NdeI. Two clones displayed the expected sizes of the DNA fragments. These clones were analyzed by sequencing and correct integration was confirmed.

The functionality of the modified shRNA4 containing targeting vector was checked by co-transfection of HEK 293 cells with the rtTA expression plasmid pUHrT 62-1 and expression analysis similar to section 3.2.

The final targeting vector containing the targeting cassette TRE-GFP-shRNA4 inserted in between of two homology arms homologous to the Col1a1 locus was subsequently microinjected together with of Col1a1 ZFN mRNA (section 2.1.11) in the pronucleus of fertilized oocytes FVBB6 F1 background. Microinjection was performed at the Transgenic Facility Mainz (TARC, University Medical Center, Mainz, Germany). Details of this procedure can be found in section 2.2.5.2. Tail DNA from mice derived from the DNA/mRNA microinjection was screened by PCR using GFP primers (section 2.1.15). Three positive transgenic founder mice (F1, F2, F3) were detected from a total of 92 offspring (3.3%). Long range PCR was performed using the DNA of the three founder mice, to confirm correct integration of the target construct in the Col1a1 locus. The long range PCR primers were as follows:

1. From 5' Col1a1 locus outside of the homologous arm to a region inside of the cassette using Col1a1 (ZFN) forward and TGM (ZFN) reversal primers (Table 2.1.14) that released in 1690bp DNA band.

2. From a region inside of the cassette to 3' Col1a1 locus outside of the homologous arm using TGM (ZFN) forward and Col1a1 (ZFN) reversal primers (Table 2.1.14) releasing in 1516bp DNA band. The results of the agarose gel electrophoresis showed correct sizes of the DNA bands for two putative transgenic founder mice N 1 and N 3 (Figure 27).

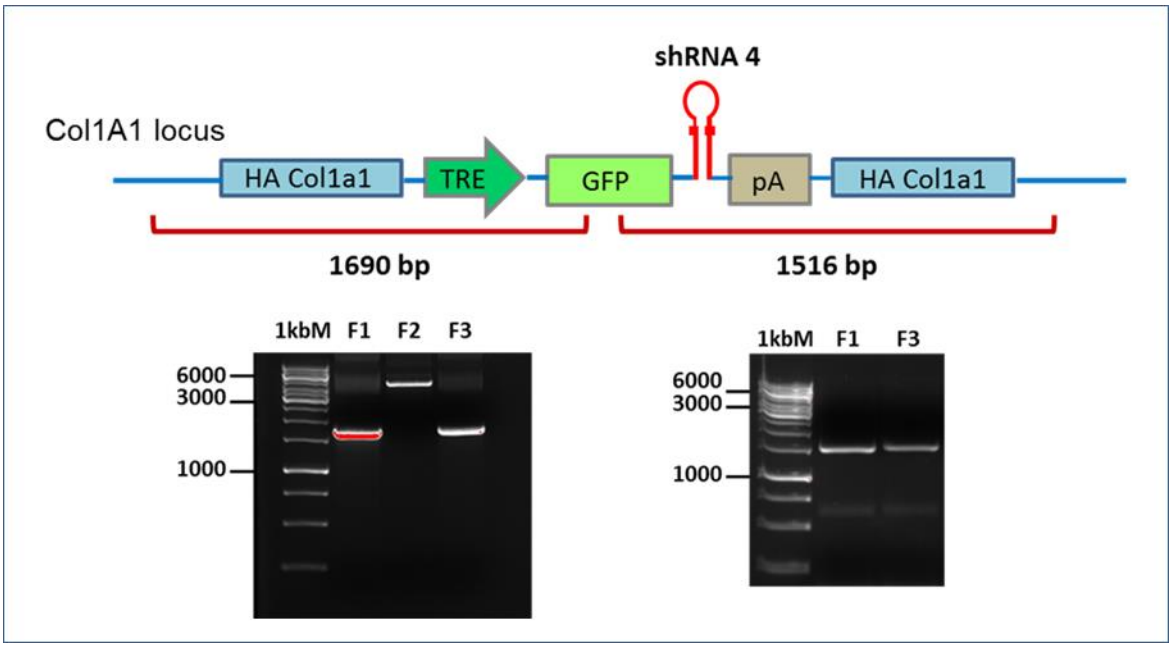

Figure 27. Long range PCR results showing correct integration of the targeting cassette TRE-GFP-shRNACol1a1-4 into the Col1a1 locus.

Finally, long range PCR products derived from the DNA of the founder mice F1 and F3 were sequenced which confirmed that the targeting cassette was correctly incorporated in both cases. To establish a transgenic mouse colony, these two individual founders were crossed to the wildtype C57BL6/J strain. Since the mice from the line ZFN-shRNACol1a1-4/Line3 showed poor viability, only the line ZFN-shRNACol1a1-4/Line1 (indicated below as ZFN-Line1) was used for the future experiments.

3.5. Characterization of mouse lines RMCE-Clone4 and ZFN-Line1

3.5.1. Functionality and inducibility of new transgenic mouse lines

The functionality of the transgenic mouse lines RMCE-Clone3 and RMCE-Clone4 that were generated by recombinase mediated cassette exchange had already been shown directly using chimeric mice that were produced from KH2 ES cells, but they showed a high degree of chimerism (section 3.3. Figure 22). In order to test functionality of the new transgenic mouse line ZFN-Line1 generated with ZFN, the mice were bred with the Rosa26-rtTA strain (59) that provides widespread expression of the reverse tetracycline-controlled transactivator (rtTA-M2) (28) protein. Bi transgenic Rosa26-rtTA/ZFN-Line1 mice were fed doxycycline (625 mg/kg in food pellets) for four days

and then analyzed using *in vivo* fluorescence imaging (section 2.2.9). A strong GFP signal was observed in the body and in the separated organs. Rosa26-rtTA/RMCE-Clone4 used as a positive control (Figure 28).

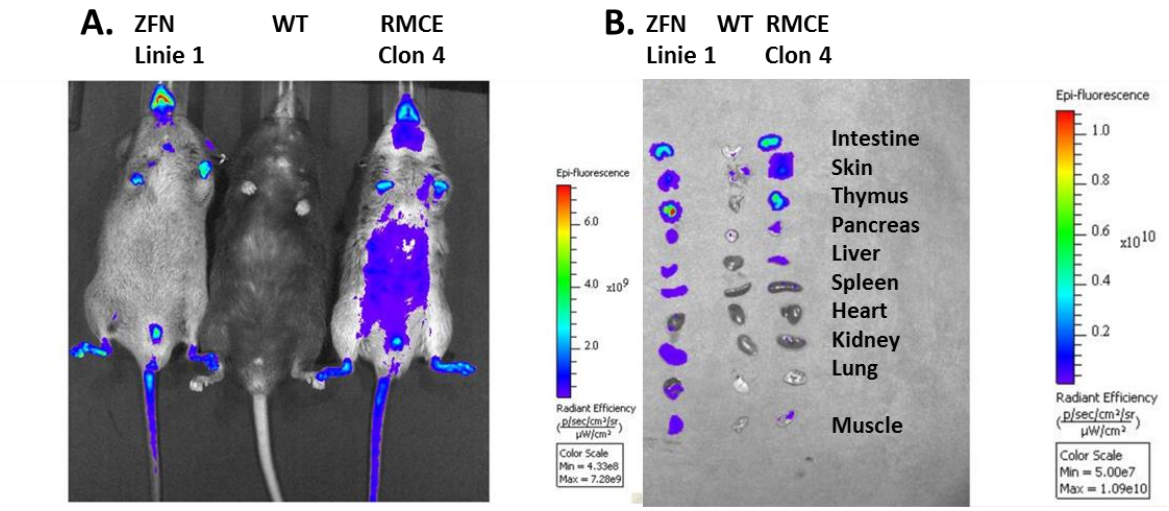

Figure 28. *In vivo* fluorescence imaging analysis of bi transgenic mice Rosa26-rtTA/ZFN-Line1; Rosa26/RMCE-Clone4 used as a positive control. A. In vivo imaging of Rosa26-rtTA/ZFN-Line1 mouse demonstrates a strong GFP signal in the body after four days of treatment with doxycycline (625 mg/kg food). B. GFP signal in the separated organs: positivity in intestine, skin, thymus, pancreas, liver, spleen, kidney, lung and muscle.

3.5.2. Doxycycline-dependent GFP expression in the fibrotic liver of bi-transgenic mice

Two analyze the new tetracycline inducible RNAi Col1a1 transgenic mice, all three lines RMCE-Clone3, RMCE-Clone4 and ZFN-Line1 were bred with the R26-rtTA strain, to generate sufficient animals for the induction of liver fibrosis. Bi transgenic mice were treated with escalating doses of oral CCl_4, a model that robustly induces parenchymal liver fibrosis (52), for three weeks (section 2.2.8.1). During induction, mice received oral doxycycline to induce expression of GFP and Col1A1 shRNAs (section 2.2.8.2). Single Col1a1 transgenic littermates (indicated below as WT) treated with CCL_4 and doxycycline served as controls. Livers were analyzed using confocal laser scanning microscopy (CLSM), quantitative real-time PCR, H&E histology, immunofluorescence and immunohistochemistry.

GFP expression in the fibrotic livers was analased *in vivo* using confocal laser scanning microscopy (CLSM). All bi transgenic mice lines showed a comparable promounced GFP signal in comparison with wild type control group (Figure 29, shown Rosa26-rtTA/RMCE-Clone4 mice line only).

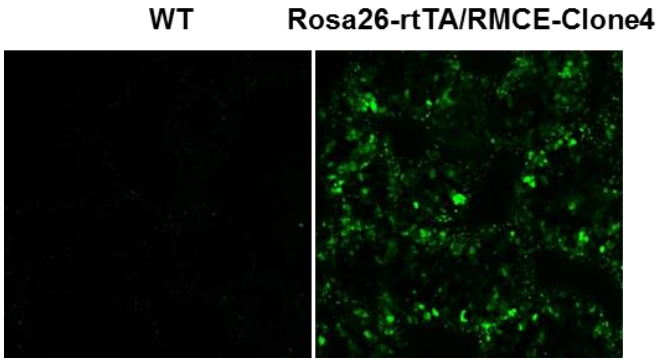

Figure 29. Doxycycline depended GFP expression in the fibrotic liver of Rosa26-rtTA/RMCE-Clone4 bi-transgenic mice (CLSM).

The expression level of GFP in the fibrotic liver was determined using quantitative real-time PCR (section 2.2.3.3). Rosa26-rtTA/RMCE-Clone4 and Rosa26-rtTA/ZFN-Line1 bi transgenic mice lines showed same high level of GFP expression ($P<0.01$). Compared to these two groups the Rosa26-rtTA/RMCE-Clone3 bi transgenic mice line did not show any significance and in spite of the same high level of GFP expression was excluded from the following experiments (Figure 30).

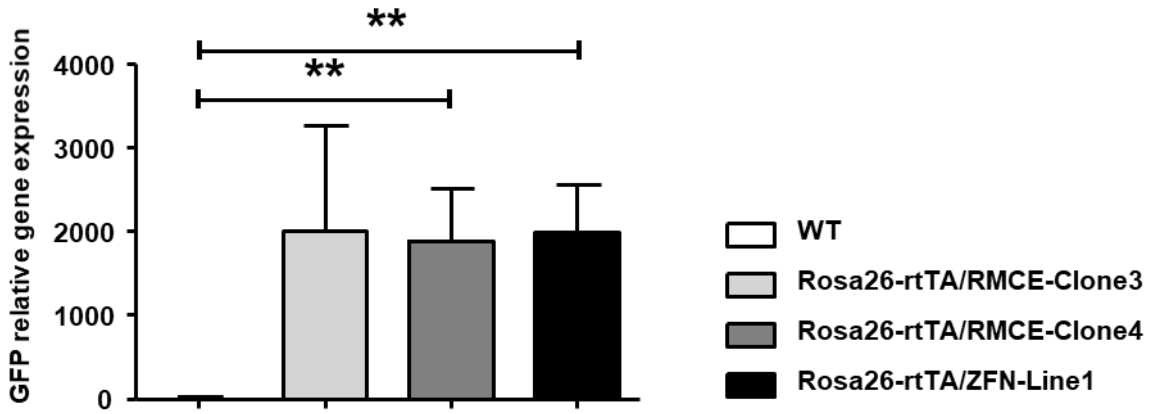

Figure 30. GFP expression levels in the fibrotic liver. Quantitative real-time PCR relative to Gapdh mRNA as standard. Data are expressed as means ± SEMs. Rosa26-rtTA/RMCE-Clone3 mice, N=4; Rosa26-rtTA/RMCE-Clone4 mice, N=5; Rosa26-rtTA/ZFN-Line1 mice, N=7; control WT mice, N=7.

3.5.3. Regulation of the expression of Col1a1 and other different collagen types in ear fibroblasts of bi transgenic mice

In order to continue analyzing of the inducibility and functionality of the new tetracycline inducible RNAi targeting Col1a1 mice models the ear fibroblasts of bi transgenic mice lines were cultivated (section 2.2.4.2) without und with doxycycline (1µg/ml) for four days. Appropriate GFP signal was observed in all cell dishes incubated in the presents of doxycycline (Figure 31).

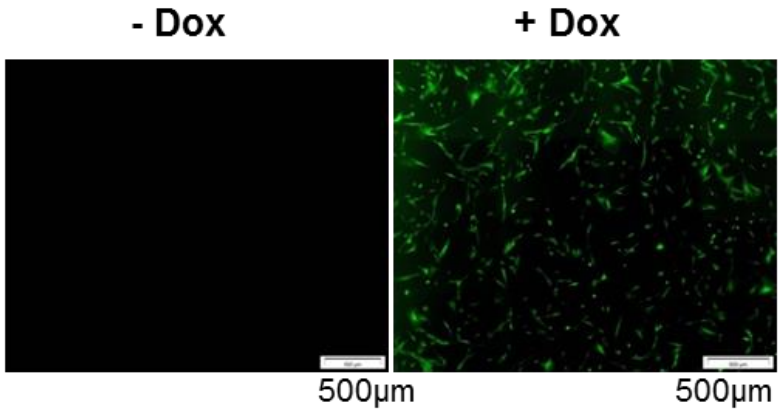

Figure 31. GFP signal in the culture of ear fibroblasts of bi transgenic mice lines; only Rosa26-rtTA/ZFN-Line1 example is shown.

After harvesting the cells mRNA was isolated and expression level of Col1a1 as well as of some other pro-collagens (Col3a1, Col4a1, Col5a1, Col6a1, Col6a3) were determinated by quantitative real-time PCR (Figure 32).

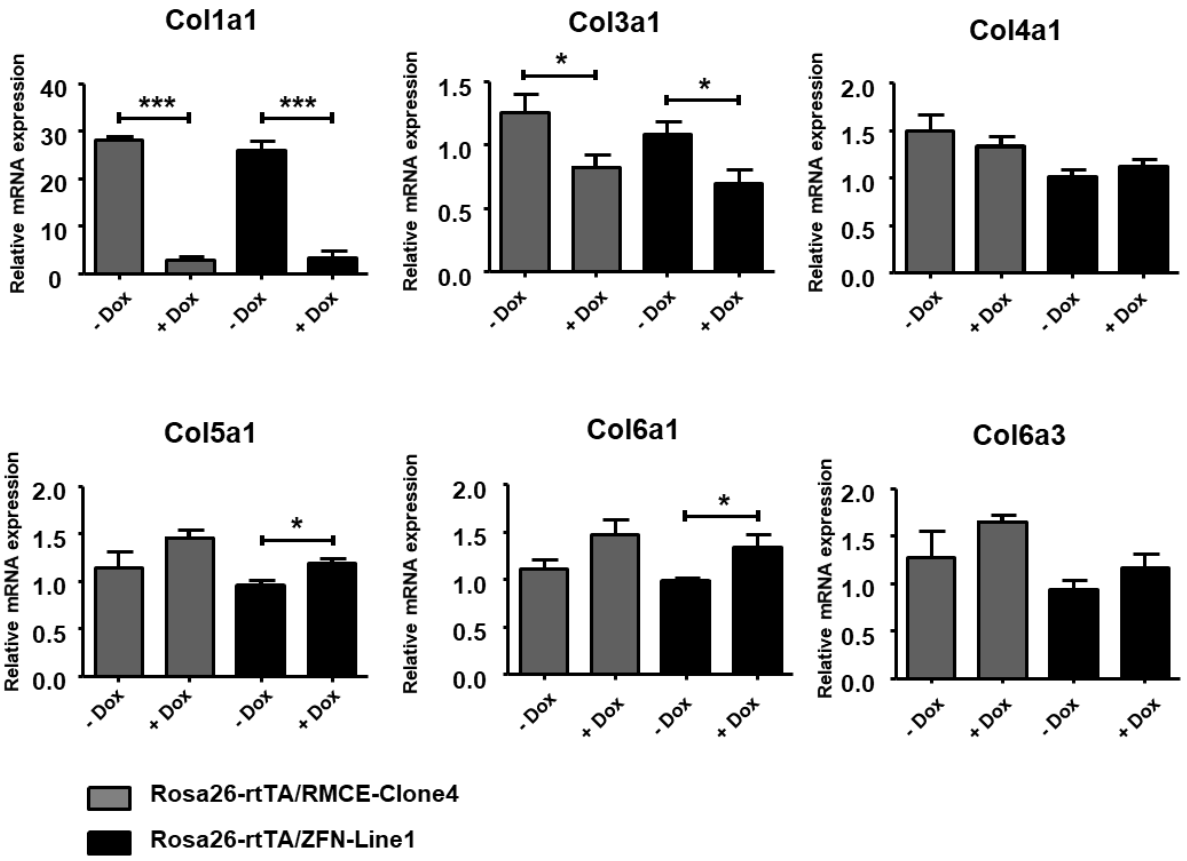

Figure 32. Expression levels of various major procollagen types in ear fibroblasts of bi transgenic mouse lines Rosa26-rtTA/RMCE-Clone4 (N=4) and Rosa26-rtTA/ZFN-Line1 (N=5). Quantitative real-time PCR relative to Gapdh mRNA as standard. Data are expressed as means ±SEMs.

Both of the lines demonstrated a high degree of down regulation of the targeted gene Col1a1 in ear fibroblasts ($p<0.001$): 89% for Rosa26-rtTA/RMCE-Clone4 and 80% for Rosa26-rtTA/ZFN-Line1. Interestingly, silencing of Col1a1 expression lead to downregulation of another important component of scar tissue, Col3a1 ($p<0.05$): 35% for Rosa26-rtTA/RMCE-Clone4 and 30% for ZFN-Line1. At the same time procollagen genes Col5a1 and Col6a1 were upregulated, with significance only for the more potent Rosa26-rtTA/ZFN-Line1 ($p<0.05$): upregulation 20% and 28%, respectively. Expression levels of procollagens Col4a1 and Col6a3 were regulated in parallel, but this did not reach statistical significance.

3.5.4 Regulation of the expression of Col1a1 and other different collagen types in the fibrotic liver tissue of bi transgenic mice

When bi transgenic mice and wild type controls were treated with escalating doses of oral CCl_4 for three weeks to induce parenchymal liver fibrosis and fed chow enrichen with Dox to induce expression of shRNAs targeting Col1a1 and GFP, mRNAs of the livers were isolated (section 2.2.3.1), a significant suppression of Col1a1 and fibrosis in general was observed. Thus Col1a1 expression was suppressed by 89% for Rosa26-rtTA/RMCE-Clone4 ($p<0.001$) and by 88% for Rosa26-rtTA/ZFN-Line1 ($p<0.001$). Similarly, Col3a1, the second most abundant fibrillar collagen, was downregulated by 73% for Rosa26-rtTA/RMCE-Clone4 ($p<0.01$) and by 65% for Rosa26-rtTA/ZFN-Line1 ($p<0.01$), well in line the effect found in the cultures of ear fibroblasts. In contrast to the cell culture studies with fibroblasts, expression of Col6a3 was significantly ($p<0.05$) suppressed by 56% for Rosa26-rtTA/RMCE-Clone4 and by 59% for Rosa26-rtTA/ZFN-Line1 vs the wildtype controls. Other collagenes Col4a1, Col5a1, Col6a1 showed a trend that was down regulated by 20-40% (Figure 33).

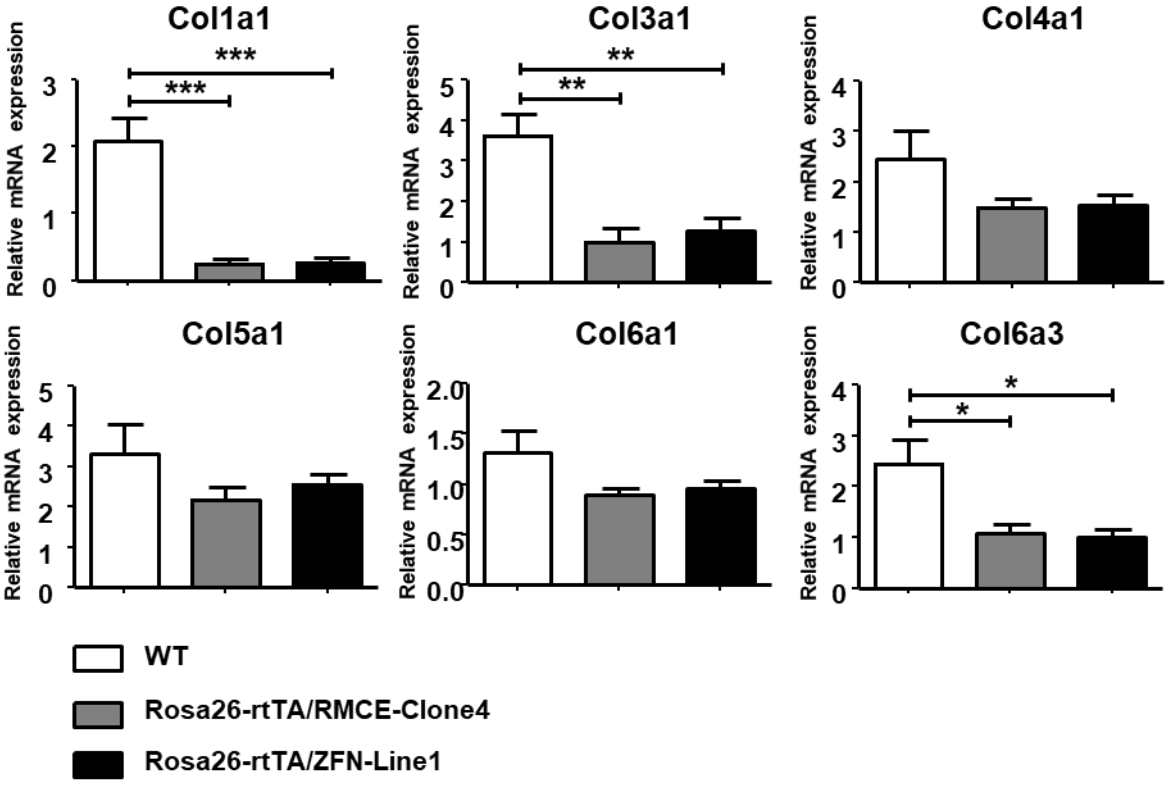

Figure 33. Expression level of procollagens in fibrotic livers of bi transgenic mouse lines Rosa26-rtTA/RMCE-Clone4 (n=5), Rosa26-rtTA/ZFN-Line1 (n=7), WT control (n=7). Quantitative real-time PCR relative to Gapdh mRNA as standard. Data are expressed as means ±SEMs.

Frozen sections of the livers were stained with anti-collagen type I (section 2.2.6.1) and anti-procollagen type III primary antibodies (section 2.2.6.2), followed by fluorescent-labelled secondary antibodies and visualized under the fluorescence microscope (Figure 34). Quantification of the stained areas showed a significant reduction of collagen type I deposition: 64% for Rosa26-rtTA/RMCE-Clone4 ($p<0.01$) and 73% for Rosa26-rtTA/ZFN-Line1 ($p<0.01$) compared to wildtype mice. Similarly, collagen type III deposition was reduced by 39% for Rosa26-rtTA/RMCE-Clone4 ($p<0.05$) and 35% for Rosa26-rtTA/ZFN-Line1 ($p<0.05$). These results confirmed the down regulation of expression of Col1a1 and Col3a1 genes, as quantified by real time PCR, on the protein level.

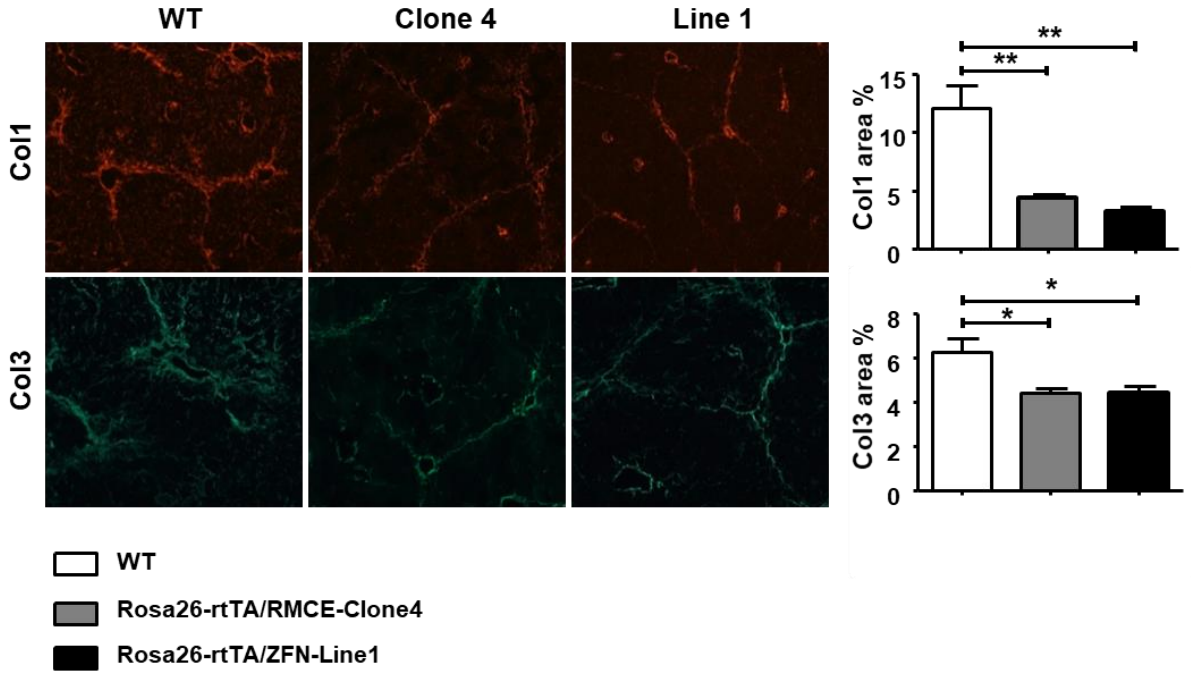

Figure 34. Immunofluorescent images of collagen type I and procollagen type III stainings in liver sections. Rosa26-rtTA/RMCE-Clone4 (n=5), Rosa26-rtTA/ZFN-Line1 (n=7), WT control (n=7). Data are expressed as means ±SEMs.

3.5.5. Quantification of the total amount of collagen in the fibrotic liver tissue of bi transgenic mice

The overall collagen content in the livers was determined biochemically via quantification of the collagen-specific amino acd hydroxyproline (Hyp) in tissue hydrolysates (section 2.2.7). Total collagen in the fibrotic livers of Rosa26-rtTA/RMCE-Clone4, Rosa26-rtTA/ZFN-Line1 and wildtype control mice fully corresponded to the suppression of Col1a1 (and in part the other collagens) *in vivo* as quantified by quantitative real-time PCR. The Hyp concentration (per 100 mg of liver tissue) was significantly reduced by 56% for the Rosa26-rtTA/RMCE-Clone4 ($p<0.01$) and by 39% for the Rosa26-rtTA/ZFN-Line1 ($p<0.05$) mice. The total amount of Hyp (amount per total liver) equally showed a significant reduction by 49% for the Rosa26-rtTA/RMCE-Clone4 ($p<0.05$) and by 43% for the Rosa26-rtTA/ZFN- Line1 ($p<0.05$) mice (Figure 35).

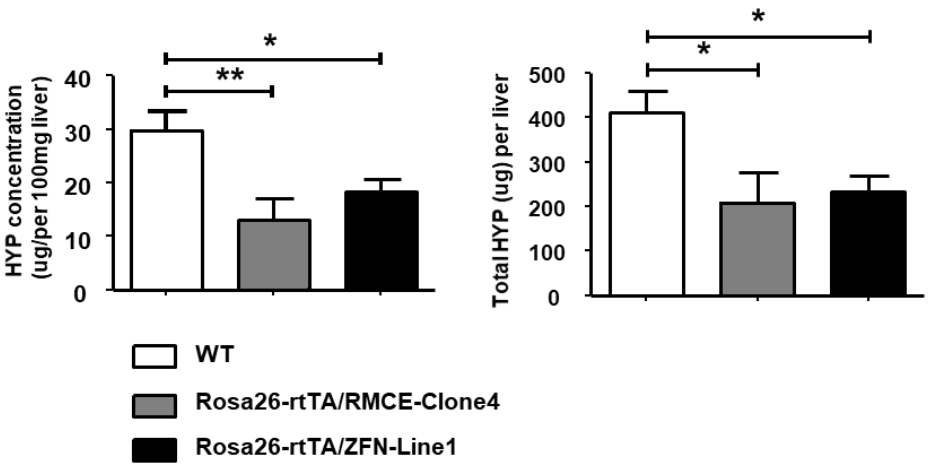

Figure 35. Hydroxyproline (Hyp) concentrations in the livers of the bi-transgenic mice vs control mice after 3 weeks of fibrosis induction with CCL_4. Rosa26-rtTA/RMCE-Clone4 (n=5), Rosa26-rtTA/ZFN-Line1 (n=7), WT control (n=7). Data are expressed as means ±SEMs.

These results were confirmed by morphometric assessment using Sirius red morphometry (section 2.2.6.4) which determined significant ($p<0.001$) redaction of collagen content by 47% for Rosa26-rtTA/RMCE-Clone4 and by 42% for Rosa26-rtTA/ZFN-Line1 (Figure 36).

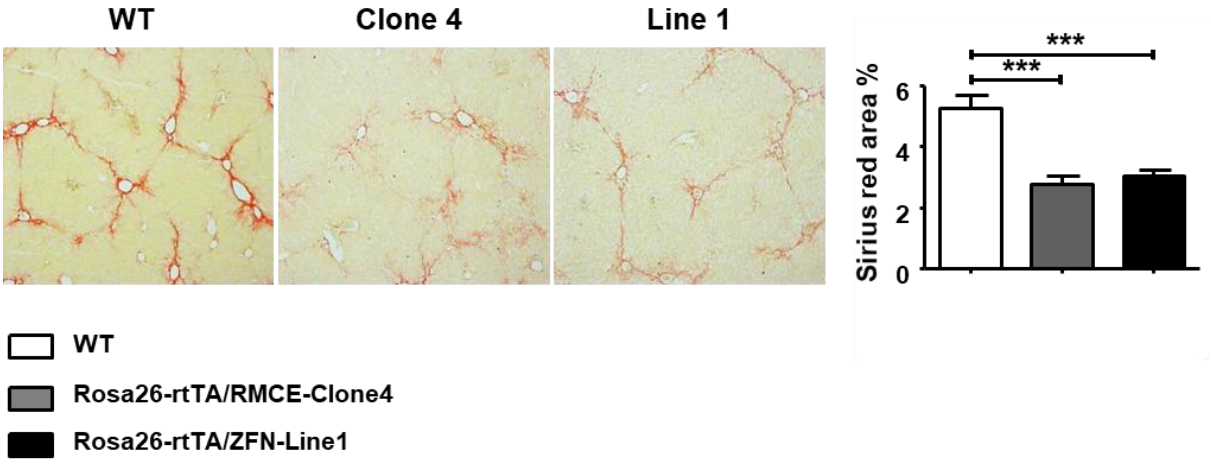

Figure 36. Photomicrographs of Sirius red-stained collagen in liver sections. Rosa26-rtTA/RMCE-Clone4 (n=5), Rosa26-rtTA/ZFN-Line1 (n=7), WT control (n=7). Data are expressed as means ±SEMs.

3.5.6. Analysis of fibrosis related gene expression in the livers of bi-transgenic mice

Silencing of Col1a1 affected several other genes related to liver fibrosis, such as α-SMA, TIMP-1, TGF-β. Quantitative real-time RCP showed downregulation of MMP-8, MMP-13, TIMP-1, TGF-β and α-SMA (Figure 37).

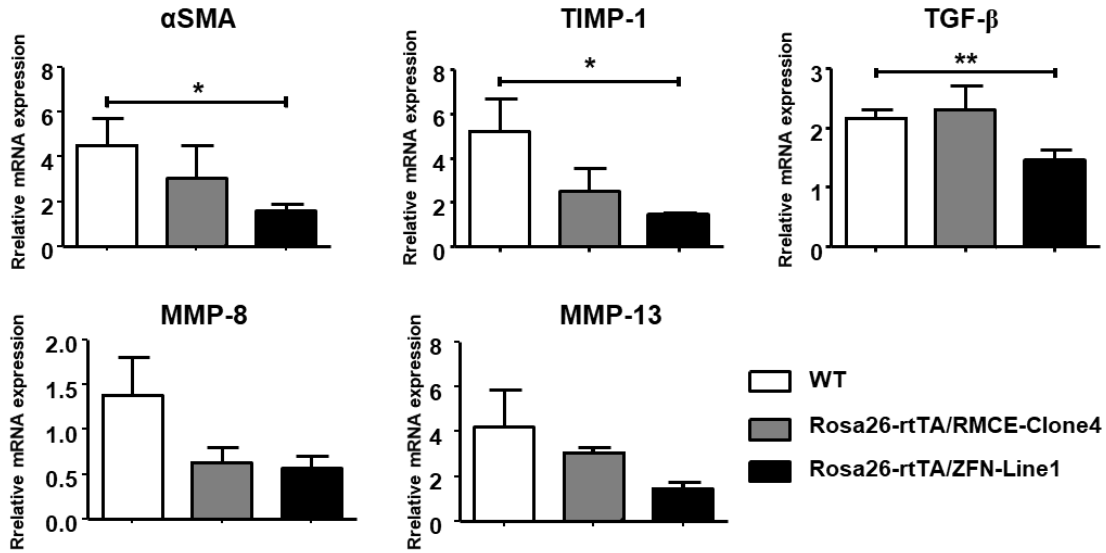

Figure 37. Expression of fibrous factors in the liver. Rosa26-rtTA/RMCE-Clone4 (n=5), Rosa26-rtTA/ZFN-Line1 (n=7), WT control (n=7). Quantitative real-time PCR relative to Gapdh mRNA as standard. Data are expressed as means ±SEMs.

In addition, paraffin sections of the liver were stained with anti-α-SMA, representing (section 2.2.6.3) the area occupied by activated hepatic stellate cells was quantified by computerized image analysis to demonstrate a significant reduction in both bi-transgenic mouse lines by 26% for Rosa26-rtTA/RMCE-Clone4 ($p<0.001$) and by 42% for Rosa26-rtTA/ZFN-Line1 ($p<0.001$), respectively (Figure 38).

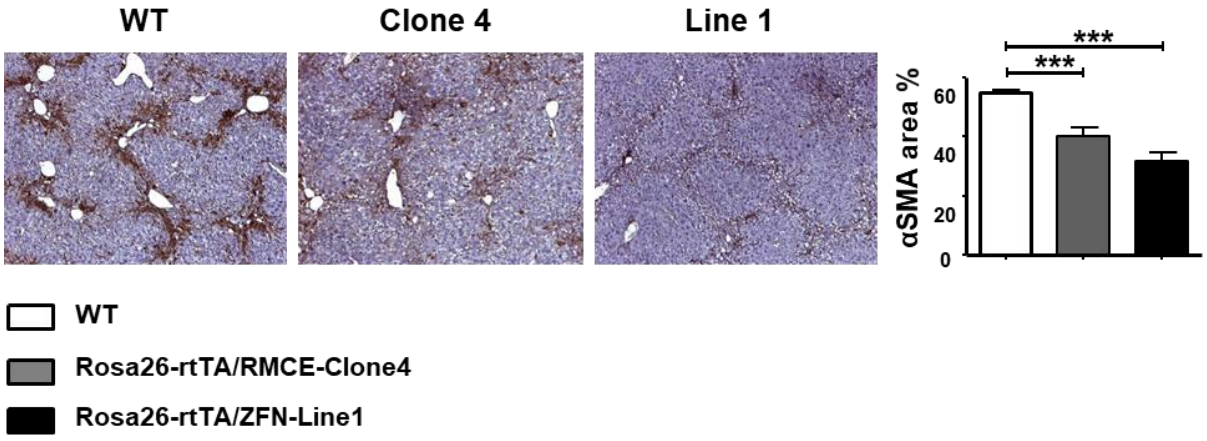

Figure 38. Micrographs and morphometric analysis of α-SMA-stained liver sections. Rosa26-rtTA/RMCE-Clone4 (n=5), Rosa26-rtTA/ZFN-Line1 (n=7), WT control (n=7). Data are expressed as means ±SEMs.

3.5.7. Analysis of inflammation related genes in the livers of bi-transgenic mice

Silencing of Col1a1 also lead to a significant suppression of major inflammation-related genes such as TNF-α and CD68+ (for macrophages) ($p<0.05$), in Rosa26-rtTA/ZFN-Line1). Moreover, in Rosa26-rtTA/ZFN-Line1 the serum levels of transaminases reflecting liver inflammation were reduced (Figure 39).

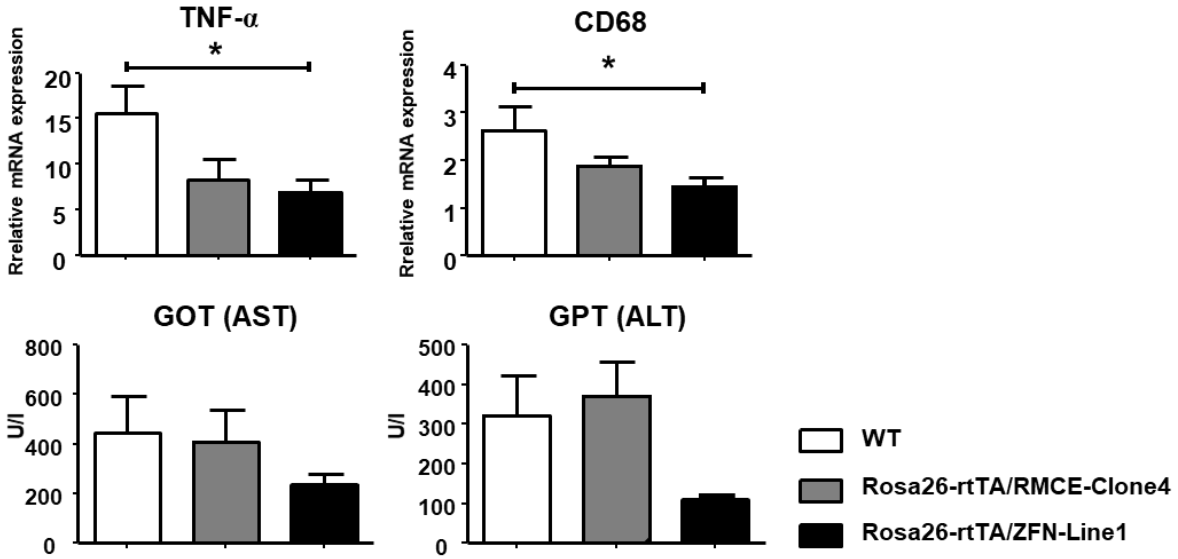

Figure 39. Inflammation factors and transaminases in the liver. Rosa26-rtTA/RMCE-Clone4 (n=5), Rosa26-rtTA/ZFN-Line1 (n=7), WT control (n=7). Quantitative real-time PCR relative to Gapdh mRNA as standard. Data are expressed as means ±SEMs.

4. Discussion

4.1. First transgenic mouse model for an inducible Col1a1 knockdown

Collagen type I is the major protein component of fibrotic tissues and has been considered a highly relevant therapeutic target to prevent or treat fibrotic diseases, which account for almost 50% of worldwide morbidity and mortality. Prominent examples are fibrosis of lungs, kidneys and liver (60). However, agents that would specifically antagonize procollagen type I synthesis in the relevant target cells, i.e. activated fibroblasts or myofibroblasts remain elusive. Importantly, potential adverse effects of the procollagen type I ablation in vivo remain unknown. Notably, ablation of the alpha 1(I) chain gene (Col1a1) that in contrasts to the alpha 2(I) chain gene of the triple helical procollagen type I molecule (that is composed of two alpha1 and one alpha2 chain) prevents collagen triple helix formation, since unlike alpha1 chain trimers, alpha2 chain trimers are unstable (61). Previously generated transgenic mice introduced a constitutive knockout of the alpha1 chain or constitutive mutations that are found in bone disease, i.e., osteogenesis imperfecta (43,62). These mice have a prominent and early bone phenotype and are unsuitable to study soft tissue fibrosis. Moreover, they do not reflect pharmacological intervention in a living organism. In the presented work I therefore developed three transgenic mouse strains with a doxycycline-(Dox) inducible knockdown by activation of shRNAs targeting the Col1a1 gene. Importantly, the tetracycline responsive element (TRE) is expressed downstream of the Col1a1 gene, a safe integration site that does not interfere with Col1a1 gene expression when no Dox is added (33,59). Moreover, in these mice the shRNA, which is directed against Col1a1 in our present study, can be exchanged by a shRNA against any other gene of interest using the same vector and tools that we applied in the present study. Finally, these are the first transgenic mice that permit an inducible Col1a1 knockdown.

4.2. Two different technologies for gene insertion: recombinase-mediated cassette exchange vs ZFN mediated gene targeting

Two different technologies for gene insertion at the predefined site downstream of the Col1a1 gene were employed which finally yielded comparable results, i.e. a highly efficient and reproducible knockdown of the target gene, Col1a1: 1) recombinase-mediated cassette exchange (63) in KH2 embryonic stem cells developed by the Jaenisch laboratory (33) and modified by Premsrirut et al. (35,53,57) allowing Tet-inducible fluorescent-linked shRNA expression; 2) ZFN mediated gene targeting in fertilized oocytes to insert the Tet-inducible shRNA expression cassette; both being downstream of the Col1a1 locus.

Genetically modified mice are an extremely important instrument for understanding gene function and for modeling human disease. Gene targeting in mouse embryonic stem cells is a conventional method that introduces mutations through homologous recombination (HR) in mouse ES cells it usually occurs with very low efficiency, and the generation of mutant mice is costly and time-consuming, since an enormous number gene-targeted ES cell clones need to be selected (64).

RMCE in KH2 ES cells has increased efficiency for correct integration compared to conventional homologous recombination in ES cells (34,35), thereby reducing time-consuming screening of ES cell clones by a factor of 50- to 100. For the RMCE construct, two of five clones were shRNA positive, which confirms the finding that time-consuming screening of ES cell clones can be avoided with the KH2 RMCE technology. Due to the high level of chimerism, the resulting chimeras allow a fast assessment of effectiveness of knock-down *in vivo* without further breeding for the appearance of general germline transmission. After blastocyst transfer of both modified KH2 clones the chimeric mice could be screened rapidly and successfully for correct transgene expression *in vivo* without additional breeding steps. Here, the target gene Col1a1 was significantly downregulated in primary ear fibroblasts from chimeric mice after doxycycline treatment.

The direct gene targeting in fertilized oocytes, using site-specific nucleases such as zinc-finger nuclease, is even more efficient. This technology obviates the need for prior cell culture work and allows the direct generation of germline modified transgenic

founder mice and as such greatly reduces both cost and time for generating the transgenic mice. I have demonstrated the feasibility of this approach in targeting the Col1a1 locus which resulted in 3 out 92 targeted transgenic animals. The efficacy of homologous recombination might be further improved by optimizing the components used during microinjection or longer homology arms; however, the efficacy was high enough to obtain transgenic founder mice by routine procedures and therefore allows the faster generation of transgenic knockdown mouse models compared to the RMCE technology. In addition, using this approach the vector backbone including the selection cassette was not integrated into the mouse genome, which might otherwise interfere with transgenic or Col1a1 expression under some circumstances. Furthermore, this strategy allows targeting the Col1a1 locus in the genetic background of choice and is not dependent on the genetic background of the KH2 cells.

Finally both strategies finally yielded comparable results and resulted in a highly efficient knockdown of the target gene, although RMCE seems to be more costly and time-consuming then ZFN approach (Table 3).

	RMCE in KH2 ES cells	ZFN
Donor vector cloning	Yes	Yes
Cell culture work, clone screening	Yes, 6-8 weeks	No
Selection cassette	Integrated into the mouse genome	No
Microinjection	Blastocyst microinjection	Fertilized oocytes
Germline transmission generation	Yes, 6 weeks	No
Background	C57BL/6 x 129Sv	Background of choice
First analysis	Directly in chimeric mice because of a high percentage of chimerism	1-2 generations of breeding with an effector mouse line, 6-9 weeks
Mice lines (number)	Two	One

Table 3. Comparison of technologies: RMCE in KH2 ES cells vs ZFN.

4.3. Future perspectives of gene targeting

Gene targeting technology, particularly utilization of site-specific nucleases, has developed continually and extremely quickly in the past several years. The recent development of the “clustered regularly interspaced short palindromic repeat”

(CRISPR)/CRISPR-associated protein (Cas) system has enabled direct manipulation of the genome with extremely high efficiency (64). Based on the adaptive immune system in bacteria and archaea, the CRISPR/Cas system does not require additional plasmid cloning of zinc-finger nucleases (ZFNs) or transcription activator–like effector nucleases (TALENs) and subsequent production of appropriate mRNAs. The system comprises CRISPR-coded RNAs (crRNAs), trans-activating crRNA (tracrRNAs) and Cas9 endonuclease (from *Streptococcus pyogenes*) (Figure 40). The optimized CRISPR/Cas system consists of a fusion between the crRNA and the tracrRNA, providing a chimeric single-guide RNA (sgRNA) that can be used to produce sequence-specific DSBs (65).

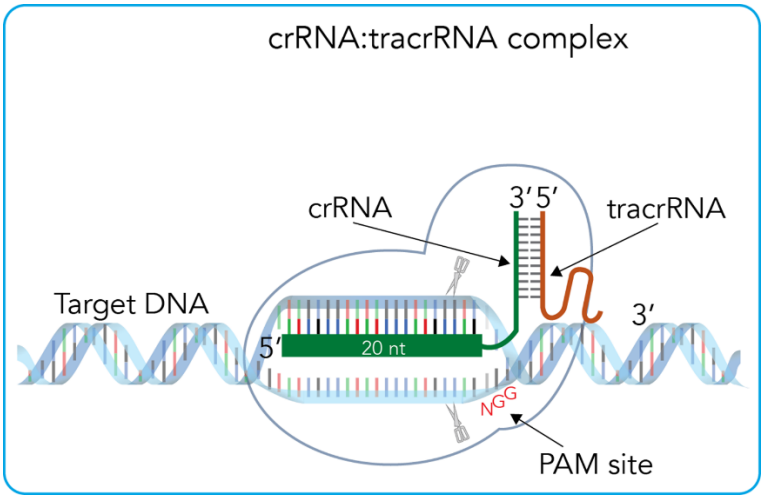

Figure 40. The chemically synthesized crRNA and tracrRNA hybridyze and join the Cas9 endonuclease, targeting it to cleave DNA in a sequence specific way. 20 nucleotides of crRNA are complementary to the target sequence, right upstream the protospacer adjacent motif (66) site on the opposite DNA strand. DNA is cleaved upstream the protospacer adjacent motif (PAM) site.

Compared with ZFNs and TALENs, the CRISPR/Cas-mediated genome editing is more efficient and easy to design, construct and deliver multiple sgRNAs, that allows multiplexed manipulation in genome. Utilization of ssDNAs as a donor is a new promising approach for productive and uncomplicated exogenous transgene insertion (knock-in) without additional donor vector cloning (67). Although more studies are needed to further improve the CRISPR/Cas system for *in vivo* genome editing, the recent findings suggest that this technology has great potential to be highly efficient and specific (68).

4.4. Utilization of inducible shRNA mice models for studying liver fibrosis: highly efficient knockdown of the target gene Col1a1

The Col1a1 knockdown was rigorously validated and examined in a model of progressive liver fibrosis, induced by three weekly injections of CCL4 for 3 weeks. Here, induced suppression of procollagen α1(I) production had dramatic effects not only on collagen accumulation, but also suppressed other collagens, both interstitial and basement membrane collagens, and modulated the expression of MMPs. Moreover, and unexpectedly, the inducible procollagen type I knockdown attenuated liver inflammation. Overall, it induced beneficial features throughout that were not predictable before and that go beyond mere antifibrotic activities.

RNA interference (RNAi) is a natural mechanism for gene silencing characterized by expression of non-coding small interfering RNA (siRNA) or short hairpin RNA (shRNA) complementary to the target mRNA transcript (12,13). Artificial siRNA mediated knock-down of endogenous gene expression is a widely exploited experimental approach to study gene functions (18). It was optimized for inducible *in vivo* system by using prediction tools for optimal knockdown efficacy. This allowed pretesting knockdown efficiency for Col1a1 in fibroblast cultures and selection of the most effective siRNAs, before they were inserted into the backbone of a naturally occurring primary microRNA precursor (miR30) which permits its integration into a shRNA-like environment with a more efficient suppression of gene expression than traditional stem-loop shRNAs (34). Despite the different technologies to generate the Dox-inducible Col1a1 shRNA-harboring mouse lines (Tet-controlled shRNACol1a1-7 using recombinase-mediated cassette exchange in the noncoding Col1a1 locus in embryonic stem cells; Tet-controlled shRNACol1a1-4 using ZFN assisted homologous recombination directly in fertilized oocytes), the results obtained in the liver fibrosis studies were almost identical, supporting not only the efficacy but also the reliability of these approaches.

Breeding these two mouse lines, carrying the cassette expressing the Tet regulated EGFP reporter protein and shRNA targeting Col1a1, with the R26-M2rtTA mouse strain, which secures widespread expression of the reverse tetracycline transactivator (rtTA), generated the final bi-transgenic mice. In both strains primary ear fibroblasts from bi-transgenic animals of both Col1a1 shRNA models, GFP fluorescence was only

detected after induction with Dox, paralleled by >80% reduced Col1a1 expression. Notably, in these cells the functional suppression of Col1a1 induced transcriptional changes of a number of other major collagens that are relevant in liver fibrosis, with a significant downregulation of Col3a1, while Col5a1 and Col6a1 were significantly upregulated, suggesting that dysregulation of single ECM component (here collagen type I) can significantly alter the fibroblast synthetic phenotype, likely via a different, e.g., integrin-mediated sensing of the cells environment.

Many but not all of these effects were replicated in fibrotic liver *in vivo* where Dox-induced activation of the Col1a1 shRNA resulted in a massive GFP fluorescence signal in bi-transgenic mice and an almost 50% reduction of collagen deposition, an antifibrotic efficacy not reached with most antifibrotic agents (3,69). The target gene Col1a1 was downregulated by almost 90% compared to controls and the gene of the other major fibrillar collagen, Col3a1 by 65-70%. However, unlike the cell culture results, all other collagen genes analyzed in the fibrotic livers were downregulated, most significantly Col6a1 by almost 60%. Suppression of collagen accumulation was confirmed on the protein level, as assessed by quantitative morphometry of specifically stained liver sections, with a 60-70% reduction for collagen type I and 35-39% reduction for collagen type III compared to the non-Dox-induced littermates. Finally, all specific fibrosis related data were completely in accordance with the observed decrease in biochemical collagen (hydroxyproline content) and collagen morphometry on Sirius red stained liver sections.

4.5. Reduction of collagen type I in the fibrotic liver tissue led to attenuation of ECM mechanical stress

The ECM is a complex interacting system of structural as well as functional molecules including various distinct collagens, glycosaminoglycans, proteoglycans, noncollagenous glycoproteins, stored growth factors/cytokines and different cell types embedded in it (6,70). Changes in this microenvironment, including quantitative changes of mainly structural components like collagen type I, lead not only to tissue morphological changes but also to a different environment for the cells that are anchored to the ECM, especially activated (myo)fibroblasts. Thus integrin (the major ECM receptors) mediated signals to these myofibroblasts sense mechanical stress, as in wound healing, when these cells receive cues to proliferate and lay down a novel

ECM via their integrin-ECM (collagen)-contacts, a physiological regulatory response that is aimed at “filling the gap” (63,71). This mechanical stress which is e.g. mediated via the collagen type I binding integrin α2β1 induces myofibroblast activation and enhanced transcription of ECM genes, including the here studied Col3a1, Col4a1, Col5a1, Col6a1 and Col6a3 genes, while several MMPs that are mainly involved in the degradation of collagens and other ECM components are suppressed (6,71-73). On the other hand, reduction of collagen type I in the fibrotic liver tissue, as was induced in the here generated transgenic mice, could have led to attenuation of mechanical stress sensing by the myofibroblasts, with the observed downregulation of other ECM genes. This mechanism would not be equally transferable to the above-described fibroblast cultures which attach to tissue culture plastic (also via a spectrum of integrins) in an artificial, mechanically stressed 2D environment, as compared to the 3D environment *in vivo*, which could explain some of the observed differences between the used *in vitro* and *in vivo* systems. Moreover, MMP transcripts that are associated both with fibrolysis and fibrogenesis, depending on the context, were decreased when Col1a1 was suppressed in fibrotic mice.

4.6. Anti-inflammatory effect of collagen type I suppression

As shortly mentioned above, the attenuation of the inflammatory response by induced specific downregulation of Col1a1 expression in the CCl_4-fibrosis model is an intriguing novel finding. At first glance this is unexpected, since fibrolytic responses, as occur in these models, are usually driven by or associated with classical inflammatory Th1 T cells and M1 macrophages (74). With the induced knockdown of procollagen type I production, transcription of for MMP-8 and MMP-13 that are mainly produced by neutrophils and macrophages and that cleave interstitial collagens type I and III (75) the CD68 macrophage marker and macrophage infiltration in the liver was significant suppressed, suggesting a reduced recruitment and/or activation of these MMP-expressing inflammatory cells in the collagen type I reduced livers. This anti-inflammatory effect of collagen type I suppression was also reflected by a decreased serum ALT and AST, both serum markers of liver inflammation. Therefore, a quantitative reduction, but not complete absence, of collagen type I, appears to attenuate inflammatory cell activation and recruitment in the damaged liver.

4.7. Conclusion

Taken together, I generated Tet-inducible RNAi knockdown mouse lines that provide highly efficient and inducible downregulation of Col1a1 using two different gene targeting strategies. These mouse lines will serve as valuable novel tools to study the role of cell-specific genes in fibrotic or inflammatory conditions. They already led to relevant novel insights into the role of collagen type I in the regulation of fibrosis, of other ECM related genes and the inflammatory cell response to liver damage. In addition, the models will permit a prediction as to, yet to be developed, collagen type I specific antifibrotic therapies.

5. Summary

Hepatic fibrosis results from a chronic wound-healing response of the liver. It may progress to cirrhosis and primary liver cancer, which are the major causes of liver related morbidity and mortality. Hepatic fibrosis is characterized by chronic inflammation that causes excess deposition of scar tissue (extracellular matrix, ECM), mainly composed of interstitial collagens such as collagen type I and other structural and functional components of the ECM.

This study focused on generation of RNAi mouse models that provide a highly efficient downregulation of Col1a1 (alpha-1 type I procollagen) to address the role of collagen type I in development of liver fibrosis and to predict the effect novel specific, collagen type I directed anti-fibrotic therapies.

To create mice with inducible RNA interference (RNAi) to knockdown Col1a1, two modern efficient methods of gene targeting were used: recombinase-mediated cassette exchange (RMCE) in embryonic stem cells and zinc-finger nuclease (ZFN)-aided genomic targeting. Using these methods, a targeting cassette carrying the tetracycline responsive element (TRE), enhanced green fluorescent protein (EGFP) and sh(short hairpin)RNA targeting Col1a1 were inserted in the predefined locus downstream 3' UTR of the Col1a1 gene.

For this propose two different shRNAs were screened, validated and cloned in the context of miR30, which permits a more efficient suppression of gene expression than traditional stem-loop shRNAs. ShRNACol1a1-7 was used for creating the Tet-regulated shRNA expressing mice using RMCE in KH2 embryonic stem (ES) cells, while the Tet-controlled shRNACol1a1-4 was integrated in the same genomic location using ZFN assisted homologous recombination directly in fertilized oocytes.

To analyze the new tetracycline inducible RNAi Col1a1 transgenic mice, they were bred with the Rosa26-M2rtTA strain that provides widespread expression of the reverse tetracycline-controlled transactivator (rtTA-M2) protein. Transgenic mice and the wild type (WT) control group were treated with escalating doses of oral CCl_4 for three weeks to induce parenchymal liver fibrosis and at the same time with doxycycline to induce expression of Col1A1 shRNAs and EGFP reporter protein.

Bi-transgenic mice showed an 80-90% suppression of procollagen alpha1(I) transcription and a 40-50% reduction in hepatic collagen accumulation in comparison with the fibrotic WT controls. Interestingly, the induced procollagen alpha1(I) knockdown downregulated procollagens type III, IV and VI and other fibrosis related parameters. This was associated with attenuation of chronic inflammation, suggesting that collagen type I serves not only as major scar component, but also as a modulator of other collagens and of chronic inflammation.

6. Zusammenfassung

Die Leberfibrose ist eine chronische Wundheilungsreaktion der Leber bei chronischer Schädigung. Sie kann zur Zirrhose und zum Leberzellkarzinom führen, die die Hauptursachen der erhöhten Morbidität und Mortalität chronischer Lebererkrankungen sind. Die Leberfibrose ist durch eine überschüssige Ablagerung von Narbengewebe (extrazellulärer Matrix, EZM) charakterisiert, die hauptsächlich aus interstitiellen Kollagenen besteht, mit Kollagen Typ I als einer Hauptkomponenete und zahlreichen andere strukturellen und funktionellen Molekülen.

In dieser Arbeit wurde RNAi-Mausodelle genereiert, die einen hocheffizienten „Knockdown“ von Col1a1, welches für die essenzielle Kette des tripelhelikalen Prokollagen Typ I kodiert, um die Rolle des Kollagen Typ I bei der Entwicklung der Leberfibrose zu untersuchen und den Effekt neuartiger, spezifischer, auf die Kollagen Typ I-Synthese abzielender anti-fibrotischer Therapien vorherzusagen.

Um durch RNA-Interferenz (RNAi) induzierbare Mausmodelle mit einem Col1a1 „Knockdown“ zu generieren, wurden zwei verschiedene effektive Methoden eingesetzt: Kassettenaustauschverfahren in embryonalen Stammzellen und Zinkfingernuklease-mediierte Genom-Editierung. Beide Methoden wurden so eingesetzt, dass die Targeting Kassette, die das „enhanced green fluorescent protein“ (EGFP) und „short hairpin-RNA (shRNA) targeting Col1a1“ enthalten, in den Locus des Prokollagen α1(I) Gens (jenseits des 3’ UTR Col1a1-Locus) eingebracht wurde. Zu diesem Zweck wurde zwei verschiedenen shRNAs selektiert und validiert, und in den Kontext des miR30 Lokus einkloniert worden.

ShRNACol1a1-7 wurde für die Herstellung der die Tetrazyklin (Tet)-regulierbaren shRNA exprimierenden Mäuse bei dem Kassettenaustauschverfahren in KH2 embryonalen Stammzellen verwendet. Das (Tet)-regulierbare shRNACol1a1-4 Gen wurde im gleichen Genort bei der ZFN-abhängigen homologen Rekombination unmittelbar in befruchteten Eizellen eingesetzt.

Um die neuen induzierbaren RNAi Col1a1 transgenen Mäuse zu charakterisieren, wurden die Tiere mit der Rosa26-M2rtTA Linie, die die weit verbreitete Expression des reversen Tetrazyklin-abhängigen Transaktivators (rtTA) erlaubt, gekreuzt. Die

transgene Mäuse und die Wildtyp (WT)-Kontrolltiere wurden drei Wochen lang mit eskalierenden Dosen CCl_4 behandeln, um eine parenchymatöse Leberfibrose und die gleichzeitige Expression der shRNAs Col1a1 und des EGFP Reporterprotein zu induzieren.

Die Tet-induzierten bi-transgenen Mäuse zeigten eine 80-90%ige Suppression der der Prokollagenes α1(I) mRNA-Expression und eine 40-50%ige Reduzierung der Kollagen-Ablagerung in der Leber im Vergleich zu den fibrotischen WT-Mäusen. Interessanterweise führte der Prokollagen α1(I) “knockdown” auch zu einer Suppression der Expression, sondern auch der Expression der Prokollagene Typ III, IV und VI sowie andere Fibrose-assoziierter Gene. Dies war mit einer Abschwächung der chronischen Entzündung begleitet, was darauf hindeutet, dass Kollagen Typ I nicht nur eine wichtige Komponente des Narbengewebes darstellt, sondern auch als Modulator anderer Kollagene und als Promoter der chronischen Entzündung selbst dient.

7. Abbreviations

αSMA - α-smooth muscle actin

Ago2 - Argonaute 2

Col1a1 - procollagen α1(I) gene (alpha-1 type I collagen)

CCL2 - chemokine ligand 2

Dox – doxycycline

dsRNA - double-stranded RNA

ECM - extracellular matrix

ES cells - embryonic stem cells

EGFP - enhanced green fluorescent protein

Flp – flippase (Flp recombinase)

frt - flippase recognition target sites

HSC - hepatic stellate cells

IL-1β - interleukin-1β

IL-6 - interleukin 6

IL-8 - interleukin 8

MF - myofibroblast

miR30 - microRNA precursor

MMPs - matrix metalloproteinases

MCP-1 - monocyte chemoattractant protein 1

miRNA - microRNA

RMCE - recombinase-mediated cassette exchange

RNAi - RNA interference

RNA-induced silencing complex (RISC)

rtTA - reverse tetracycline transactivator

siRNA - small interfering RNA

shRNA - short (small) hairpin RNA

SSR - site-specific recombination

TGM - TRE-GFP-miR30 targeting construct

TGFß1 - transforming growth factor beta 1

Tet - tetracycline

tTA - tetracyclin-controlled transactivator

TIMPs - tissue inhibitors of MMPs

TNFα - tumor necrosis factor alpha

TRE - tetracycline responsive element

ZFN - zinc-finger nuclease

8. References

1. Schuppan, D. (2015) Liver fibrosis: Common mechanisms and antifibrotic therapies. *Clinics and research in hepatology and gastroenterology*, **39 Suppl 1**, S51-59.
2. Wynn, T.A. and Ramalingam, T.R. (2012) Mechanisms of fibrosis: therapeutic translation for fibrotic disease. *Nat Med*, **18**, 1028-1040.
3. Schuppan, D. and Kim, Y.O. (2013) Evolving therapies for liver fibrosis. *The Journal of clinical investigation*, **123**, 1887-1901.
4. Sun, M. and Kisseleva, T. (2015) Reversibility of liver fibrosis. *Clinics and research in hepatology and gastroenterology*, **39 Suppl 1**, S60-63.
5. Trautwein, C., Friedman, S.L., Schuppan, D. and Pinzani, M. (2015) Hepatic fibrosis: Concept to treatment. *J Hepatol*, **62**, S15-24.
6. Schuppan, D., Ruehl, M., Somasundaram, R. and Hahn, E.G. (2001) Matrix as a modulator of hepatic fibrogenesis. *Semin Liver Dis*, **21**, 351-372.
7. Mouw, J.K., Ou, G. and Weaver, V.M. (2014) Extracellular matrix assembly: a multiscale deconstruction. *Nat Rev Mol Cell Biol*, **15**, 771-785.
8. Schuppan, D. (1990) Structure of the extracellular matrix in normal and fibrotic liver: collagens and glycoproteins. *Semin Liver Dis*, **10**, 1-10.
9. Fire, A., Xu, S., Montgomery, M.K., Kostas, S.A., Driver, S.E. and Mello, C.C. (1998) Potent and specific genetic interference by double-stranded RNA in Caenorhabditis elegans. *Nature*, **391**, 806-811.
10. Karsdal, M.A., Nielsen, S.H., Leeming, D.J., Langholm, L.L., Nielsen, M.J., Manon-Jensen, T., Siebuhr, A., Gudmann, N.S., Ronnow, S., Sand, J.M. *et al.* (2017) The good and the bad collagens of fibrosis - Their role in signaling and organ function. *Adv Drug Deliv Rev*.
11. Shoulders, M.D. and Raines, R.T. (2009) Collagen structure and stability. *Annual review of biochemistry*, **78**, 929-958.
12. Hammond, S.M., Caudy, A.A. and Hannon, G.J. (2001) Post-transcriptional gene silencing by double-stranded RNA. *Nature reviews. Genetics*, **2**, 110-119.
13. Jinek, M. and Doudna, J.A. (2009) A three-dimensional view of the molecular machinery of RNA interference. *Nature*, **457**, 405-412.
14. Mocellin, S. and Provenzano, M. (2004) RNA interference: learning gene knock-down from cell physiology. *Journal of translational medicine*, **2**, 39.

15. Moran, Y., Agron, M., Praher, D. and Technau, U. (2017) The evolutionary origin of plant and animal microRNAs. *Nat Ecol Evol*, **1**.
16. Fellmann, C. and Lowe, S.W. (2014) Stable RNA interference rules for silencing. *Nat Cell Biol*, **16**, 10-18.
17. Dickins, R.A., Hemann, M.T., Zilfou, J.T., Simpson, D.R., Ibarra, I., Hannon, G.J. and Lowe, S.W. (2005) Probing tumor phenotypes using stable and regulated synthetic microRNA precursors. *Nature genetics*, **37**, 1289-1295.
18. Kim, D.H. and Rossi, J.J. (2007) Strategies for silencing human disease using RNA interference. *Nature reviews. Genetics*, **8**, 173-184.
19. Tuettenberg, A., Steinbrink, K. and Schuppan, D. (2016) Myeloid cells as orchestrators of the tumor microenvironment: novel targets for nanoparticular cancer therapy. *Nanomedicine*, **11**, 2735-2751.
20. Babinet, C. (2000) Transgenic mice: an irreplaceable tool for the study of mammalian development and biology. *Journal of the American Society of Nephrology : JASN*, **11 Suppl 16**, S88-94.
21. Turan, S., Zehe, C., Kuehle, J., Qiao, J. and Bode, J. (2013) Recombinase-mediated cassette exchange (RMCE) - a rapidly-expanding toolbox for targeted genomic modifications. *Gene*, **515**, 1-27.
22. Kim, H. and Kim, J.S. (2014) A guide to genome engineering with programmable nucleases. *Nature reviews. Genetics*, **15**, 321-334.
23. Kohan, D.E. (2008) Progress in gene targeting: using mutant mice to study renal function and disease. *Kidney international*, **74**, 427-437.
24. Baron, U. and Bujard, H. (2000) Tet repressor-based system for regulated gene expression in eukaryotic cells: principles and advances. *Methods in enzymology*, **327**, 401-421.
25. Gossen, M. and Bujard, H. (1992) Tight control of gene expression in mammalian cells by tetracycline-responsive promoters. *Proceedings of the National Academy of Sciences of the United States of America*, **89**, 5547-5551.
26. Pattanayak, V., Guilinger, J.P. and Liu, D.R. (2014) Determining the specificities of TALENs, Cas9, and other genome-editing enzymes. *Methods Enzymol*, **546**, 47-78.
27. Kistner, A., Gossen, M., Zimmermann, F., Jerecic, J., Ullmer, C., Lubbert, H. and Bujard, H. (1996) Doxycycline-mediated quantitative and tissue-specific

control of gene expression in transgenic mice. *Proceedings of the National Academy of Sciences of the United States of America*, **93**, 10933-10938.

28. Urlinger, S., Baron, U., Thellmann, M., Hasan, M.T., Bujard, H. and Hillen, W. (2000) Exploring the sequence space for tetracycline-dependent transcriptional activators: novel mutations yield expanded range and sensitivity. *Proceedings of the National Academy of Sciences of the United States of America*, **97**, 7963-7968.
29. Geerts, A., Schuppan, D., Lazeroms, S., De Zanger, R. and Wisse, E. (1990) Collagen type I and III occur together in hybrid fibrils in the space of Disse of normal rat liver. *Hepatology*, **12**, 233-241.
30. Branda, C.S. and Dymecki, S.M. (2004) Talking about a revolution: The impact of site-specific recombinases on genetic analyses in mice. *Developmental cell*, **6**, 7-28.
31. Wirth, D., Gama-Norton, L., Riemer, P., Sandhu, U., Schucht, R. and Hauser, H. (2007) Road to precision: recombinase-based targeting technologies for genome engineering. *Current opinion in biotechnology*, **18**, 411-419.
32. Birling, M.C., Gofflot, F. and Warot, X. (2009) Site-specific recombinases for manipulation of the mouse genome. *Methods in molecular biology*, **561**, 245-263.
33. Beard, C., Hochedlinger, K., Plath, K., Wutz, A. and Jaenisch, R. (2006) Efficient method to generate single-copy transgenic mice by site-specific integration in embryonic stem cells. *Genesis*, **44**, 23-28.
34. Dickins, R.A., McJunkin, K., Hernando, E., Premsrirut, P.K., Krizhanovsky, V., Burgess, D.J., Kim, S.Y., Cordon-Cardo, C., Zender, L., Hannon, G.J. *et al.* (2007) Tissue-specific and reversible RNA interference in transgenic mice. *Nature genetics*, **39**, 914-921.
35. Premsrirut, P.K., Dow, L.E., Kim, S.Y., Camiolo, M., Malone, C.D., Miething, C., Scuoppo, C., Zuber, J., Dickins, R.A., Kogan, S.C. *et al.* (2011) A rapid and scalable system for studying gene function in mice using conditional RNA interference. *Cell*, **145**, 145-158.
36. Kim, Y.G., Cha, J. and Chandrasegaran, S. (1996) Hybrid restriction enzymes: zinc finger fusions to Fok I cleavage domain. *Proceedings of the National Academy of Sciences of the United States of America*, **93**, 1156-1160.

37. Doyon, Y., Vo, T.D., Mendel, M.C., Greenberg, S.G., Wang, J., Xia, D.F., Miller, J.C., Urnov, F.D., Gregory, P.D. and Holmes, M.C. (2011) Enhancing zinc-finger-nuclease activity with improved obligate heterodimeric architectures. *Nature methods*, **8**, 74-79.

38. Miller, J.C., Holmes, M.C., Wang, J., Guschin, D.Y., Lee, Y.L., Rupniewski, I., Beausejour, C.M., Waite, A.J., Wang, N.S., Kim, K.A. *et al.* (2007) An improved zinc-finger nuclease architecture for highly specific genome editing. *Nature biotechnology*, **25**, 778-785.

39. Krempen, K., Grotkopp, D., Hall, K., Bache, A., Gillan, A., Rippe, R.A., Brenner, D.A. and Breindl, M. (1999) Far upstream regulatory elements enhance position-independent and uterus-specific expression of the murine alpha1(I) collagen promoter in transgenic mice. *Gene Expr*, **8**, 151-163.

40. Kisseleva, T., Uchinami, H., Feirt, N., Quintana-Bustamante, O., Segovia, J.C., Schwabe, R.F. and Brenner, D.A. (2006) Bone marrow-derived fibrocytes participate in pathogenesis of liver fibrosis. *J Hepatol*, **45**, 429-438.

41. Kisseleva, T., Cong, M., Paik, Y., Scholten, D., Jiang, C., Benner, C., Iwaisako, K., Moore-Morris, T., Scott, B., Tsukamoto, H. *et al.* (2012) Myofibroblasts revert to an inactive phenotype during regression of liver fibrosis. *Proceedings of the National Academy of Sciences of the United States of America*, **109**, 9448-9453.

42. Magness, S.T., Bataller, R., Yang, L. and Brenner, D.A. (2004) A dual reporter gene transgenic mouse demonstrates heterogeneity in hepatic fibrogenic cell populations. *Hepatology*, **40**, 1151-1159.

43. Weis, S.M., Emery, J.L., Becker, K.D., McBride, D.J., Jr., Omens, J.H. and McCulloch, A.D. (2000) Myocardial mechanics and collagen structure in the osteogenesis imperfecta murine (oim). *Circ Res*, **87**, 663-669.

44. Wendling, O., Bornert, J.M., Chambon, P. and Metzger, D. (2009) Efficient temporally-controlled targeted mutagenesis in smooth muscle cells of the adult mouse. *Genesis*, **47**, 14-18.

45. Cuttler, A.S., LeClair, R.J., Stohn, J.P., Wang, Q., Sorenson, C.M., Liaw, L. and Lindner, V. (2011) Characterization of Pdgfrb-Cre transgenic mice reveals reduction of ROSA26 reporter activity in remodeling arteries. *Genesis*, **49**, 673-680.

46. Muzumdar, M.D., Tasic, B., Miyamichi, K., Li, L. and Luo, L. (2007) A global double-fluorescent Cre reporter mouse. *Genesis*, **45**, 593-605.

47. Henderson, N.C., Arnold, T.D., Katamura, Y., Giacomini, M.M., Rodriguez, J.D., McCarty, J.H., Pellicoro, A., Raschperger, E., Betsholtz, C., Ruminski, P.G. *et al.* (2013) Targeting of alphav integrin identifies a core molecular pathway that regulates fibrosis in several organs. *Nat Med*, **19**, 1617-1624.
48. Fausther, M. and Dranoff, J.A. (2014) Integrins, myofibroblasts, and organ fibrosis. *Hepatology*, **60**, 756-758.
49. Gaj, T., Gersbach, C.A. and Barbas, C.F., 3rd. (2013) ZFN, TALEN, and CRISPR/Cas-based methods for genome engineering. *Trends Biotechnol*, **31**, 397-405.
50. Mullis, K.B. (1990) The unusual origin of the polymerase chain reaction. *Sci Am*, **262**, 56-61, 64-55.
51. Tucker, K.L., Wang, Y., Dausman, J. and Jaenisch, R. (1997) A transgenic mouse strain expressing four drug-selectable marker genes. *Nucleic Acids Res*, **25**, 3745-3746.
52. Popov, Y., Sverdlov, D.Y., Sharma, A.K., Bhaskar, K.R., Li, S., Freitag, T.L., Lee, J., Dieterich, W., Melino, G. and Schuppan, D. (2011) Tissue transglutaminase does not affect fibrotic matrix stability or regression of liver fibrosis in mice. *Gastroenterology*, **140**, 1642-1652.
53. Dow, L.E., Premsrirut, P.K., Zuber, J., Fellmann, C., McJunkin, K., Miething, C., Park, Y., Dickins, R.A., Hannon, G.J. and Lowe, S.W. (2012) A pipeline for the generation of shRNA transgenic mice. *Nature protocols*, **7**, 374-393.
54. Vert, J.P., Foveau, N., Lajaunie, C. and Vandenbrouck, Y. (2006) An accurate and interpretable model for siRNA efficacy prediction. *BMC bioinformatics*, **7**, 520.
55. Filhol, O., Ciais, D., Lajaunie, C., Charbonnier, P., Foveau, N., Vert, J.P. and Vandenbrouck, Y. (2012) DSIR: assessing the design of highly potent siRNA by testing a set of cancer-relevant target genes. *PloS one*, **7**, e48057.
56. Fellmann, C., Zuber, J., McJunkin, K., Chang, K., Malone, C.D., Dickins, R.A., Xu, Q., Hengartner, M.O., Elledge, S.J., Hannon, G.J. *et al.* (2011) Functional identification of optimized RNAi triggers using a massively parallel sensor assay. *Molecular cell*, **41**, 733-746.
57. McJunkin, K., Mazurek, A., Premsrirut, P.K., Zuber, J., Dow, L.E., Simon, J., Stillman, B. and Lowe, S.W. (2011) Reversible suppression of an essential gene

in adult mice using transgenic RNA interference. *Proceedings of the National Academy of Sciences of the United States of America*, **108**, 7113-7118.

58. Buchholz, F., Angrand, P.O. and Stewart, A.F. (1998) Improved properties of FLP recombinase evolved by cycling mutagenesis. *Nature biotechnology*, **16**, 657-662.
59. Hochedlinger, K., Yamada, Y., Beard, C. and Jaenisch, R. (2005) Ectopic expression of Oct-4 blocks progenitor-cell differentiation and causes dysplasia in epithelial tissues. *Cell*, **121**, 465-477.
60. Wynn, T.A. (2008) Cellular and molecular mechanisms of fibrosis. *J Pathol*, **214**, 199-210.
61. Kuznetsova, N.V., McBride, D.J. and Leikin, S. (2003) Changes in thermal stability and microunfolding pattern of collagen helix resulting from the loss of alpha2(I) chain in osteogenesis imperfecta murine. *J Mol Biol*, **331**, 191-200.
62. Forlino, A., Porter, F.D., Lee, E.J., Westphal, H. and Marini, J.C. (1999) Use of the Cre/lox recombination system to develop a non-lethal knock-in murine model for osteogenesis imperfecta with an alpha1(I) G349C substitution. Variability in phenotype in BrtlIV mice. *J Biol Chem*, **274**, 37923-37931.
63. Georges, P.C., Hui, J.J., Gombos, Z., McCormick, M.E., Wang, A.Y., Uemura, M., Mick, R., Janmey, P.A., Furth, E.E. and Wells, R.G. (2007) Increased stiffness of the rat liver precedes matrix deposition: implications for fibrosis. *Am J Physiol Gastrointest Liver Physiol*, **293**, G1147-1154.
64. Yang, H., Wang, H. and Jaenisch, R. (2014) Generating genetically modified mice using CRISPR/Cas-mediated genome engineering. *Nature protocols*, **9**, 1956-1968.
65. Jinek, M., Chylinski, K., Fonfara, I., Hauer, M., Doudna, J.A. and Charpentier, E. (2012) A programmable dual-RNA-guided DNA endonuclease in adaptive bacterial immunity. *Science*, **337**, 816-821.
66. Shi, C., Jia, T., Mendez-Ferrer, S., Hohl, T.M., Serbina, N.V., Lipuma, L., Leiner, I., Li, M.O., Frenette, P.S. and Pamer, E.G. (2011) Bone marrow mesenchymal stem and progenitor cells induce monocyte emigration in response to circulating toll-like receptor ligands. *Immunity*, **34**, 590-601.
67. Miura, H., Quadros, R.M., Gurumurthy, C.B. and Ohtsuka, M. (2018) Easi-CRISPR for creating knock-in and conditional knockout mouse models using long ssDNA donors. *Nature protocols*, **13**, 195-215.

68. Ran, F.A., Cong, L., Yan, W.X., Scott, D.A., Gootenberg, J.S., Kriz, A.J., Zetsche, B., Shalem, O., Wu, X., Makarova, K.S. *et al.* (2015) In vivo genome editing using Staphylococcus aureus Cas9. *Nature*, **520**, 186-191.

69. Popov, Y. and Schuppan, D. (2009) Targeting liver fibrosis: strategies for development and validation of antifibrotic therapies. *Hepatology*, **50**, 1294-1306.

70. Karsdal, M.A., Manon-Jensen, T., Genovese, F., Kristensen, J.H., Nielsen, M.J., Sand, J.M., Hansen, N.U., Bay-Jensen, A.C., Bager, C.L., Krag, A. *et al.* (2015) Novel insights into the function and dynamics of extracellular matrix in liver fibrosis. *Am J Physiol Gastrointest Liver Physiol*, **308**, G807-830.

71. Hinz, B., Phan, S.H., Thannickal, V.J., Galli, A., Bochaton-Piallat, M.L. and Gabbiani, G. (2007) The myofibroblast: one function, multiple origins. *Am J Pathol*, **170**, 1807-1816.

72. Eckes, B., Zweers, M.C., Zhang, Z.G., Hallinger, R., Mauch, C., Aumailley, M. and Krieg, T. (2006) Mechanical tension and integrin alpha 2 beta 1 regulate fibroblast functions. *J Investig Dermatol Symp Proc*, **11**, 66-72.

73. Langholz, O., Rockel, D., Mauch, C., Kozlowska, E., Bank, I., Krieg, T. and Eckes, B. (1995) Collagen and collagenase gene expression in three-dimensional collagen lattices are differentially regulated by alpha 1 beta 1 and alpha 2 beta 1 integrins. *J Cell Biol*, **131**, 1903-1915.

74. Mehal, W.Z. and Schuppan, D. (2015) Antifibrotic therapies in the liver. *Semin Liver Dis*, **35**, 184-198.

75. Giannandrea, M. and Parks, W.C. (2014) Diverse functions of matrix metalloproteinases during fibrosis. *Disease models & mechanisms*, **7**, 193-203.

9. Erklärung

Ich versichere, dass ich die von mir vorgelegte Dissertation selbständig angefertigt, die benutzten Quellen und Hilfsmittel vollständig angegeben und die Stellen der Arbeit – einschließlich Tabellen, Karten und Abbildungen -, die anderen Werken im Wortlaut oder dem Sinn nach entnommen sind, in jedem Einzelfall als Entlehnung kenntlich gemacht habe; dass diese Dissertation noch keiner anderen Fakultät oder Universität zur Prüfung vorgelegen hat; dass sie - abgesehen von Kongresspräsentationen in Abstraktform (wie unten angegeben) und einer gerade akzeptierten Originalpublikation (Molokanova O, Schönig K, Weng SY, Wang X, Bros M, Diken M, Ohngemach S, Karsdal M, Strand D, Nikolaev A, Eshkind L, Schuppan D. Inducible knockdown of procollagen I protects mice from liver fibrosis and leads to dysregulated matrix genes and attenuated inflammation. Matrix Biol. 2018, eingereicht) noch nicht veröffentlicht worden ist sowie, dass ich eine solche Veröffentlichung vor Abschluss des Promotionsverfahrens nicht vornehmen werde. Die Bestimmungen dieser Promotionsordnung sind mir bekannt. Die von mir vorgelegte Dissertation ist von Herrn Prof. Dr. Dr. …….. betreut worden.

Mainz, im 2018

Olena Molokanova

10. Acknowledgements

11. Curriculum vitae